2017

OLFACTORY SENSORY NEURON AND OLFACTORY BULB RESPONSES TO NOVEL PUTATIVE PHEROMONE COMPONENTS AND COMBINATIONS IN THE SEA LAMPREY (Petromyzon marinus)

Gianfranco Grande
University of Windsor

Follow this and additional works at: https://scholar.uwindsor.ca/etd

OLFACTORY SENSORY NEURON AND OLFACTORY BULB RESPONSES TO NOVEL
PUTATIVE PHEROMONE COMPONENTS AND COMBINATIONS IN THE SEA
LAMPREY (*Petromyzon marinus*)

By

Gianfranco Grande

A Thesis
Submitted to the Faculty of Graduate Studies
through the Department of Biological Sciences
in Partial Fulfilment of the Requirements for
the Degree of Master of Science
at the University of Windsor

Windsor, Ontario, Canada

2017

OLFACTORY SENSORY NEURON AND OLFACTORY BULB RESPONSES TO NOVEL
PUTATIVE PHEROMONE COMPONENTS AND COMBINATIONS IN THE SEA
LAMPREY (*Petromyzon marinus*)

by

Gianfranco Grande

APPROVED BY:

_____
C. Semeniuk
Great Lakes Institute for Environmental Research

_____
D. Higgs
Biological Sciences

_____
B. Zielinski, Advisor
Biological Sciences

May 5th, 2017

Declaration of Originality

I hereby certify that I am the sole author of this thesis and that no part of this thesis has been published or submitted for publication.

I certify that, to the best of my knowledge, my thesis does not infringe upon anyone's copyright nor violate any proprietary rights and that any ideas, techniques, quotations, or any other material from the work of other people included in my thesis, published or otherwise, are fully acknowledged in accordance with the standard referencing practices. Figures 2.5, 2.6, 2.7, and 2.22 were produced with or exclusively by Michelle Farwell based on data produced with the help of or exclusively by Michelle Farwell. Furthermore, to the extent that I have included copyrighted material that surpasses the bounds of fair dealing within the meaning of the Canada Copyright Act, I certify that I have obtained a written permission from the copyright owner(s) to include such material(s) in my thesis and have included copies of such copyright clearances to my appendix.

I declare that this is a true copy of my thesis, including any final revisions, as approved by my thesis committee and the Graduate Studies office, and that this thesis has not been submitted for a higher degree to any other University or Institution.

Abstract

The olfactory system of fishes mediates a wide array of behaviours including migration and spawning. These olfactory-mediated behaviours are elicited by chemical mixtures known as pheromones, released by a conspecific with the intent of communicating to a conspecific. Olfactory sensory neurons expressing the complementary odour receptor for an odorant will bind it, initiating an intracellular cascade resulting in the depolarization of the cell and propagation of sensory information toward brain structures known as olfactory bulbs. While generalist olfactory sensory neurons (OSNs) have been observed in insects, some OSNs in the main olfactory epithelium of mammals as well as fish express odour receptors that show high specificity for a single odorant or structurally similar odorants. Although the male sea lamprey (*Petromyzon marinus*) sex pheromone components 3 keto-petromyzonol sulfate (3kPZS) and 3,12-diketo-4,6-petromyzonene-24-sulfate (DKPES) stimulate responses at the level of the olfactory epithelium, only 3kPZS and a DKPES/3kPZS mixture has elicited a behavioural response from ovulating females. Thus, it was hypothesized that the OSNs of the sea lamprey respond to a single pheromone odorant, and the objective of my thesis was to determine the cellular response specificity of sea lamprey OSNs and to characterize neural responses from the olfactory bulb, the location of the first order synapses and associated interneurons. We used calcium imaging to investigate the specificity of odorant responses by individual OSNs to amino acid and pheromone odorants and found that sea lamprey OSNs showed high specificity in responding to single amino acids and pheromone odorants. At the level of the olfactory bulb, the local field potential detection thresholds for several pheromone odorants were determined and several previously untested single pheromone odorants were found to stimulate responses from the dorsal bulbar region. This study characterises, for the first time in the sea lamprey, the specificity of individual OSN responses to pheromone odorants and describes the olfactory responses to 4 newly elucidated putative sea lamprey pheromone odorants that were found to elicit responses from both the olfactory epithelium and olfactory bulb.

This work is dedicated to my mother and father, to my nonni, to my brothers, to Melina, and to striving towards harmony

eundum quo nemo ante iit

Acknowledgements

First and foremost, I would like to thank my mother and father, Colomba and Giovanni, my nonni Angela and Salvatore, my brothers Domenico and Michele, and my girlfriend Melina for their unwavering and invaluable support throughout this endeavour. It cannot be overstated how much it meant to me to know that I was not the only one who believed in what I was working towards. A special thanks to my parents for their steadfast guidance and their plentiful wisdom; I am who I am and have accomplished all I have accomplished thus far because of the fine example each of you has set for me.

My sincerest thanks go to my advisor, Dr. Barbara Zielinski. Your patient and wise guiding hand afforded me the opportunity to grow as a scientist and your passion spurred my own scientific curiosity. You opened my eyes to the world of olfaction and introduced me to the lamprey, an ancient, exquisitely hideous marvel.

A special thank you to Scott Miehls and Nick Johnson at Hammond Bay Biological Station for their expertise and their careful collection of the vast majority of the sea lamprey I used in my studies. The quality was top drawer and a testament to their skill and knowledge.

I would also like to thank Weiming Li and Ke Li from Michigan State University for their collaboration and generous supply of all the pheromone odorants I tested throughout my studies. Thanks are also extended to Dr. Gheylen Daghfous and Dr. Réjean Dubuc for their expertise and vital help with getting the calcium imaging experiments up and running.

A very warm thank you to the staff of the biology building, including Nancy Barkley, Martha Hiuser, Bob Hodge, Ingrid Churchill, Rodica Lieu, Linda Sterling and many others. Thank you to my fellow graduate students as well for helping to make our department a welcoming and fun place to learn and work, I am happy to have made great new friends during this experience.

To my committee, I would like to thank you very much for finding the time in your chaotic schedules, amongst countless other committees you are a part of, to offer the guidance and support that you have provided throughout this endeavour.

I would also like to thank my labmates, past and present: Michelle Farwell, Karl Boyes, Tina Suntres, Jenna Jones, Ahsan Muhammad, Gillian Hughes, Kristyn Quenneville, Alex Zygowska, and Zeenat Aurangzeb. Thank you for your help, your advice, and for making sure the valleys were not too deep.

Finally, I would like to thank our family dog Nico for being the best writing partner a graduate student could ever ask for.

Table of Contents

List of Tables

List of Figures

List of Abbreviations

3kACA	3-keto allocholic acid
3kPZS	3-keto petromyzonol sulphate
ACA	Allocholic acid
AOO	Accessory olfactory organ
cAMP	cyclic adenosine monophosphate
DFO	Fisheries and Oceans Canada
DKPES	3,12-diketo-4,6-petromyzonene-24-sulfate
EOG	Electro-olfactogram
EPSP	Excitatory post-synaptic potential
GPCR	G protein coupled receptor
IPSP	Inhibitory post-synaptic potential
LFP	Local field potential
MLR	Mesencephalic locomotor region
MOE	Main olfactory epithelium
OB	Olfactory bulb
OE	Olfactory epithelium
OR	Odour receptor
OSN	Olfactory sensory neuron
PADS	Petromyzonamine disulphate
PN	Projection neuron
PSDS	Petromyzonolsterol disulphate
PZS	Petromyzonol sulphate
SMW	Spermiated male washings
USFWS	U.S. Fish and Wildlife Service
VNO	Vomeronasal organ

CHAPTER 1 *GENERAL INTRODUCTION*

Survival and reproduction for any organism are dependent upon the ability of that organism to process the wide range of sensory information available from its surrounding environment at a neural level in order to elicit appropriate behaviours. Perceiving and decoding this sensory information is accomplished by sensory systems including the visual, auditory, and olfactory systems. Behaviours including feeding, migration, and spawning are mediated by the olfactory systems of organisms ranging from insects (Kaissling 1971) to mammals (Eisenberg and Kleiman 1972) to fishes (Hara 1986). In fishes, olfaction plays a prominent role in facilitating chemical communication both among inter- and intraspecific organisms as the olfactory system of fishes is capable of detecting a wide variety of chemicals including amino acids, gonadal steroids, bile acids, and prostaglandins (Hara 1994). Olfactory cues have been found to guide migration to suitable spawning habitat in species including salmon (Hasler and Scholz 1983) and sea lamprey (Teeter 1980). In addition, identification of gender and reproductive status of conspecifics, facilitating reproduction in a number of fish species, has also featured the exploits of the olfactory system (Drickamer 1999; Sorensen and Stacey 1999). With this sensory system also having a role in eliciting behaviours such as feeding, kin recognition, and predator avoidance across aquatic taxa, the importance of the olfactory system cannot be understated.

To understand how olfaction mediates behaviour, an understanding of how the olfactory system is organized as well as the nature of the signalling pathways inherent in this system is required. To this end, much has been learned from the study of vertebrate and invertebrate organisms (Hildebrand and Shepherd, 1997), with the neural pathway from olfaction to

locomotion having been described in an invertebrate (*C. elegans*) (Gray *et al.* 2005) and also in the sea lamprey (*Petromyzon marinus*) (Derjean *et al.* 2010). Given their large and easily accessed olfactory bulbs relative to the rest of their brain (Stoddart 1990), the sea lamprey is a model species for the study of olfaction and has been subject of rigorous study. The olfactory pathway in sea lamprey (and in all other vertebrates) begins when an odour ligand binds to its odour receptor expressed by an olfactory sensory neuron (OSN) on the surface of the main olfactory epithelium (MOE) or accessory olfactory organ (Li and Sorensen 1997). Generalist OSNs, which bind and respond to a number of varying odorants, have been observed on the antennae of insects (Schneider 1969; Stengl *et al.* 1992) and in the OSNs projecting to necklace glomeruli of the mouse (Greer *et al.* 2016). However, OSNs in the main olfactory epithelium of mammals (Ressler *et al.* 1994; Vassar *et al.* 1994) as well as fish (Specca *et al.* 1999; Laberge and Hara 2001) have been shown to express odour receptors that exhibit high affinity for a particular ligand property of an odorant. The odour receptors expressed by sea lamprey OSNs are members of a seven-transmembrane G-protein coupled receptor superfamily (Libants *et al.* 2009). The binding of an odour ligand to the odour receptor initiates a signal transduction cascade involving second messengers opening cyclic nucleotide gated channels as well as other ion channels on the surface of the OSN (Figure 1.1), spurring the depolarization of the cell, producing a generator potential detectable by electro-olfactogram recordings, and culminating in an action potential once the membrane potential threshold is met (Restrepo *et al*. 1996). The electrical impulses propagate along OSN axons via voltage-gated sodium channels to the axon terminus in an associated glomerular region of neuropil found in the olfactory bulb. Local field potentials (LFPs) can be recorded from the surface of the olfactory bulb when odorant responses occur (Schild and Restrepo 1998). The olfactory bulb surface is organized into regions based on

the response characteristics of the OSNs within each region (Rubin and Katz 1999). In the sea lamprey, OSNs from the main olfactory epithelium have been shown, through tract tracing experiments, to extend to the medial, dorsal, and lateral regions of the ipsilateral olfactory bulb while sensory neurons within the accessory olfactory organ project axons solely to the medial region of the olfactory bulb (Figure 1.2) (Frontini *et al.* 2003; Ren *et al.* 2009). The dendrites of olfactory bulb projection neurons extend into the glomeruli to receive synaptic input from the OSNs of the main olfactory epithelium and accessory olfactory epithelium (Derjean *et al.* 2010). Projection neurons from the medial region of the olfactory bulb project their axons to the posterior tuberculum before relaying to the mesencephalic locomotor region containing neurons which project to reticulospinal neurons responsible for locomotion. Projection neurons from the lateral olfactory bulb project to the lateral pallium and other forebrain regions (Figure 1.2) (Derjean *et al.* 2010).

This thesis refers to the intentionally released, male sex pheromone components as chemical signals, while referring to the components more passively released by larvae, as chemical cues (Wisenden 2015). The use of chemical signals and cues by the sea lamprey (*Petromyzon marinus*) to mediate critical behaviours over the course of its complex life-cycle (Figure 1.3) has been well documented (Kleerekoper 1972; Teeter 1980; Mallatt 1983; Bjerselius *et al.* 2000; Li *et al.* 2002). An ancient agnathan, the sea lamprey can have its origin traced back about 500 million years ago (Forey and Janvier 1993). While native to the Atlantic Ocean, this anadromous species has successfully invaded all the Great Lakes as well as several of the Finger Lakes in North America (Smith and Tibbles 1980; Bryan *et al.* 2005). Each spring, males and females mate in spawning streams where males construct nests for the tens of thousands of eggs deposited by a single female attracted to the nests by male sex pheromone components including

3-keto petromyzonol sulphate (3kPZS) (Figure 1.4b) and 3-keto allocholic acid (3kACA) (Figure 1.4b) (Li *et al*. 2002; Siefkes *et al*. 2003). 3kPZS stimulates directional movement and search behaviour by females, thereby attracting them to the pheromone's source while also increasing swimming speed and inducing rapid tail beating (Li *et al*. 2002; Siefkes *et al*. 2003; Johnson *et al*. 2005; 2009). While males do release 3kACA, this compound failed to elicit a behavioural response on its own and did not increase female trap retention when released as part of a mixture with 3kPZS compared to 3kPZS released on its own (Luerhing *et al*. 2010). Soon after spawning, the male and female die (Applegate, 1950). Blind, filter-feeding young referred to as ammocoetes then hatch from the developed embryos and live in streams for 3-20 years (Smith and Tibbles 1980). The time spent as ammocoetes depends on the time taken to reach a critical size and condition required for metamorphosis into juveniles. With large olfactory systems and rasping oral discs, parasitic stage lamprey will swim downstream to open waters (ie. associated river, lake, or ocean) where they will actively parasitize fishes present (Youson 2003). One to two years of rapid growth occur during this parasitic phase, with these individuals being transported widely by the hosts they are feeding from. At the onset of sexual maturity, they are guided to appropriate spawning rivers by the migratory cues released by larvae within their streambeds including petromyzonol sulphate (PZS) (Figure 1.4b), allocholic acid (ACA) (Figure 1.4b), and two disulphated aminosterol derivatives known as petromyzonamine disulphate (PADS) (Figure 1.4b) and petromyzonolsterol disulphate (PSDS) (Figure 1.4b) (Li *et al*. 1995; Bjerselius *et al*. 2000; Sorensen *et al*. 2005). It has been shown through mark-recapture studies that sea lampreys do not necessarily return to their specific natal streams, and instead follow the aforementioned migratory cues towards streams containing high numbers of larvae (Bergstedt and Seelye, 1995; Moore and Schleen, 1980; Sorensen and Vrieze, 2003). This behavioural

strategy results in significantly lower numbers of sea lamprey entering rivers where lampricides have decimated larvae numbers. Once the lampreys have entered a spawning river during a spring-time run, males will construct their nests, spawning ensues, followed by death of the spawning individuals all within a few weeks.

Presently, sea lampreys remain a constant threat to commercially and ecologically important fishes, and controlling this species remains a necessity in order to maintain a healthy and sustainable ecosystem in the Great Lakes. As such, the Great Lakes Fishery Commission, in conjunction with the Fisheries and Oceans Canada (DFO) and the U.S. Fish and Wildlife Service (USFWS), continues to implement an integrated pest management program to control sea lamprey populations in the Great Lakes.

As evidenced by having set strategic goals including the deployment of a new alternative-control method by 2010, the GLFC continues to actively pursue potential advances to their control program in terms of increasing efficiency, reducing cost, and limiting environmental impact (GLFC, 2001). The research spurred on by this initiative has resulted in the elucidation and subsequent synthesis of a number of migratory and sex pheromone components released by sea lamprey, as outlined above. Recent studies by Li *et al.* (2013) have since demonstrated that ovulating female lamprey show a pervasive preference for spermiated male washings when exposed to spermiated male washings and isolated 3kPZS in a two-choice maze, indicating the likelihood of there being another male sex pheromone component. The identity of this component was determined to be 3,12-diketo-4,6-petromyzonene-24-sulfate (DKPES) (Figure 1.4a). The putative pheromone petromyzestrosterol (Li *et al*. 2012) has also been recently isolated and its structure elucidated from water conditioned by spermiated male lamprey. From water conditioned by larval lamprey, the putative pheromone petromyzonin (Li *et al*. 2013) has

too been isolated and its structure elucidated. More recently, PAMS-24 (Figure 1.4a) has been

identified as a putative pheromone component obtained from reproductive male lamprey and is

believed to act as a territory marker, averting other conspecific males from the releasing male's

nest (Brant 2015). In addition, two other newly isolated putative pheromone components, 971

and 973 (Figure 1.4a), have been obtained from larval lamprey and are to be investigated to

determine their function (Brant 2015). The migratory and sex pheromone components isolated

from sea lamprey to date have been characterized in terms of electrophysiological responsiveness

at the level of the olfactory epithelium through electro-olfactogram recordings (Li *et al*. 1995,

2002, 2013; Bjerselius *et al*. 2000; Siefkes *et al*. 2003; Sorensen *et al*. 2005). The same cannot be

said however of our knowledge concerning the processing of this sensory input within the brain.

The potential for synergistic effects on behaviour when DKPES and 3kPZS are released as a

mixture was demonstrated in 2013 when Li *et al.* observed a 73% increase in the proportion of

sexually mature females entering nests when they were baited with a mixture of DKPES and

3kPZS (2:29.8) compared to nests baited with only 3kPZS. These pheromone components are

likely bound by specific odour receptors expressed by olfactory sensory neurons within the

peripheral olfactory organ. Much can be gained then from imaging experiments at the peripheral

olfactory organs as well as electrophysiological investigations at the olfactory bulb in terms of

better characterising how each of these pheromone components are detected and processed by

the olfactory system. As well, the relative importance of each component with regard to

stimulating motor output may be determined.

Given the potential synergistic interactions between 3kPZS and DKPES, the overall

hypothesis of this thesis is that each epithelial olfactory sensory neuron of the sea lamprey

responds to a single pheromone component, rendering pheromone component combinations

more stimulatory than single components. The general aim of my research is thus to assess whether the olfactory sensory neurons are each exclusively responding to a single odour or to multiple odours. Additionally, I wish to determine whether synergistic affects arise in the form of greater or lesser electrophysiological response amplitudes when pheromone components are released as a mixture compared to when each component is released alone. To address this, I employed electrophysiological and calcium imaging techniques to gain multiple perspectives of and subsequently better characterise the relative responses generated by pheromone components themselves compared to mixtures of these components.

To this end, calcium imaging techniques were employed to determine the level of cellular specificity with regard to OSN responses to different odours. The calcium binding fluorophore Calcium green dextran loaded olfactory epithelia were exposed to various odorants and odorant mixtures of interest and the relative change in fluorescence in each of the OSNs observed was recorded. In this way, specificity was determined based on whether similar fluorescence changes are observed from the same OSNs in response to different odours or whether completely different subsets of OSNs fluoresce in response to different odours.

Neural activity in the form of summed inhibitory and excitatory postsynaptic potentials from the surface of the OB, in response to sea lamprey pheromone components and mixtures, was examined by recording local field potential (LFP) responses from dorsal and lateral olfactory bulb regions. As well, detection thresholds for these components were determined in adult lamprey at the level of the olfactory bulb.
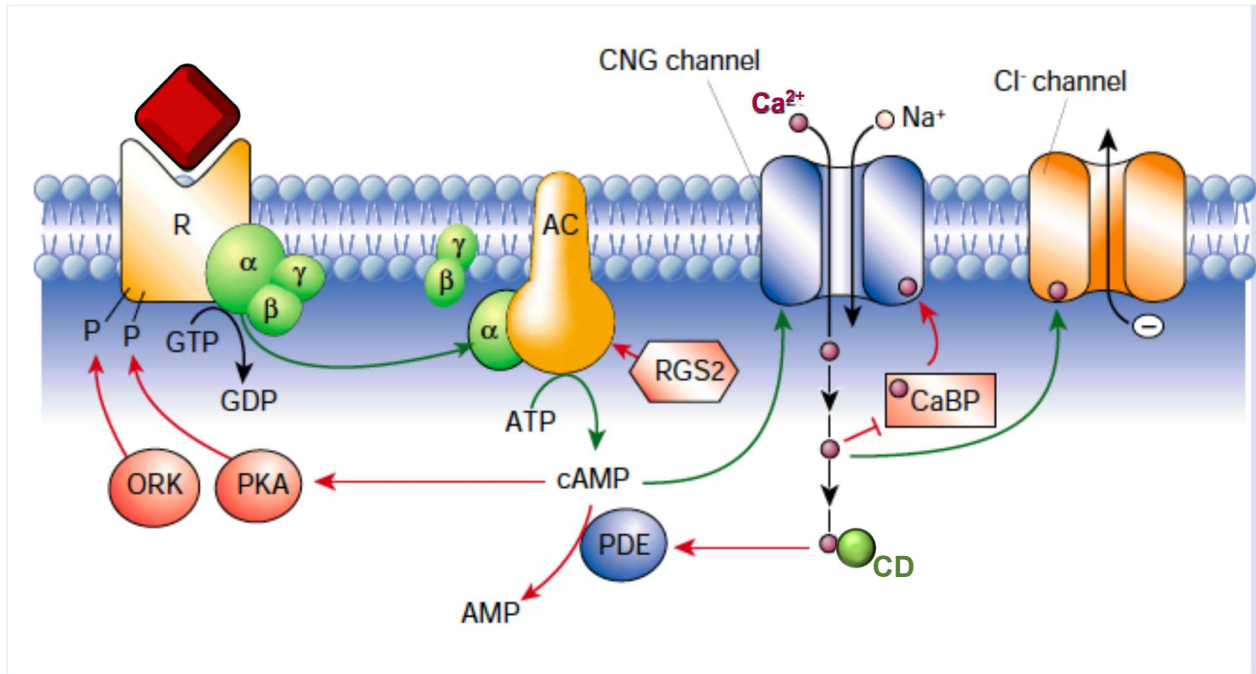
Figure 1.1 The olfactory signal transduction cascade involving the second messenger cyclic adenosine monophosphate (cAMP). Binding of an odour to a G-protein coupled receptor (R) releases the α subunit from the receptor, which binds to, and activates adenylyl cyclase (AC). The activated AC uses adenosine triphosphate (ATP) to produce cAMP, which in turn binds to cyclic nucleotide-gated channels (CNG). The CNG channels open and Ca2+ and Na+ ions enter the intracellular environment, where calcium dextran molecules (CD) can bind with the Ca^{2+}. The increase in intracellular Ca2+ and Na+ ions causes a chloride channel to open, allowing Cl- ions to flow into the extracellular environment. The movement of Ca2+ and Na+ ions inward and Cl- ions outward depolarizes the olfactory sensory neuron generating an action potential. Illustration modified from Firestein, 2001. Nature Vol 413: 211-218.
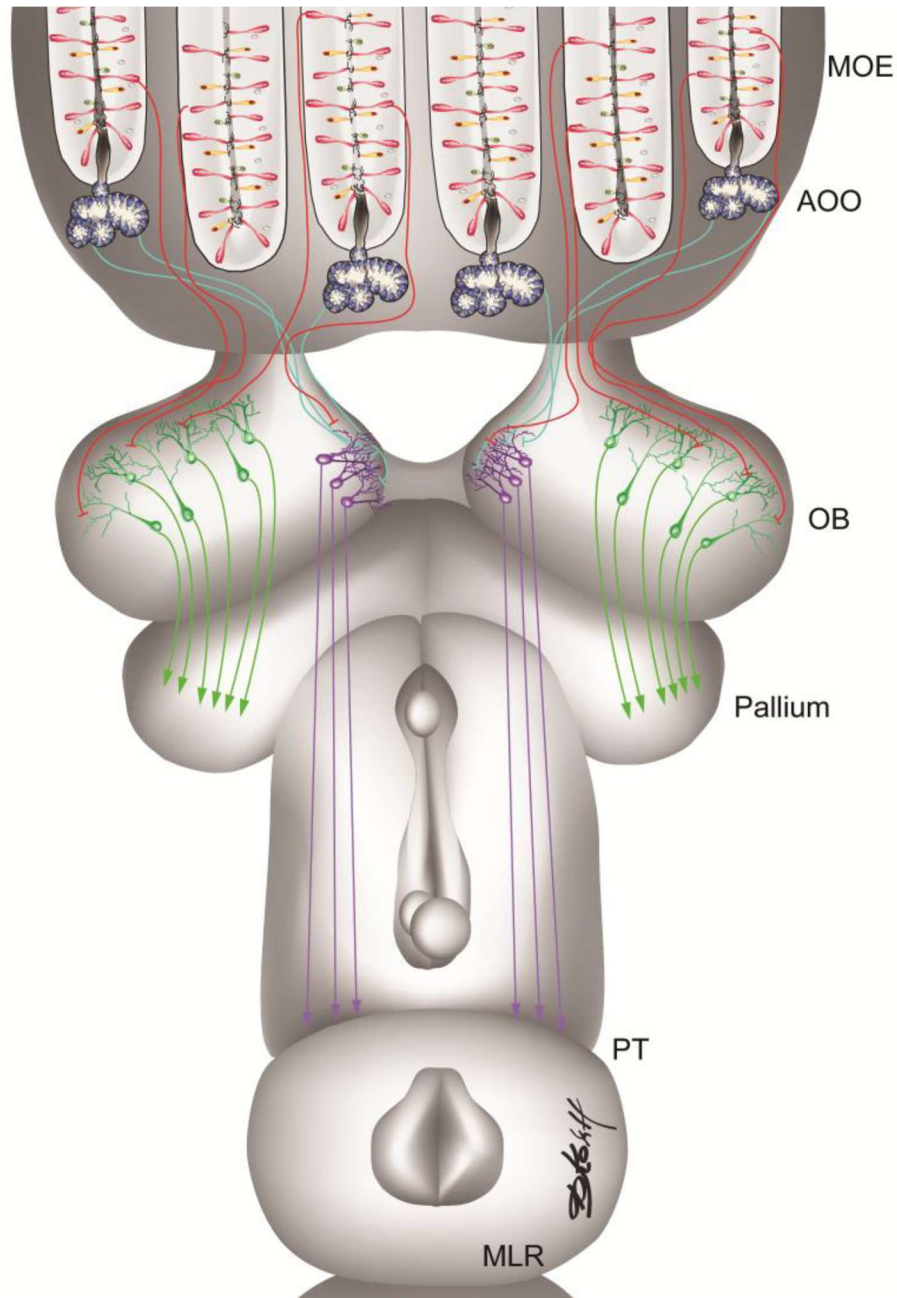
Figure 1.2 An illustration of the parallel processing pathways of the olfactory bulb in the sea lamprey. The accessory olfactory organ (AOO) OSNs (blue) project solely to the medial region of the olfactory bulb. The main olfactory epithelium (MOE) OSNs (red) project to the medial, dorsal, and lateral regions of the olfactory bulb. The medial olfactory bulb sends the axons of its primary projection neurons (purple) to the posterior tuberculum (PT). Neurons of the PT project to the mesencephalic locomotor region (MLR) where reticulospinal cells, responsible for initiating locomotion, synapse with PT axons. The primary projection neurons of the non-medial regions of the olfactory bulb (green), receiving inputs solely from the MOE (red), project their axons (green) to pallial regions of the forebrain. It is proposed that this pathway is involved with further olfactory information integration (Illustration from Derjean *et al.* 2010. PLoS Biol 8(12):e1000567).
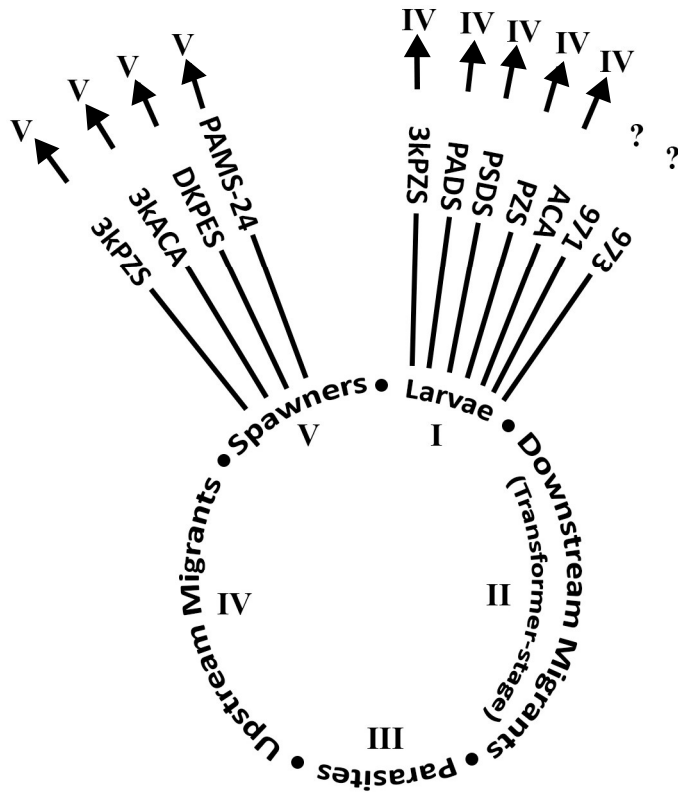
Figure 1.3 The sea lamprey life-cycle and associated pheromone components. The life-cycle stages are numbered I though V. Pheromone components released by a particular stage are seen branching from that stage. The Roman numeral of the life stage affected by each component is found branching from that component. "?" denotes currently unknown component target. Li *et al.* 2002 (3kPZS); Li *et al.* 2013 (DKPES); Brant 2015 (971, 973, and PAMS-24); Sorensen *et al.* 2005 (PSDS and PADS); Siefkes *et al.* 2003 (3kACA); Li *et al.* 1995 (PZS); and Bjerselius *et al.* 2000 (ACA).
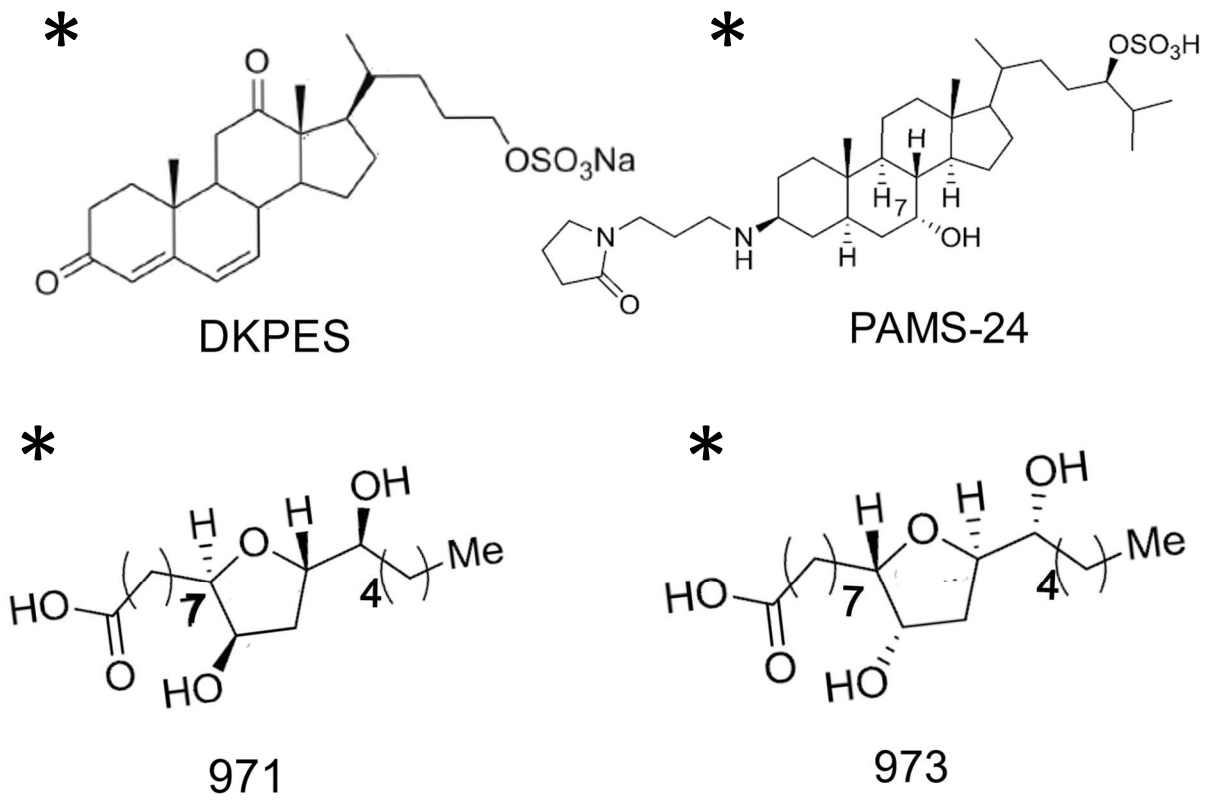
Figure 1.4a Elucidated chemical structures of putative sea lamprey migratory cues and male sex pheromone components. Putative pheromone components are denoted with '*' (Li *et al*. 1995, 2002, 2013; Bjerselius *et al*. 2000; Siefkes and Li 2004; Sorensen *et al*. 2005).

3kPZS

PZS

3kACA

ACA

PSDS

PADS
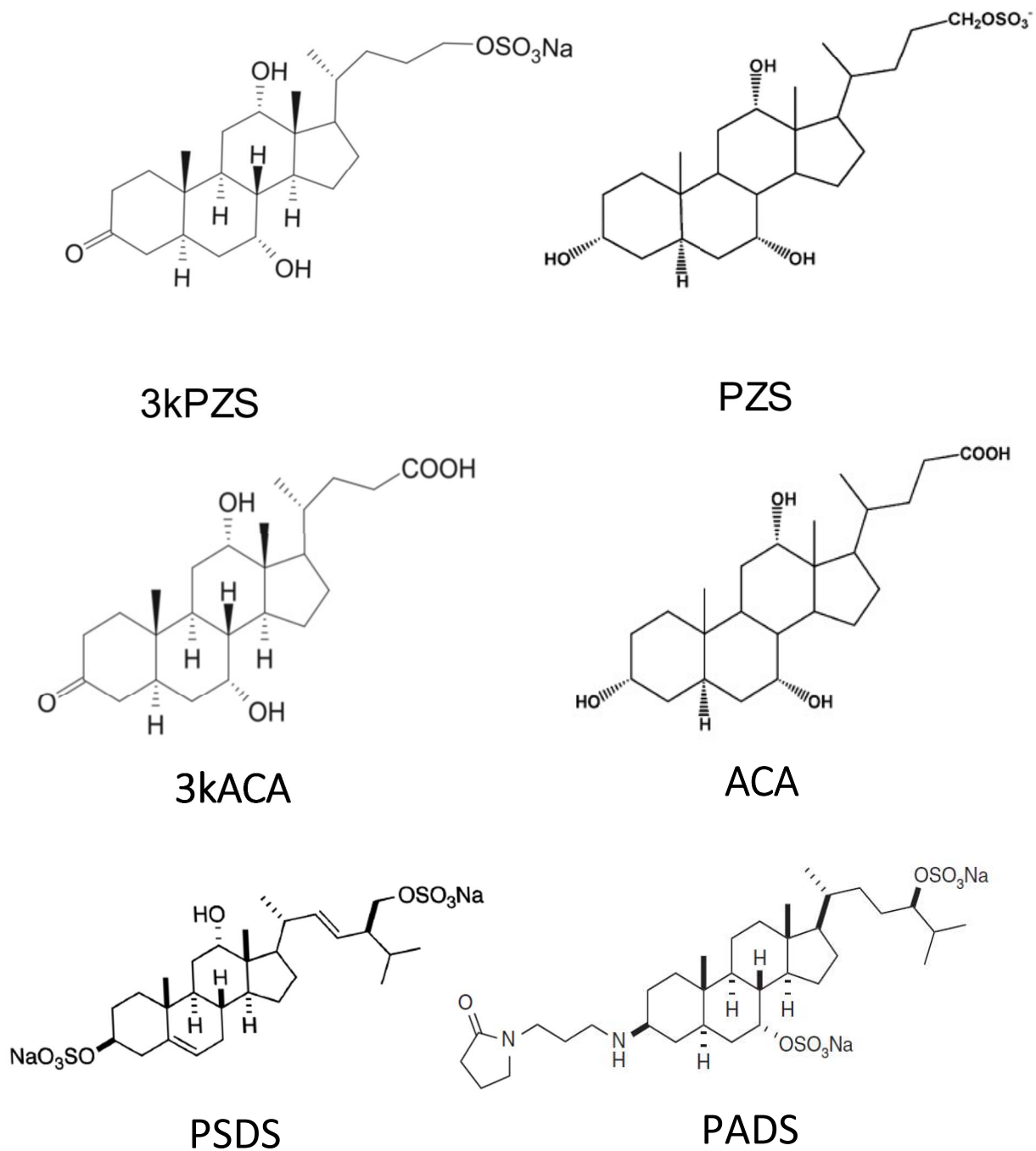
Figure 1.4b Elucidated chemical structures of known sea lamprey migratory cues and male sex pheromone components. (Li *et al*. 1995, 2002, 2013; Bjerselius *et al*. 2000; Siefkes and Li 2004; Sorensen *et al*. 2005).

CHAPTER 2 *CHARACTERIZATION OF OLFACTORY RESPONSES TO NOVEL PUTATIVE SEA LAMPREY (*Petromyzon marinus*) PHEROMONE COMPONENTS AND COMBINATIONS*

2.1. Introduction

2.1.1 Is there cellular specificity of olfactory sensory neuron responses to pheromones?

The peripheral olfactory organs of an organism house the repertoire of olfactory sensory neurons, within which, olfactory sensory reception occurs. Olfactory sensory neurons on the antennae of invertebrates (Tolbert and Hildebrand 1981; Christensen *et al*. 1995), olfactory sensory neurons within the main olfactory epithelium and vomeronasal organ of mammals (Shepherd and Greer 1998; Ma 2007), and olfactory sensory neurons within the olfactory epithelium of teleost fish (Ngai *et al.* 1993) express the odour receptors that bind their respective odour ligands to initiate sensory reception. While generalist olfactory sensory neurons that bind, and respond to a variety of odorants have been observed on the antennae of insects (Schneider 1969; Stengl *et al.* 1992) as well as on olfactory sensory neurons that project to specific glomeruli termed the necklace glomeruli of the mouse (Greer *et al.* 2016), olfactory sensory neurons in the main olfactory epithelium of mammals (Ressler *et al.* 1994; Vassar *et al.* 1994) as well as teleost fish (Speca *et al.* 1999; Laberge and Hara 2001) are known to express odour receptors which exhibit specificity to a single odorant or to a specific ligand group that can be present on several odorant molecules. In fish, the peripheral olfactory organ detects a number of chemical classes, including amino acids, gonadal steroids, nucleotides, bile acids, and prostaglandins (Hara 1994; Hara and Zielinski 2007). The olfactory sensory neurons expressing the complementary odour receptor protein for each of these odour classes are relatively more

organised in mammals in terms of zones of receptor expression when compared to fish (Ressler *et al*. 1993; Laberge and Hara 2001). In mammals, zones of receptor expression will overlap in the main olfactory epithelium, and a particular odour receptor may be expressed in several zones across the surface of the epithelium (Ressler *et al.* 1993; Buck 1996; Iwema *et al.* 2004; Miyamichi *et al.* 2005; Ma 2007). Conversely, odour receptors expressed by olfactory sensory neurons in fish are distributed stochastically throughout the olfactory epithelium (Speca *et al.* 1999; Laberge and Hara 2001). In all vertebrates, the axons of olfactory sensory neurons from the olfactory epithelium spread over the surface of the olfactory bulb and enter spherical regions of neuropil known as glomeruli. Spatial patterning of bulbar activity elicited by particular odour stimulants is referred to as chemotopy, and this has been observed in mammals (Johnson *et al.* 1998; Johnson and Leon 2007) as well as various fish species (Friedrich and Korsching 1997, 1998; Nikonov and Caprio 2001) and the sea lamprey (Green *et al.* 2017).

In sea lamprey, electrophysiological recordings by Green *et al.* (2017) have shown that the medial olfactory bulb region responds to amino acid, bile acid, and pheromone odorants. Conversely, odorant specificity was observed in nonmedial olfactory bulb regions, with the dorsal territory responding most readily to lamprey sex and migratory pheromone components while basic amino acids were best able to elicit responses from the lateral territory. Tract-tracing experiments have shown that these distinct olfactory bulb regions receive projections from olfactory sensory neurons that are scattered throughout the main olfactory epithelium (Green *et al.* 2017). Still to be determined is whether, in the case of bile acids for example, the individual epithelial olfactory sensory neurons responding to bile acids respond to all or to specific bile acids.

Olfactory sensory reception requires an odour ligand to successfully bind to a complementary odour receptor protein expressed by an olfactory sensory neuron. This binding initiates an intracellular, cyclic adenosine monophosphate second messenger cascade that sees an influx of extracellular calcium ions into the olfactory sensory neuron coupled with an efflux of chloride ions resulting in depolarization of the cell (Schild and Restrepo 1998; Firestein 2001). Calcium imaging is a technique which takes advantage of the calcium influx inherent in olfactory sensory neurons responding to successfully bound odour ligands to their odour receptors. Calcium imaging experiments have been employed in olfactory organ imaging studies of species including the mouse, *Mus musculus* (Leinders-Zufall *et al.* 1998; Wachowiak and Cohen 2001; Bozza *et al.* 2002), frog (Sansone *et al.* 2015), salamander, *Ambystoma tigrinum* (Firestein *et al.* 1991), and zebrafish, *Danio rerio* (Friedrich and Korsching 1997). This study represents the first use of calcium imaging techniques in the sea lamprey, thus the methods used were adapted from previous examinations of other animal models. This technique uses a calcium-sensitive dye that is loaded into the olfactory sensory neurons of interest prior to imaging taking place. The dye may potentially be naturally endocytosed into OSNs (Doving *et al.* 2009), however a solution of triton x-100 can be used to solubilize the cell membrane of OSNs to allow entry of the large dextran molecule (Frontini 2003). With the dye successfully loaded into the olfactory sensory neurons, the olfactory epithelium is exposed to an olfactory stimulus, resulting in the influx of calcium into responding olfactory sensory neurons that is bound by the dye. The binding of calcium dextran to calcium in responding cells results in those olfactory sensory neurons fluorescing, thus clearly indicating cell-specific responses to olfactory stimuli.

Calcium imaging experiments were utilized in the present study to test whether olfactory sensory neurons in the sea lamprey olfactory epithelium respond to a single, specific pheromone

component, or to multiple. Epithelial olfactory sensory neurons were loaded with fluorescent Calcium-Green dextran dye, and imaging experiments captured the change in fluorescence of olfactory sensory neurons responding to odorants of interest. These imaging experiments had a focus on investing the neurophysiological basis of the synergistic affect that male sex pheromone components 3,12-diketo-4,6-petromyzonene-24-sulfate (DKPES) and 3-keto petromyzonol sulphate (3kPZS) appear to display when eliciting increased behavioural responses in ovulating females upon their release as a mixture (Li *et al.* 2013). As such, 3kPZS and DKPES responses were examined individually as well as in a mixture to determine which olfactory sensory neurons are responding to each pheromone component based on the fluorescence observed upon application of each component onto the olfactory epithelium.

2.1.2   *Characterization of sea lamprey (Petromyzon marinus) olfactory bulb responses to novel pheromone candidate molecules*

To effectively manage the invasive sea lamprey populations of the Laurentian Great Lakes, abatement strategies utilizing pheromones to disrupt migration and reproduction of sea lampreys while leaving other organisms unaffected are being investigated (Li *et al.* 2013; Brant 2015). To ensure the effectiveness of these strategies, knowledge of how potent these pheromones are at eliciting predictable behavioural responses in lampreys is essential. Recently, several putative male sex pheromone and larval migratory pheromone components have been elucidated including 3,12-diketo-4,6-petromyzonene-24-sulfate (DKPES), (+)9,(12)-oxy-10,13-dihydroxystearic acid (973), (-)9,(12)-oxy-10,13-dihydroxystearic acid (971), and petromyzonamine-24-monosulfate (PAMS-24) (Li *et al.* 2013; Brant 2015). Still to be robustly

determined however, is the relative effectiveness of these molecules at stimulating and maintaining neural activity in the olfactory epithelium and olfactory bulbs of these animals.

Each of the sea lamprey pheromone components elucidated to date have been applied to the main olfactory epithelium, where electro-olfactogram recordings have been taken to verify that each putative pheromone component was detectable at this level of the olfactory system and that the animal can in effect 'smell' these compounds (Li *et al*. 1995, 2002; Bjerselius *et al*. 2000; Siefkes *et al*. 2003; Sorensen *et al*. 2005). Detection at the level of the olfactory epithelium does not however, test for the response in the brain. Olfactory bulb recordings yielding local field potential (LFP) responses to olfactory stimuli have been used to determine whether an olfactory stimulus is detectable at the level of the organism's brain, thus indicating the likelihood that the stimulus is being processed here (Green *et al.* 2013; Li *et al*. 2013). The LFPs being produced are not necessarily the result of afferent action potentials, but rather the summed OSN, projection neuron, and associated interneuron synaptic activity.

The current study employed the use of LFP recordings from the olfactory bulb to help bridge the gap between existing olfactory epithelium response data and behavioural response data reported for sea lamprey pheromone components and expand olfactory bulb investigations by Green *et al.* (2017). As well, this work hopes to inform the implementation of newly elucidated putative pheromone components for sea lamprey population management strategies.

To better understand how putative pheromone odorants PAMS-22, 971, 973, and DKPES are physiologically detected by sea lamprey, LFP recordings were taken from both dorsal and lateral olfactory bulb regions. Additionally, in an attempt to determine the neurophysiological basis for the observed synergy between 3-keto petromyzonol sulphate (3kPZS) and DKPES with regard to stimulating behavioural output (Li *et al*. 2013), each of these pheromone components

was applied individually and in a mixture (DKPES:3kPZS 2:29.8) to identify potential synergistic affects as indicated by significantly different LFP peak amplitudes. Detection thresholds of various pheromone components represent useful information for population control efforts and as such, an aim of this study was to explore the olfactory bulb detection thresholds of migratory and sex pheromone components.

2.2 Materials and Methods

2.2.1 Experimental animals

Larval and transformer-stage (post-metamorphic stage seven) sea lamprey from the Connecticut River, Turner Falls, MA were collected and supplied by United States Geological Survey Conte Anadromous Fish Research Laboratory in the fall of 2015 and 2016. Spawning-stage sea lamprey were collected from Hammond Bay Biological Station, MI in the spring of 2015 and 2016. Sea lamprey were held at the University of Windsor at $6°C \pm 1°C$ in 420 L aquaria under static renewal conditions until used. All animal holding and experiments were conducted according to the University of Windsor Animal Care Committee (AUPP 14-05) under the Canadian Council on Animal Care.

2.2.2 Odorant test solutions

The test solutions included negative and positive control odorants, as well as pheromone test solutions. As a positive control for amino acids detection, stock solutions were prepared, then diluted to 10^{-4} M for both calcium imaging and olfactory bulb recordings. A stock solution of 10^{-2} M L-histidine or L-Arginine (Sigma-Aldrich, Oakville, ON, Canada; H-8000) used as a standard odour (Li and Sorensen 1992) was prepared on the day of experimentation in chilled

lamprey Ringer's solution. Immediately prior to experimentation, a serial dilution was made to a final concentration of 10^{-4} M L-histidine or L-arginine in chilled lamprey Ringer's solution.

All test lamprey pheromone components utilized were received in powder form from Dr. Weiming Li (Michigan State University, MI, USA) on 13 Febuary 2015 and 12 August 2016. Stock solutions of the pheromones were made by reconstituting each pheromone in a 1:1 solution of high purity methanol:ultra-pure water to 1 mg mL^{-1} and stored in aliquots at -80°C. A vehicle control of 0.0025% methanol (equivalent to the amount of methanol expected in 10^{-6} M pheromone solution) was tested on the olfactory bulb preparation used for recordings. Aliquots of 10^{-5} M pheromone components were made in chilled lamprey Ringer's solution from which working pheromone solutions were made immediately prior to experimentation via serial dilutions in chilled lamprey Ringer's solution. Li et al. (2013) determined electro-olfactogram response threshold for DKPES and 3kPZS was 10^{-7} M and 10^{-10} M, respectively, for sexually mature spawning sea lamprey, with behavioural responses to 3kPZS and a ratio of DKPES:3kPZS occurring at 10^{-13} M. Therefore, 10^{-7} M 3kPZS, 10^{-8} M DKPES, 2:29.8 DKPES:3kPZS with DKPES at 10^{-8} M and 3kPZS at 10^{-7} M were used in experiments comparing OSN and olfactory bulb responses to 3kPZS and DKPES individually and in a mixture. All other pheromone concentrations utilized for imaging experiments did not fall below the 10^{-13} M behavioural threshold nor the electro-olfactogram thresholds for each component (Table A-1) with 10^{-7} M being the concentration that pheromone components were typically diluted to prior to testing. Pheromone components to be employed during olfactory bulb experiments were serially diluted, beginning at 10^{-6} M, down to threshold during threshold experiments. A standard dilation series ranging from 10^{-13} M up to 10^{-6} M (for transformers) and 10^{-12} M up to 10^{-6} M (for adults) was also prepared for those sets of experiments.

2.2.3 Loading dye into olfactory epithelium for calcium imaging

To observe the response characteristics of individual olfactory epithelial OSNs when exposed to single odorants and odorant mixtures, the fluorescence changes occurring during OSN responses needed to be measured. Calcium imaging experiments involved loading OSNs with Calcium-Green dextran (3000 MW, Invitrogen, Eugene, OR). To load the olfactory epithelium, the sea lamprey to be used in the imaging experiment was taken from its holding aquarium and anesthetized (0.03% tricane methanesulfonate, pH 7.4; Sigma-Aldrich, Oakville, ON, Canada). Once unresponsive, the individual was removed from the anesthetic and the nasal pore was dried. A needle and syringe were then used to carefully deposit a mixture of Calcium-Green dextran crystals and 0.1% triton x-100 (in deionized water) into the nasal pore before allowing a 5-minute rest period to allow the dye to dissolve in the nasal cavity. Chilled (8-10°C) and oxygenated Ringer's solution (130 mM NaCl, 2.1 mM KCl, 2.6 mM CaCl2, 1.8 mM MgCl2, 4 mM HEPES, 4 mM dextrose, 1 mM NaHCO3, pH 7.4) was applied to the gills intermittently during this rest period. As an experimental technique that was adapted and improved during this study, later loadings of the olfactory epithelium involved a 5-minutes rest period in a solution of dechlorinated water odorized with L-arginine immediately following the 5-minute dry rest period (Doving *et al.* 2011). The individual was then returned to the holding aquaria for at least 48 h (Daghfous G, *Pers. Comm.*) to allow for complete loading of the dye prior to dissection and imaging.

2.2.4 Calcium imaging preparation of olfactory neurons

Following the 48-hour incubation period, the dye loaded sea lamprey was anesthetized (0.03% tricane methanesulfonate, pH 7.4; Sigma-Aldrich, Oakville, ON, Canada) and

decapitated at the 3rd branchiopore. The head region was submerged in chilled and oxygenated

lamprey Ringer's solution (130 mM NaCl, 2.1 mM KCL, 2.6 mM $CaCl_2$, 1.8 mM $MgCl_2$, 4 mM

HEPES, 4 mM dextrose, 1 mM NaHCO3; pH 7.4) that was replaced every 5-10 min during the

dissection. The sample was placed dorsal side up, allowing removal of muscle and cartilage to

expose the brain, olfactory nerve, nasal cavity, and olfactory epithelium. The ventral region of

the nasal cavity, containing the olfactory epithelium was then removed and prepared as a flat

mount, securely pinning and orienting the epithelium to face the inflow (Figure 2.1), taking care

not to contact the lamellae. In a custom-built perfusion dish on a microscope stage, the olfactory

epithelium had cooled, oxygenated Ringer's solution perfused over its surface and odorants were

applied intermittently, into the perfusate.

2.2.5 Calcium image acquisition

A Nikon Eclipse 800 epifluorescence microscope equipped with 10X to 40X objectives

(water immersion lens) and with a fluorescein isothiocyanate excitation/emission filter set was

used to monitor calcium responses of labeled cells (fluorophore excitation/emission was 506/531

nm) (Figure 2.1). The light emitted was captured with an intensified CCD video camera

(Photometrics CoolSNAP HQ; Roper Scientific, Tucson, AZ) and recorded (~1.5 frames per s),

using Metafluor imaging software (Molecular Devices, Sunnyvale, CA) (Figure 2.2). To

characterise the Ca^{2+} responses quantitatively for comparison, they were expressed as relative

changes in fluorescence $\Delta F/F\%$ and areas ($\Delta F/F \bullet s$) and compared between cells and stimuli

(Viana Di Prisco *et al*. 1997, 2000; Smetana *et al*., 2007, 2010; Brocard *et al*., 2010; Derjean *et

al*., 2010). Forskolin, an activator of adenylyl cyclase (Frings and Lindemann 1991; Leinders-

Zufall *et al.* 1997; Wong *et al.* 2000), was used as a positive control for calcium imaging

experiments at a concentration of 10^{-6} M. Adenylyl cyclase catalyzes the production of cyclic AMP, a second messenger that binds to cyclic nucleotide-gated channels through which calcium enters a responding cell, thus resulting in a calcium influx and eventual increase in cellular fluorescence. As a negative control, the neutral amino acid L-serine was applied to the olfactory epithelium where OSNs failed to respond, as also observed by Li (1995) during electro-olfactogram recordings of the olfactory epithelium upon exposure to L-serine. Larvae were used during initial imaging experiments as the larval life-stage has been found to have the greatest density of OSNs, thus increasing the probability of detecting a fluorescing OSN within the imaging field of view (Vandenbossche *et al.* 1995).
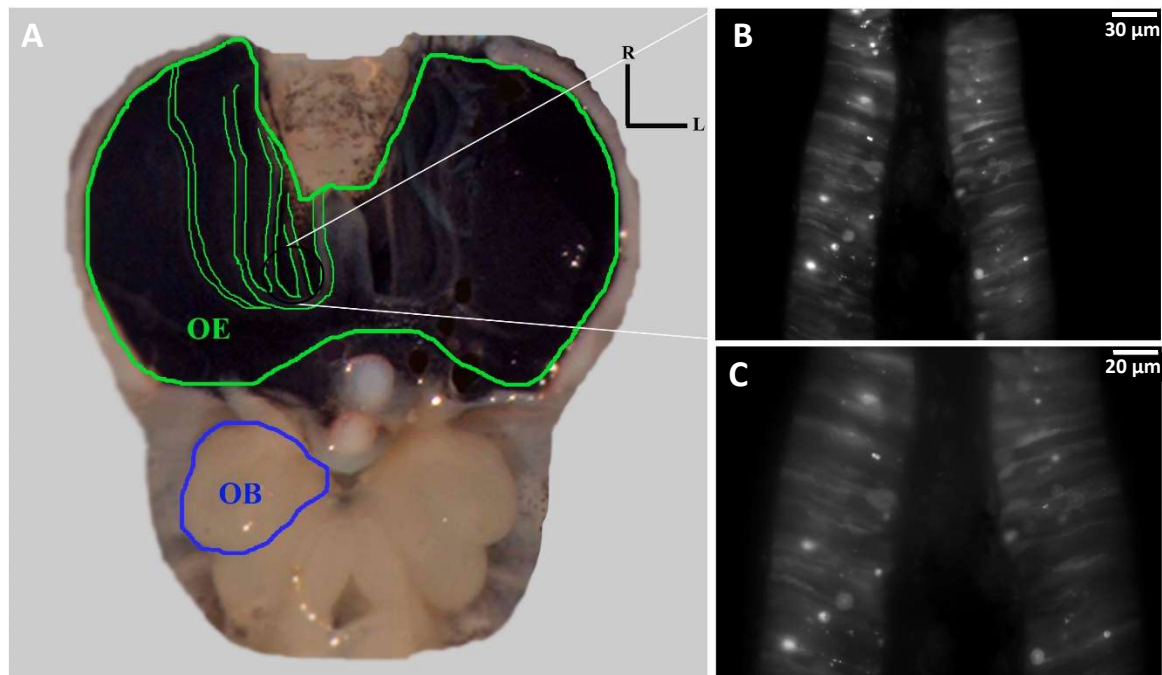
Figure 2.1 Calcium green dextran loading of sea lamprey olfactory sensory neurons. (A) The ventral olfactory epithelium (OE) with lamellar edges traced. Also visible are the olfactory

bulbs (OB) (blue trace). (B) Calcium green dextran-loaded transformer-stage olfactory sensory neurons situated along lamella. (C) Calcium green dextran-loaded cells.
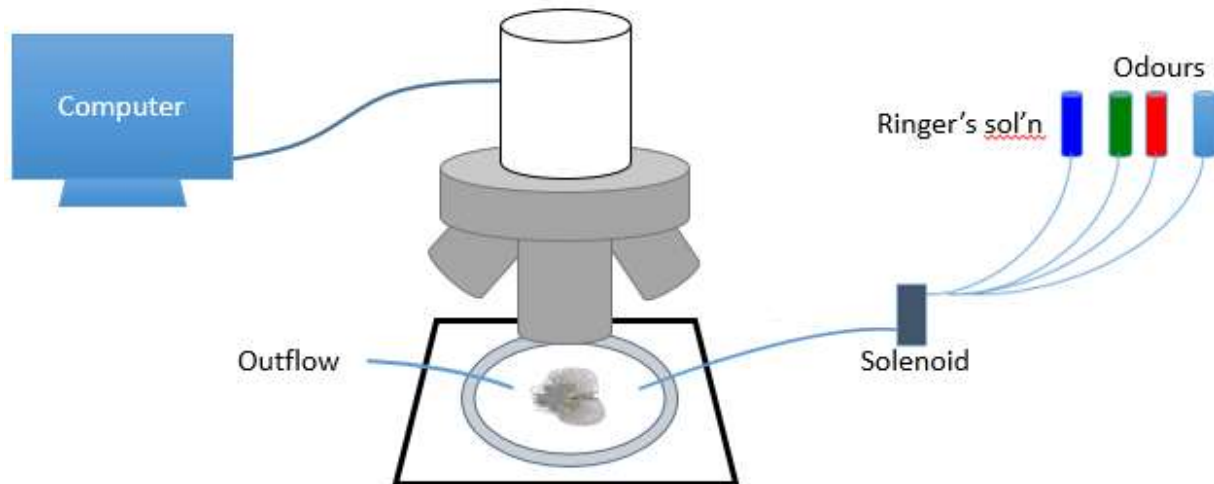
Figure 2.2 An illustration of the odorant application setup for the calcium imaging experiments. The perfusion fluid for the custom-made delivery system was kept cool with the use of a chiller. A custom-designed 3-way solenoid valve allows for rapid and accurate switching between a constant chilled-Ringer drip and any of the chilled odours onto the epithelium. Upon exposure to stimulatory solutions, fluorescence changes were captured from the olfactory epithelium via an intensified CCD video camera.

2.2.6 Electrophysiology setup

To determine if odorant and odorant mixture sensory information from OSNs of the olfactory epithelium was being relayed to the olfactory bulb, LFP responses were recorded from the dorsal region of the olfactory bulb in response to various odorant applications to the olfactory epithelium. The electrophysiological recording rig and subsequent recording protocol, developed by Green *et al.* (2013, 2017) employed a 9-chamber odour delivery system that also simultaneously chilled the odorants to be tested as well as the background medium (Ringer's solution) before delivering any of these preparations to the olfactory epithelium (Figure 2.2). Over the course of each experiment conducted using this setup, background Ringer's solution

was continuously perfused over the olfactory epithelium which was accomplished using a gravity-fed, valve-controlled odour delivery system. All Ringer's and odours applied were constantly vacuumed out of the recording chamber opposite to the inflow site. In order to switch between the background Ringer's solution to any of the experimental odorants, without interruption in flow or changes in naris pressure, a Dell computer controlled and electronically triggered three-way solenoid valve was used.

2.2.7 Ex-vivo olfactory bulb recording preparation

All samples and solutions were prepared immediately prior to neural recordings. Prior to dissection, sea lamprey were anesthetized (0.03% tricane methanesulfonate, pH 7.4; Sigma-Aldrich, Oakville, ON, Canada) and then decapitated at the 3rd branchiopore. The anterior tissue was submerged in chilled and oxygenated lamprey Ringer's solution (130 mM NaCl, 2.1 mM KCL, 2.6 mM CaCl$_2$, 1.8 mM MgCl$_2$, 4 mM HEPES, 4 mM dextrose, 1 mM NaHCO3; pH 7.4) that was replaced every 5-10 min throughout the dissection.

To begin the dissection, the removed anterior tissue was placed ventral side up and a cut made along the gill pores allowing the removal of the ventral tissue down to the level of the buccal cavity and nasopharyngeal pouch. The sample was then placed dorsal side up, allowing removal of muscle and cartilage to expose the brain (including olfactory bulbs), olfactory nerve and nasal cavities. A cut was made at the most rostral portion of the spinal cord and the olfactory epithelium was kept intact in order to detect delivered odours. The sample preparation was then placed on a chilled plate at 10°C and submerged in Ringer's solution (Figure 2.3). Neural recordings were taken 1 h post dissection to allow for tissue to recover.
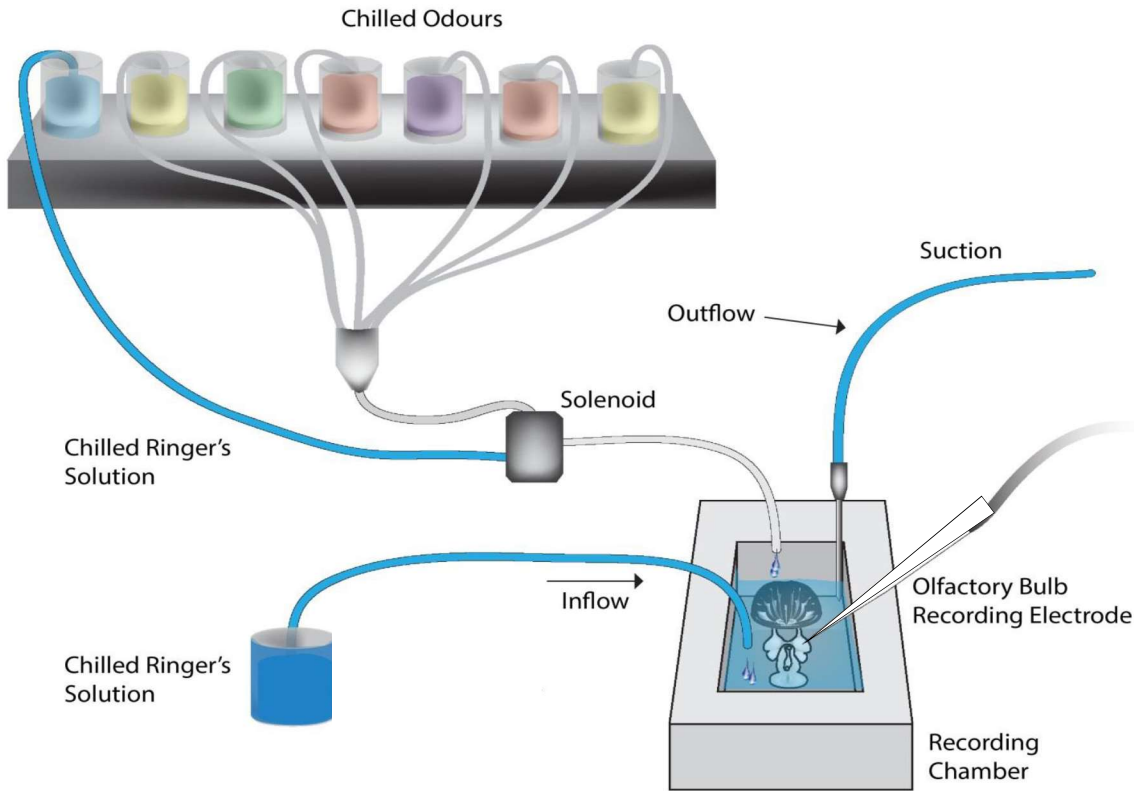
Figure 2.3 An illustration of the odorant application setup for the LFP recording experiments. The odours are stored in a custom-made delivery system and kept cool with the use of a chiller. A 3-way solenoid valve allows for rapid and accurate switching between a constant chilled-Ringer drip and any of the chilled odours onto the epithelium. Upon exposure to an odour, LFP's will be recorded from the OB while EOG recordings will be taken from the olfactory epithelium via a recording electrode, with a reference electrode being placed on the surface skin near the naris of the sea lamprey. Green *et al.* (2013, 2017).
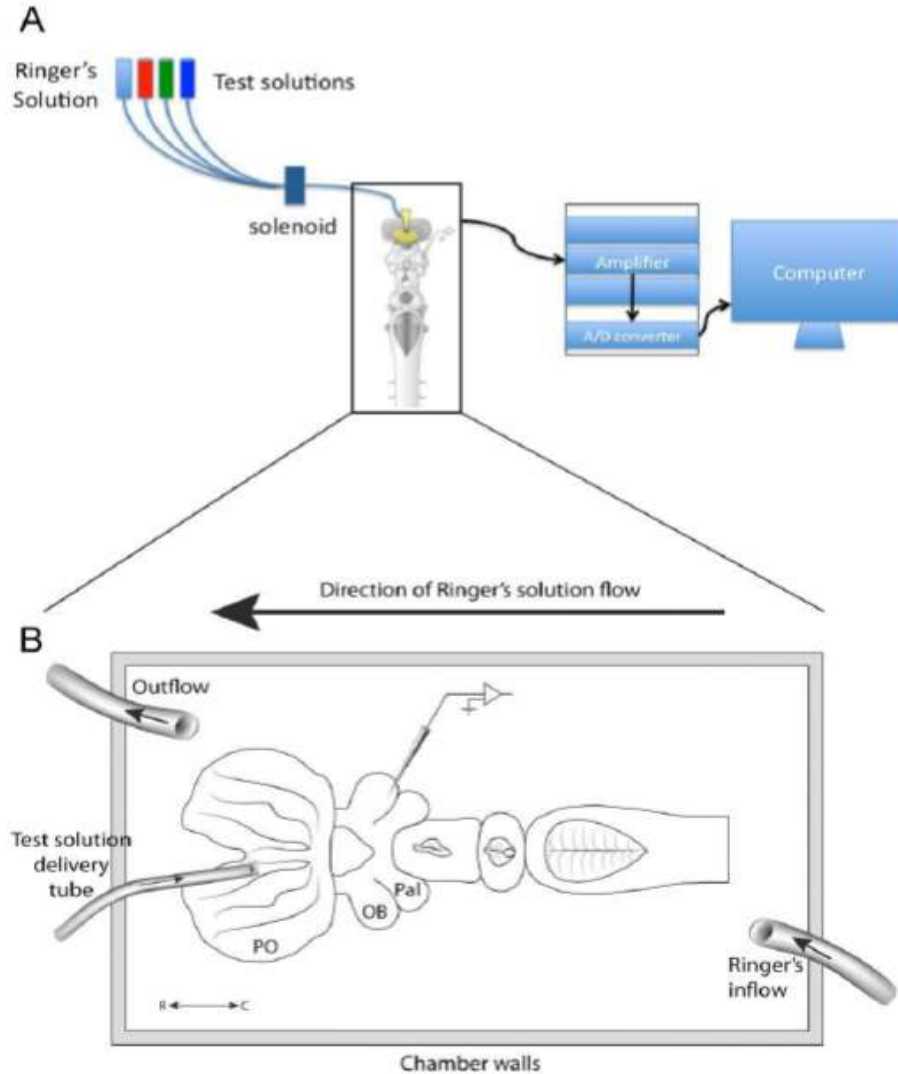
Figure 2.4 A diagram of the odour delivery apparatus (A) and recording chamber (B) containing the ex-vivo sample preparation. As illustrated, following the dissection, the peripheral olfactory organ (PO), olfactory bulb (OB), and pallium (Pal) are exposed and kept intact for the neural recordings that are read through an electrode placed on the surface of the OB. The electrode is in turn connected to an amplifier which passes the information on to an A/D converter before being displayed and stored on a connected computer. Green *et al.* (2013, 2017).

2.2.8 Local field potential recordings

Following experimental protocol as established by Green *et al.* (2013, 2017), during each

recording, all olfactory-stimulating molecules examined were delivered to the olfactory

epithelium between 3-6 times in two second pulses in addition to the intermittent delivery of a negative control (either Ringer's solution or a 10^{-4} M L-glutamine/L-serine mixture) applied to the lateral region and a positive control applied to the lateral region (10^{-4} M L-arginine). Between each unique odour delivery, lamprey Ringer's solution was delivered via the odour delivery tube in 10 second pulses until LFP responses ceased. To obtain the extracellular LFPs in the olfactory bulb, a glass micropipette (World Precision Instruments, Inc., Sarasota, FL, 1.0mm) pulled to an 5-10 μm tip diameter filled with 2M NaCl (0.1 MΩ impedance) was used. Silver wires were used to connect the micropipette to a headstage and the headstage-amplifier circuit was grounded and referenced using silver wires placed in the recording bath, that were then connected to the headstage. The signals obtained were filtered between 1 Hz and 1 kHz, before being amplified 10,000 times and then subsequently digitized at 10 kHz (Powerlab 4/30, model ML866, ADInstruments, Colorado Springs, CO, USA) (Green *et al.* 2013). In order to ensure an acceptable signal to noise ratio, spikes were viewed online during recording and subsequently analyzed offline to assess spike frequency, amplitude, and duration during odour delivery using LabChart software (version 6.1.3, ADInstruments).

For each recording, the 5 second pre-odour stimulus baseline was used to generate a baseline mean and standard deviation for each odorant response analyzed. Only responses with peak amplitudes that exceeded a value 3 times greater than the baseline standard deviation were considered to be odour-evoked responses and included in further analyses. The basic amino acid L-arginine was employed as a positive control for electrophysiological recordings taken from the olfactory bulb as this odorant functioned well in eliciting LFP responses while the neutral amino acid L-serine failed to elicit LFP responses and thus worked well as a negative control.

2.3 Results

2.3.1 *Olfactory sensory neuron responses to odorant stimuli*

To determine the response characteristics of OSNs to odorants presented to the olfactory epithelium both individually and as mixtures, calcium dextran-loaded OSNs were imaged during odorant application. Forskolin, a stimulator of adenylyl cyclase (Frings and Lindemann 1991; Leinders-Zufall *et al.* 1997; Wong *et al.* 2000), was used as a positive control (Figure 2.5a). The responses elicited by forskolin (Figure 2.5a) support the suggestion that these OSNs are employing G-protein receptors using a cyclic AMP-second messenger (Buck and Axel 1991). The neutral amino acid, L-serine, which is not an odorant to the lamprey olfactory system (Li 1994), failed to elicit OSN responses by calcium imaging (Figure 2.5b).
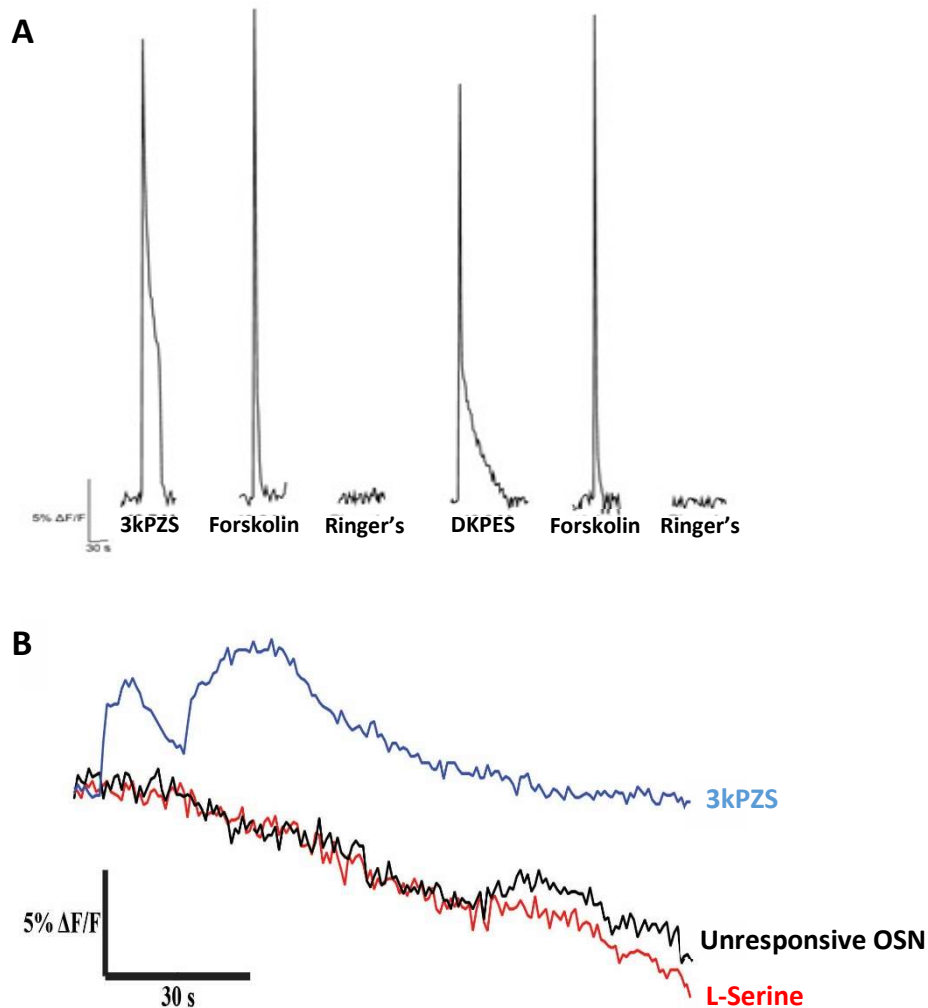
Figure 2.5 Positive and negative controls used in calcium imaging experiments. (A) Calcium transients of transformer-stage olfactory sensory neuron responses to odorant applications of 10^{-7} M 3kPZS and 10^{-6} M forskolin (positive control) compared to background (ringer's solution) baseline (left 3 transients), and odorant applications of 10^{-8}M DKPES and 10^{-6} M forskolin compared to background (ringer's solution) baseline (right 3 transients). All odorants were applied to the same olfactory epithelium preparation and each transient (produced by separate OSNs) begins at odorant stimulus offset. (B) Calcium transients of olfactory sensory neuron responses to odorant applications of 10^{-7} M Serine (red trace; negative control), 10^{-11} M 3kPZS (blue trace), and an unresponsive OSN (black trace). All odorants were applied to the same olfactory epithelium preparation and each transient (produced by separate OSNs) begins at odorant stimulus offset. Data from panel A provided by Michelle Farwell.

2.3.2 Olfactory sensory neuron discrimination between odour classes

Olfactory sensory neuron response specificity was examined at the level of pheromone and amino acid odour class discrimination. Larval olfactory sensory neurons, in a semi-intact preparation, exhibited response specificity upon exposure to a pheromone component mixture
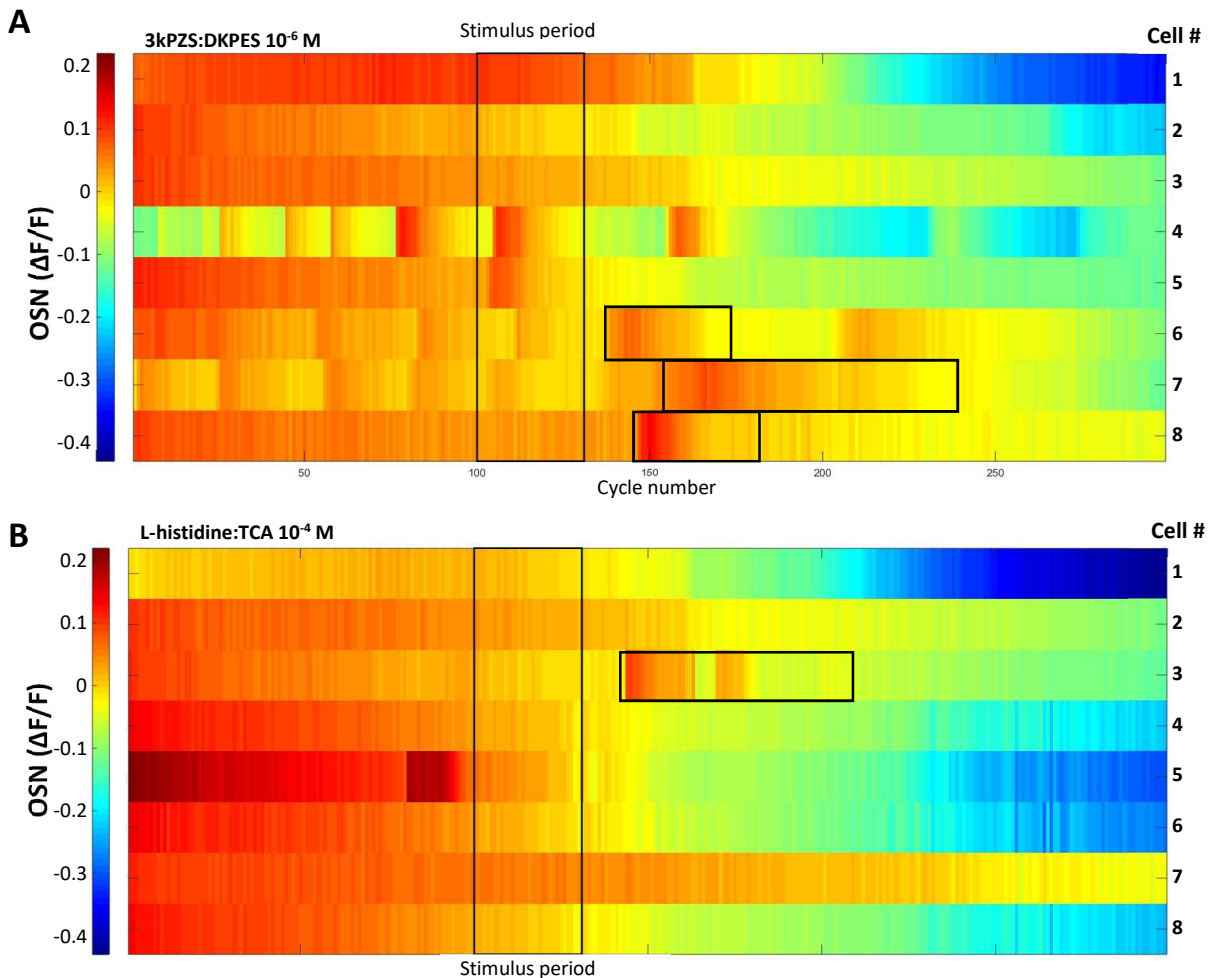
Figure 2.6 OSN discrimination between pheromone and amino acid mixtures. Changes in fluorescence of eight larval-stage olfactory sensory neuron responses to a pheromone component mixture (A), and an amino acid/bile acid mixture (B). The 8 olfactory sensory neurons depicted in panel A (cell number shown on y-axis) are the same as those in panel B (cell number shown on y-axis; on right of figure) and were imaged from the same preparation (n=1). Each row represents a distinct, recorded olfactory sensory neuron and fluorescence peaks, representing responses, are boxed. Blue colouration indicates lower fluorescence emission while red indicates higher emission. The stimulus period, during which each odorant mixture was applied, is indicated by a vertical box across all cells. Data provided by Michelle Farwell.

and an amino acid/bile acid mixture once imaged to detect changes in fluorescence emission in response to the mixtures applied (Figure 2.6). This odour class response specificity was also observed during calcium imaging experiments conducted on transformer stage sea lamprey exposed to the same amino/bile acid and pheromone component mixtures (see Appendix; Figure A-3). Olfactory sensory neurons that were observed fluorescing in response to the stimuli presented (illustrated by a sharp change from blue/green/yellow to orange/red, and then back to the pre-response colour), responded to only one of the two odorant mixtures (Figure 2.6). These neurons appeared to exhibit specificity in terms of odorant ligand binding among amino and bile acid mixtures.

2.3.3 Olfactory sensory neurons respond to specific pheromone components

Individual odorants were applied to 24 preparations of transformer stage olfactory epithelia with 137 separate cells responding (see Appendix; Figure A-7). The cells showed specificity in response upon exposure to various sets of single odorants including male sex pheromone components 3kPZS and DKPES (Figure 2.7). Ten preparations of olfactory epithelia were exposed to each pheromone component individually, then together in a mixture, eliciting responses from 23 olfactory sensory neurons (Figure 2.8). None of the responding olfactory sensory neurons were observed responding to both 3kPZS and DKPES, thus showing response specificity at the level of these individual pheromone components (Figures 2.7 and 2.8). Additionally, cells seen fluorescing to an individual pheromone component (ie. 3kPZS or DKPES) were observed responding again to a 3kPZS:DKPES mixture (Figure 2.7). The average fluorescence peak values produced by the olfactory sensory neurons (Figure 2.8) responding to a standard set of odorants including 10^{-7} M 3kPZS, 10^{-8} M 3kPZS, 10^{-8} M DKPES, and a DKPES:3kPZS mixture (10^{-8} M:10^{-7} M) are illustrated in Figure 2.9. The differences between

the fluorescence values elicited by each odorant were not determined to be statistically

significant ($f = 2.33013$, $p = 0.060427$).
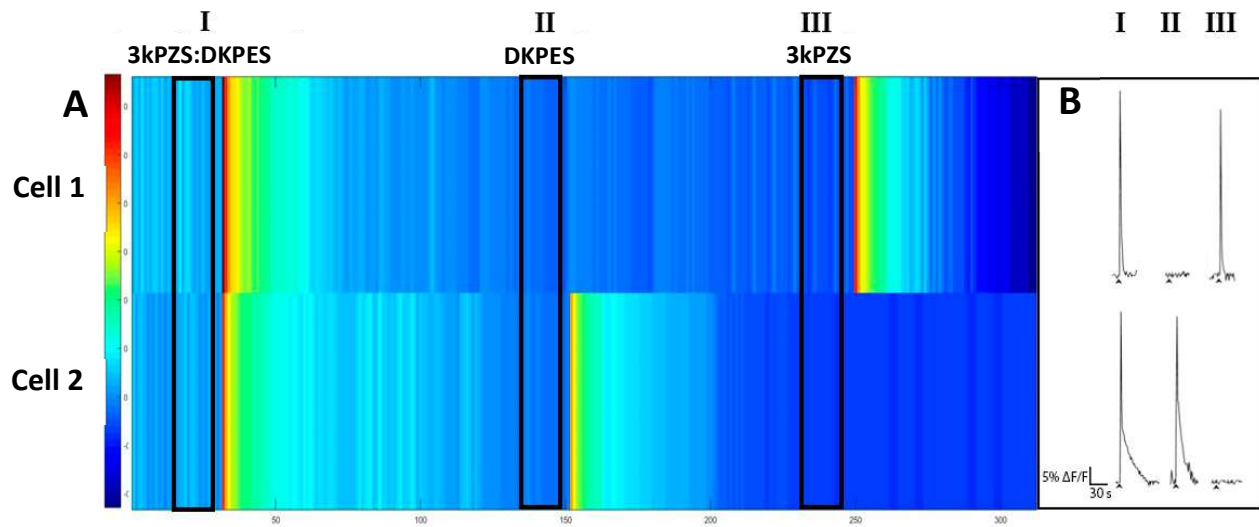
Figure 2.7 OSN fluorescence peak response patterns to 3kPZS and DKPES. Fluorescence emission from two transformer-stage olfactory sensory neurons, (1) and (2), in response to a mixture of 10^{-7} M 3kPZS:10^{-8} M DKPES (I), 10^{-8} M DKPES (II), and 10^{-7} M 3kPZS (III). Olfactory sensory neuron responses to stimuli are illustrated by vertical bands of red/orange appearing after 20 second long stimulus periods (preceding boxed area), before returning to a baseline level of fluorescence (blue). (B) Calcium transients of the responses depicted in (A). Data provided by Michelle Farwell.
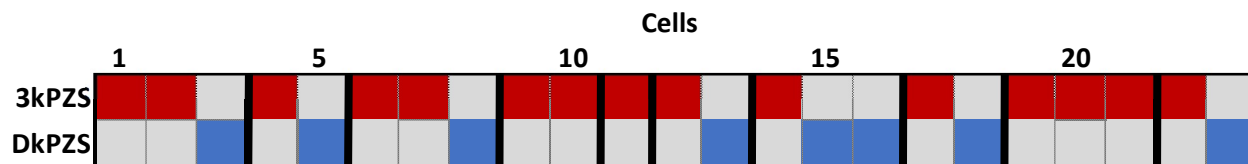
Figure 2.8 OSNs show specificity in response to 3kPZS and DKPES. An overview of transformer-stage epithelial preparations (n=10) exposed to 3kPZS and DKPES pheromone components. Each column represents a single olfactory sensory neuron, and columns grouped together by a heavier outline belong to the same preparation. Positive responses are represented by red (3kPZS) and blue (DKPES) boxes, tested odorants not responded to by a particular cell are represented by gray boxes, while untested odorants are represented by white boxes.
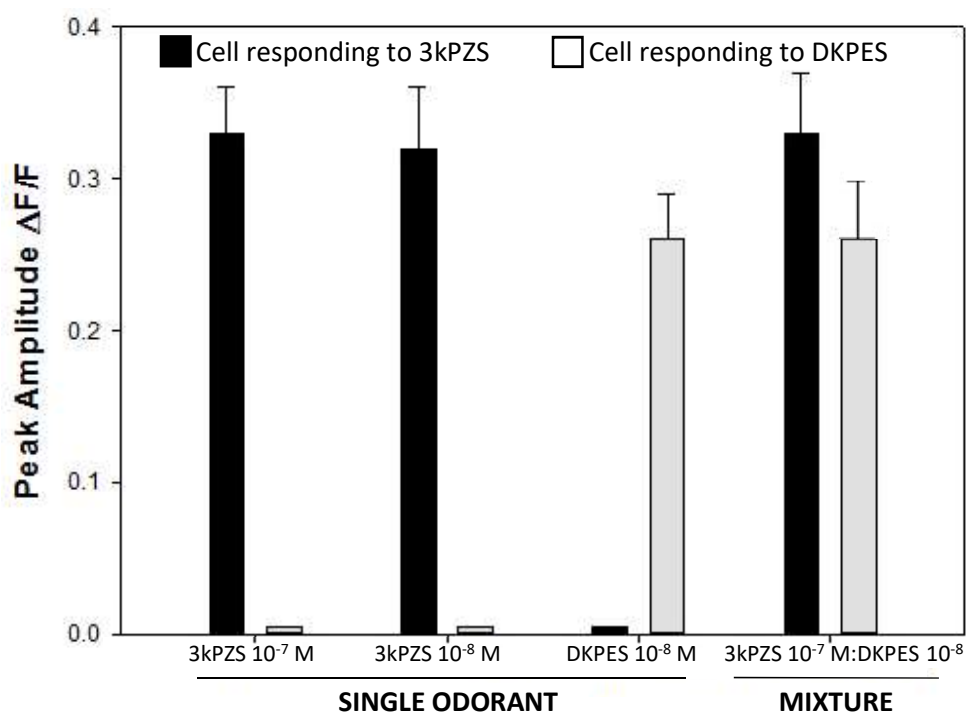
Figure 2.9 OSNs discriminate between 3kPZS and DKPES when applied as single odorants and a mixture. Average maximum peak fluorescence amplitudes produced by 23 separate transformer-stage olfactory sensory neurons over 10 preparations (n=10) of transformer stage sea lamprey epithelium. Each cell was exposed to 10^{-7} M 3kPZS, 10^{-8} M 3kPZS, 10^{-8} M DKPES, and a 10^{-7} M 3kPZS:10^{-8} M DKPES mixture. The fluorescence emission values were recorded. Cells which responded to either isolated 3kPZS concentration were classified as 3kPZS responding cells (black bars) while DKPES responding cells are represented by light gray bars for each comparison of peak fluorescence amplitudes produced by each odorant or mixture. The peak levels of fluorescence are determined by dividing the delta fluorescence by the average for a particular cell. Differences in average fluorescence peak values between odorants were not determined to be significant ($f = 2.33013$, $p = 0.060427$).

Other pairs of pheromone components were tested for specificity from olfactory sensory neurons. Putative larval migratory cues 971 and 973, enantiomers sharing the same chemical formula and mirrored structures, were delivered to two transformer stage preparations of olfactory epithelia. Each odorant was delivered individually and as a mixture, resulting in 25 cells responding to one of 971 or 973 over the two preparations. Looking at the traces identifying the cells that responded to each odour (Figure 2.10), none of the responding cells from these preparations fluoresced to both 971 and 973 odorants as seen by absence of both a yellow and magenta trace around any one cell. Furthermore, analysis of olfactory sensory neurons responding to each odorant applied revealed a number of instances involving a cell responding to one of the individual 971 or 973 odorants as well as the mixture when it was applied. One such instance is illustrated in Figure 2.11 with a 971-responding cell (outlined in blue; Figure 2.11a) producing fluorescence peaks (blue trace; Figure 2.11d) in response to applications of 10^{-7} M 971 and a 10^{-7} M 971:10^{-7} M 973 mixture. It is important to note that this cell, having responded to the 971 odorant applications, did not respond to an application of 10^{-7} M 973 (Figure 2.11d). Looking at the 973-responding cell (outlined in red; Figure 2.11a), a similar response pattern is observed with fluorescence peaks (red trace; Figure 2.11d) produced by this cell in response to odorant applications of 10^{-7} M 973 and a 10^{-7} M 971:10^{-7} M 973 mixture. None of the 25 cells
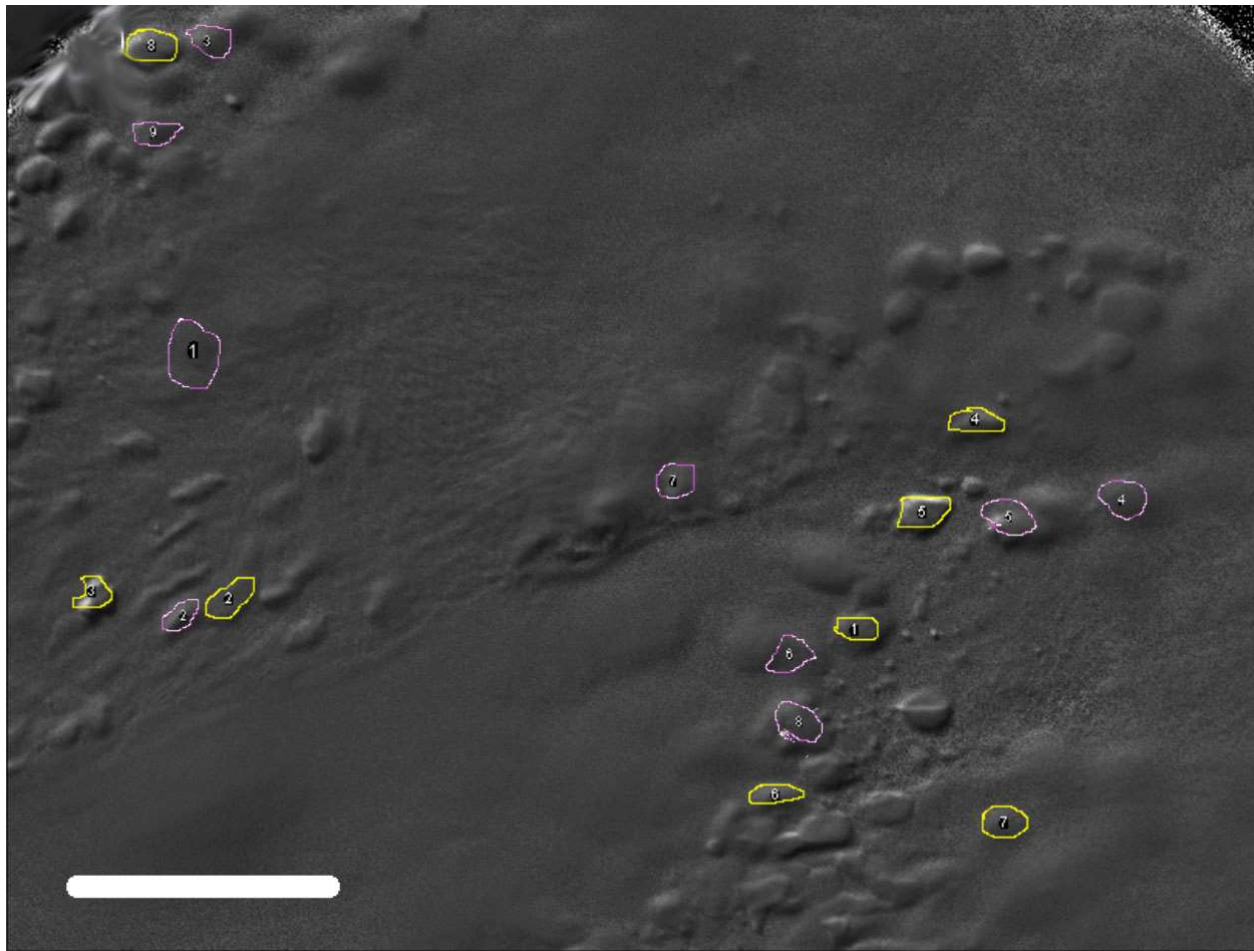
Figure 2.10 Location of transformer-stage OSNs responding to 971 and 973. The transformer-stage olfactory epithelium preparation image shown was taken from an image stack generated during the calcium imaging experiment and subsequently filtered using imageJ software. Two sets of superimposed regions of interest encompassing olfactory sensory neurons responding to 10^{-7} M 971 (yellow traces) and 10^{-7} M 973 (magenta traces; two regions have been cropped) during separate applications of each odorant onto the same olfactory epithelium. Scale bar, 60 μm.
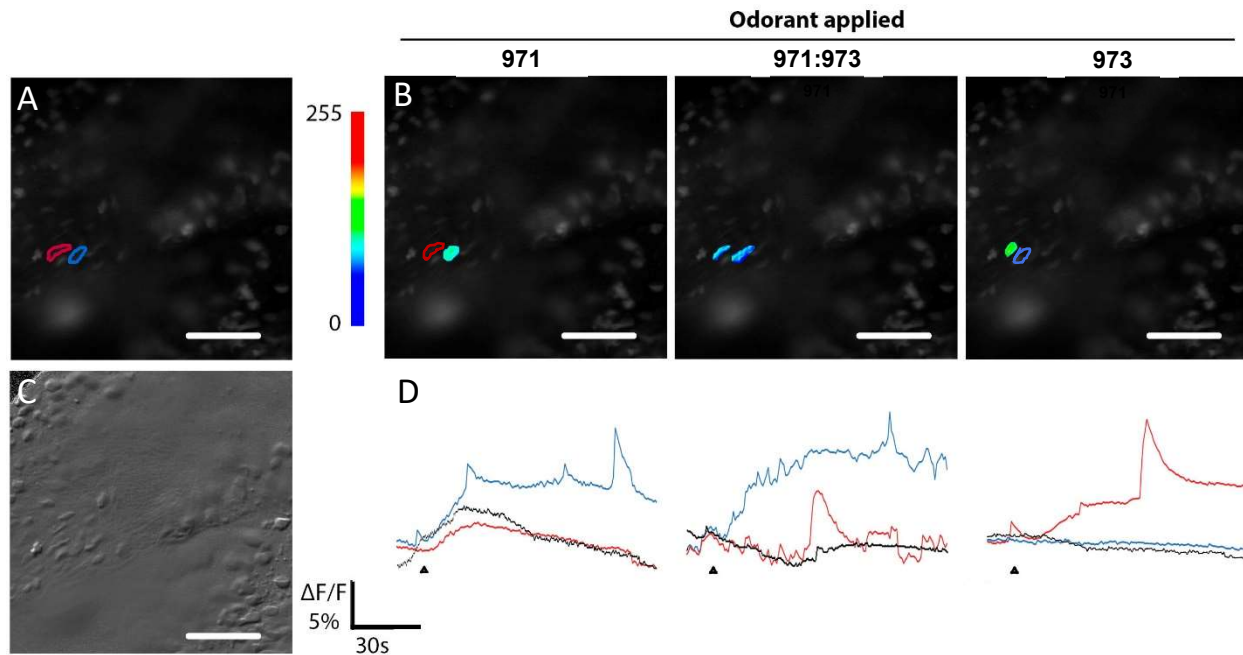
Figure 2.11 Olfactory sensory neuron discrimination between sea lamprey pheromone components 971 and 973. (A) Raw image of transformer-stage olfactory sensory neurons loaded with calcium green dextran. A cell responding to the putative pheromone component 971 is outlined in blue, while a cell responding to the putative pheromone component 973 is outlined in red. Scale bar, 60 μm. (B) Heatmap overlays of cells responding to 10^{-7} M 971 (left), a 1:1 mixture of 10^{-7} M 971:10^{-7} M 973 (center), and 10^{-7} M 973 (right). Non-responding cells are outlined in each case (971 cell in blue, 973 cell in red). Scale bars, 60 μm. (C) A filtered sample image of the preparation used for analysis. Scale bar, 60 μm. (D) Calcium transients of a 971-responding cell (blue traces), a 973-responding cell (red traces), and a control cell (black traces) in response to 10^{-7} M 971 (left), a 1:1 mixture of 10^{-7} M 971: 10^{-7} M 973 (center), and 10^{-7} M 973 (right). Odorant stimulus onset coincides with the start of each trace while black arrows beneath each trace denote offset.

which responded to either 971 (13 cells) or 973 (12 cells) were observed responding to

applications of L-arginine (Figure 2.12). Conversely, six cells that responded to L-arginine did

not respond to either 971 or 973 (Figure 2.12).
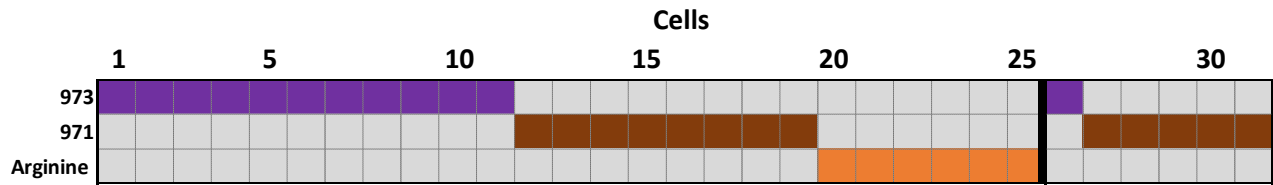
Figure 2.12 OSNs show specificity in response to 971 and 973. An overview of 2 transformer-stage epithelial preparations (n=2) exposed to 971 and 973 pheromone components. Each column represents a single olfactory sensory neuron, and columns grouped together by a heavier outline belong to the same preparation. Positive responses are represented by black boxes, tested odorants not responded to by a particular cell are represented by gray boxes, while untested odorants are represented by white boxes. Across two preparations, 25 olfactory sensory neurons responded to either 971 or 973.

Putative pheromone component PAMS-24 was tested alongside 3kPZS to determine detectability at the level of the olfactory epithelium. PAMS-24 and 3kPZS were each delivered individually to the same epithelial preparation before a mixture of both components was then applied. Again, each cell responded to either PAMS-24 or 3kPZS pheromone component and was not observed responding to both components as illustrated by response territories of PAMS-24-responding cells (magenta traces; Figure 2.13) and 3kPZS (yellow traces; Figure 2.13) not overlapping for any one cell. A specific instance of the same olfactory sensory neurons responding to both an
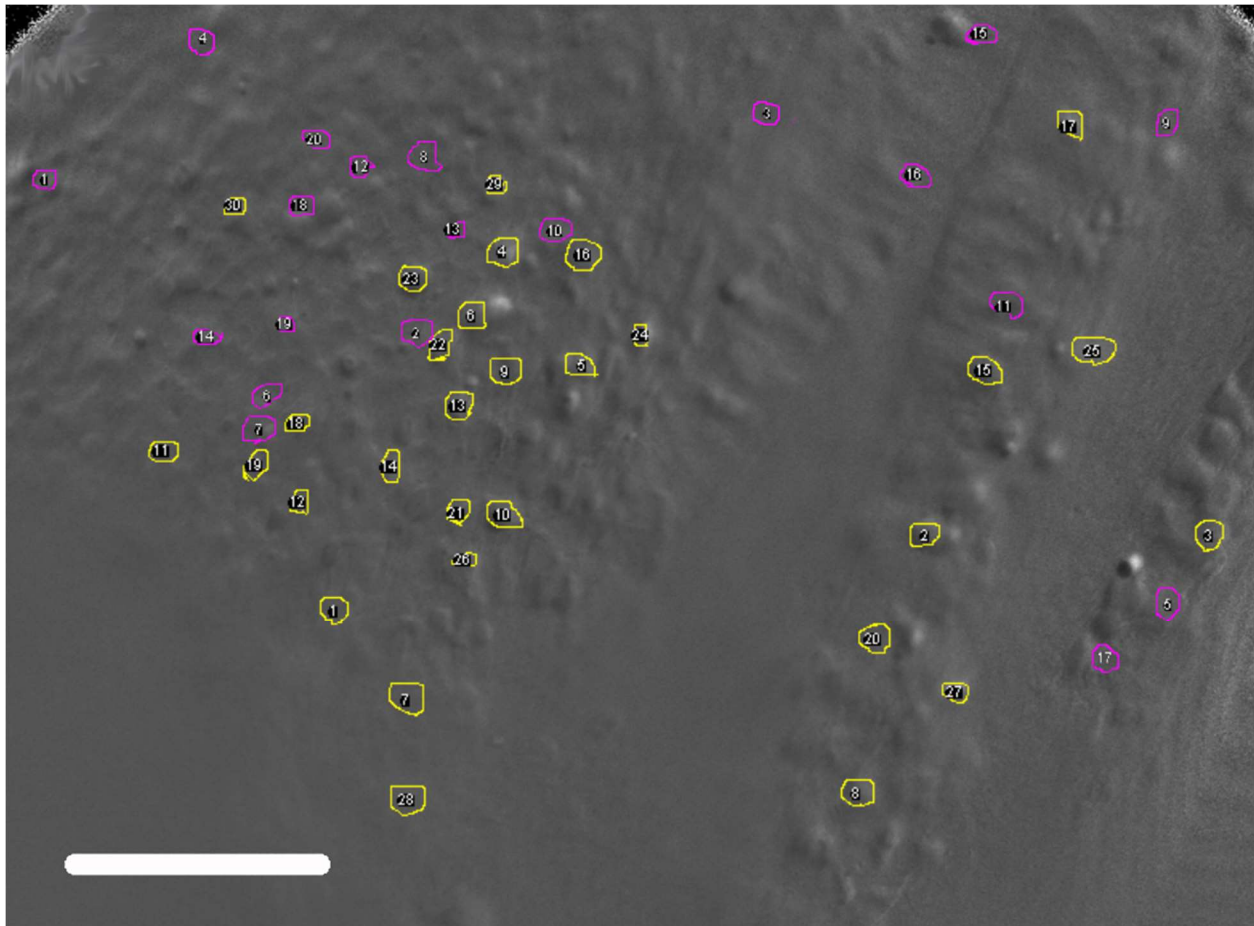
Figure 2.13 Location of OSNs responding to 3kPZS and PAMS-24. The transformer-stage olfactory epithelium preparation image shown was taken from an image stack generated during the calcium imaging experiment and subsequently filtered using imageJ software. Two sets of superimposed regions of interest encompassing olfactory sensory neurons responding to 3kPZS 10^{-7} M (yellow traces) and PAMS-24 10^{-7} M (magenta traces) during separate applications of each odorant onto the same olfactory epithelium. Scale bar, 60 μm.

individual pheromone component as well as the component mixture when applied is illustrated in

Figure 2.14. Here, a pair of responding cells; a PAMS-24-responding cell (outlined in red; Figure

2.14a) fluoresced in response to PAMS-24 10^{-7} M (Figure 2.14d; red trace, right calcium

transient set) and a 3kPZS-responding cell (outlined in blue; Figure 2.14a) fluoresced in response

to 3kPZS 10^{-7} M (Figure 2.14d; blue trace, left calcium transient set), and both responded to the

3kPZS/PAMS-24 mixture when it was applied (Figure 2.14d; middle calcium transient set).
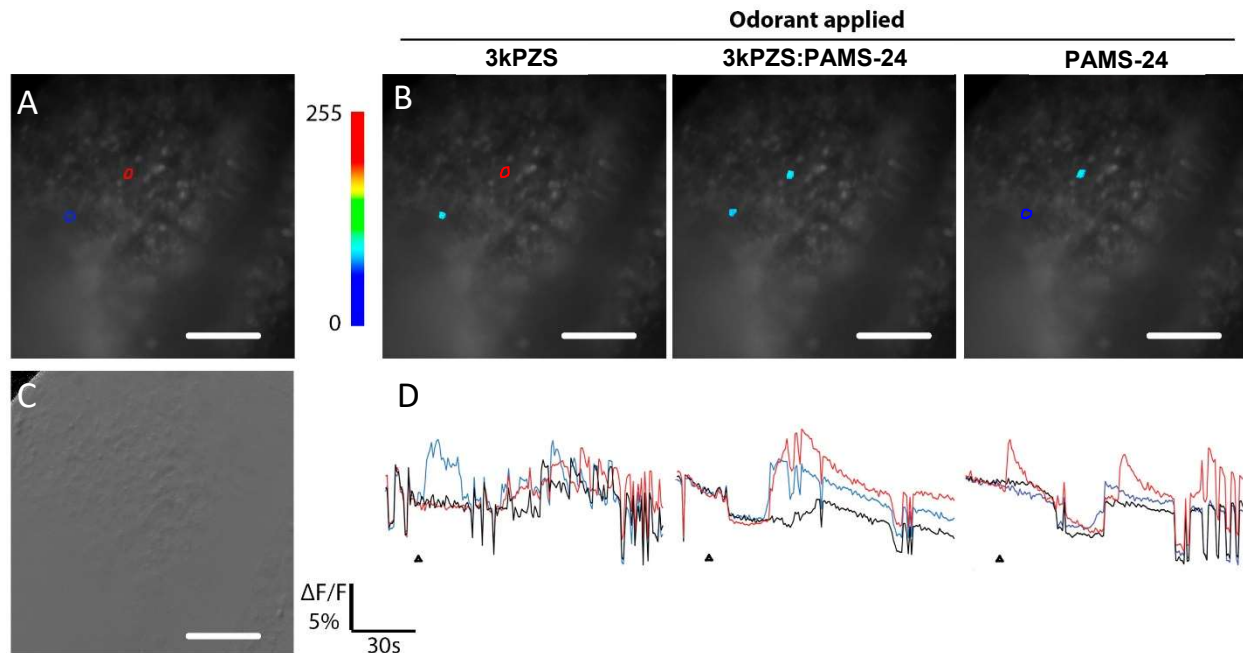
Figure 2.14 Olfactory sensory neuron discrimination between sea lamprey pheromone components 3kPZS and PAMS-24. (A) A raw image of transformer-stage olfactory sensory neurons loaded with calcium green dextran. A cell responding to the putative pheromone component 3kPZS is outlined in blue, while a cell responding to the putative pheromone component PAMS-24 is outlined in red. Scale bar, 60 μm. (B) Heatmap overlays of cells responding to 10^{-7} M 3kPZS (left), a 1:1 mixture of 10^{-7} M 3kPZS:10^{-7} M PAMS-24 (center), and 10^{-7} M PAMS-24 (right). Non-responding cells are outlined in each case (3kPZS cell in blue, PAMS-24 cell in red). Scale bars, 60 μm. (C) A filtered sample image of the preparation used for analysis. Scale bar, 60 μm. (D) calcium transients of a 3kPZS-responding cell (blue traces), a PAMS-24-responding cell (red traces), and a control cell (black traces) in response to 10^{-7} M 3kPZS (left), a 1:1 mixture of 10^{-7} 3kPZS M:10^{-7} M PAMS-24 (center), and 10^{-7} M PAMS-24 (right). Odorant stimulus onset coincides with the start of each trace while black arrows beneath each trace denote offset.

In all, 53 olfactory sensory neurons responded to one of either PAMS-24 (23 cells) or 3kPZS (30 cells). In addition to 3kPZS, DKPES, PAMS-24, 971, and 973, pheromone components PSDS and PZS were also successful in eliciting responses from olfactory sensory neurons (Figure 2.15). Cellular specificity was not only observed for pheromone components however, amino acids L-arginine and L-histidine and bile acid taurocholic acid all elicited

responses from olfactory sensory neurons, showing the same level of response specificity seen

with the aforementioned pheromone components (Figure 2.15).
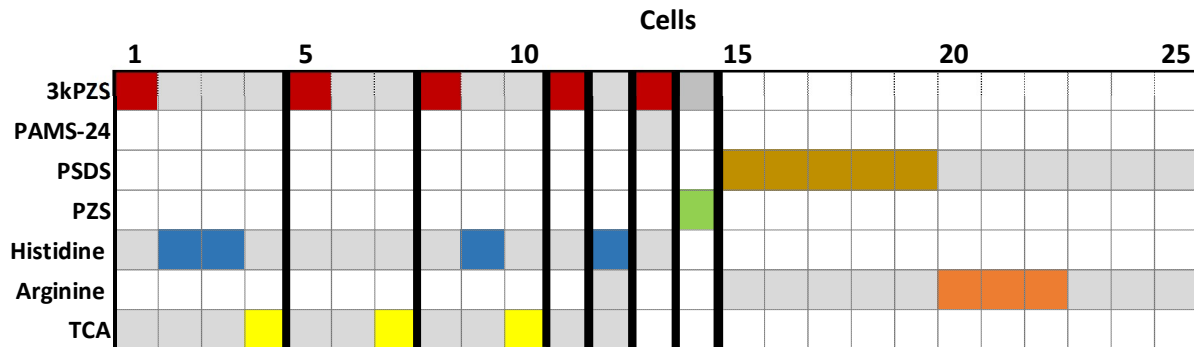
Figure 2.15 OSNs show specificity in response to a variety of odorants. An overview of transformer-stage olfactory sensory neuron responses to: pheromone components 3kPZS, PSDS, and PZS; amino acids L-histidine and L-arginine; and bile acid taurocholic acid. Each column represents a single olfactory sensory neuron, and columns grouped together by a heavier outline belong to the same preparation (n=10 preparations shown). Positive responses are represented by coloured boxes, tested odorants not responded to by a particular cell are represented by gray boxes, while untested odorants are represented by white boxes.

2.3.4 Electrophysiological olfactory bulb recordings

Local field potential recordings were made to investigate the response of the olfactory

bulb neural responses to individual canonical and newly discovered lamprey pheromone

components. Green *et al.* (2017) observed local field potential responses in the dorsal region of

the olfactory bulb to a mixture of canonical pheromone components, and the lateral bulbar region

responded only to amino acids. However, responses to individual pheromone components, or the

newly discovered pheromone components have not been tested. In our recordings, the lateral

region did not respond to the pheromone component PADS, yet the dorsal region did respond

(Figure 2.16). This finding is in agreement with the observation by Green *et al.* (2017) that the

lateral olfactory bulb did not respond to a pheromone mixture when applied, instead responding

only to amino acids.

PADS 10^{-7} M   PADS 10^{-7} M

100 µV
1 sec
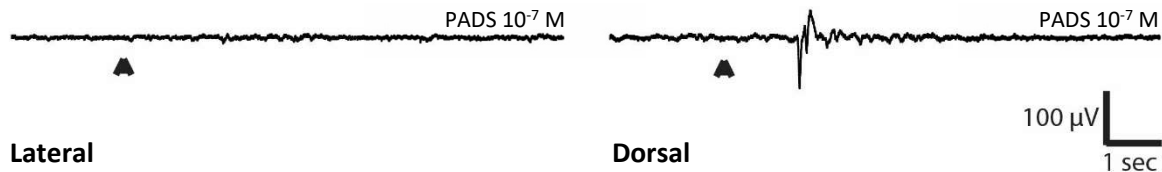
Lateral   **Dorsal**

Figure 2.16 Lateral olfactory bulb region is unresponsive during pheromone exposure.
Local field potential) recordings in the lateral and dorsal regions of the same olfactory bulb in
response to 10^{-7} M PADS. Odorant stimulus onset coincides with the start of each trace while
black arrows beneath each trace denote offset.

Each pheromone component tested arrived in powdered form and was subsequently solubilized

in a 1:1 mixture of methanol and ultra pure water. The vehicle control of 0.0025% methanol was

tested alongside 10^{-7} M 3kPZS to compare the local field potential response amplitudes

stimulated by each to ensure that the methanol vehicle control did not act as a stimulus. While

the 10^{-7} M 3kPZS application elicited a local field potential response, the methanol vehicle

control did not yield a response upon application (Figure 2.17).

0.0025% Methanol   3kPZS 10^{-7} M   100 μV   1 sec
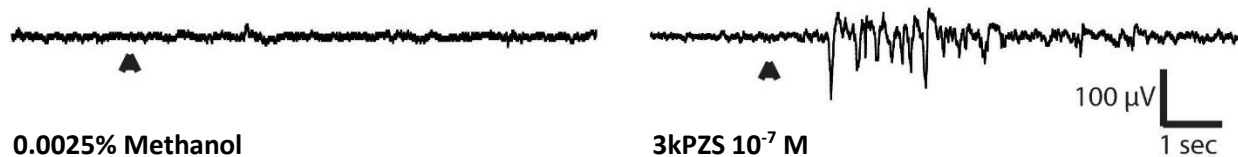
Figure 2.17 Methanol vehicle control did not elicit a response from the dorsal olfactory bulb. Electrophysiological (local field potential) recordings taken from the dorsal olfactory bulb in response to applications of 0.5% methanol and 3kPZS 10^{-7} M. Odorant stimulus onset coincides with the start of each trace while black arrows beneath each trace denote offset. Responses were elicited by 3kPZS while 0.5% methanol failed to elicit a response from the same test preparation.

The amino acids L-serine and L-arginine (Li 1994) were established as negative and positive controls respectively (Figure 2.18) as the neutral amino acid L-serine reliably failed to elicit an electrophysiological response from the dorsal olfactory bulb while the basic amino acid L-arginine functioned well as an odour stimulus.

L-serine   L-arginine   100 μV   1 sec
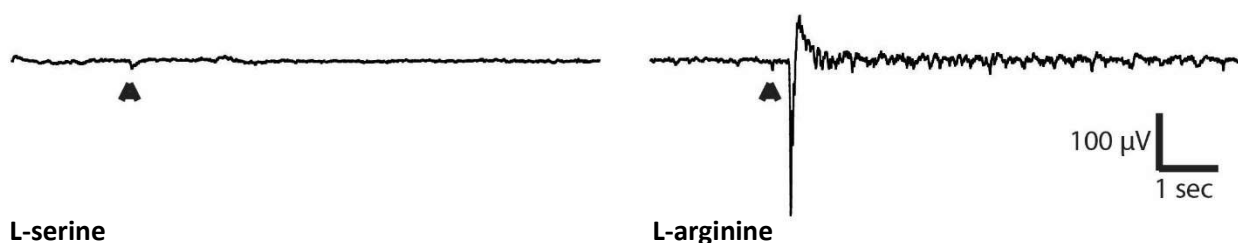
Figure 2.18 L-serine does not elicit a response from the dorsal olfactory bulb. Local field potential recordings from the dorsal olfactory bulb in response to applications of 10^{-4} M L-serine and 10^{-4} M L-arginine. Odorant stimulus onset coincides with the start of each trace while black arrows beneath each trace denote offset. Responses were elicited by L-arginine while L-serine failed to elicit a response from the same individual.

2.3.5 Threshold concentration of sea lamprey pheromone components

The response thresholds for three separate male sea lamprey sex pheromone components (n=1, Figure 2.19) as well as four larval migratory cue components (n=1, Figure 2.20) were determined from local field potential recordings from the olfactoy bulb of spawning stage sea lamprey. Each individual tested was exposed to serially decreasing concentrations of one pheromone component until response elicitation failed for three consecutive odorant stimulations (n=1 for each pheromone component tested for threshold). Concentrations indicated as 'Threshold' in Figures 2.19 and 2.20 are 10 times more concentrated than the concentration which failed to elicit an LFP responses for that pheromone component (ie. if 'threshold' is 10^{-12} M, then no response was detected at 10^{-13} M). For each recording, a 5 second pre-odour baseline mean and standard
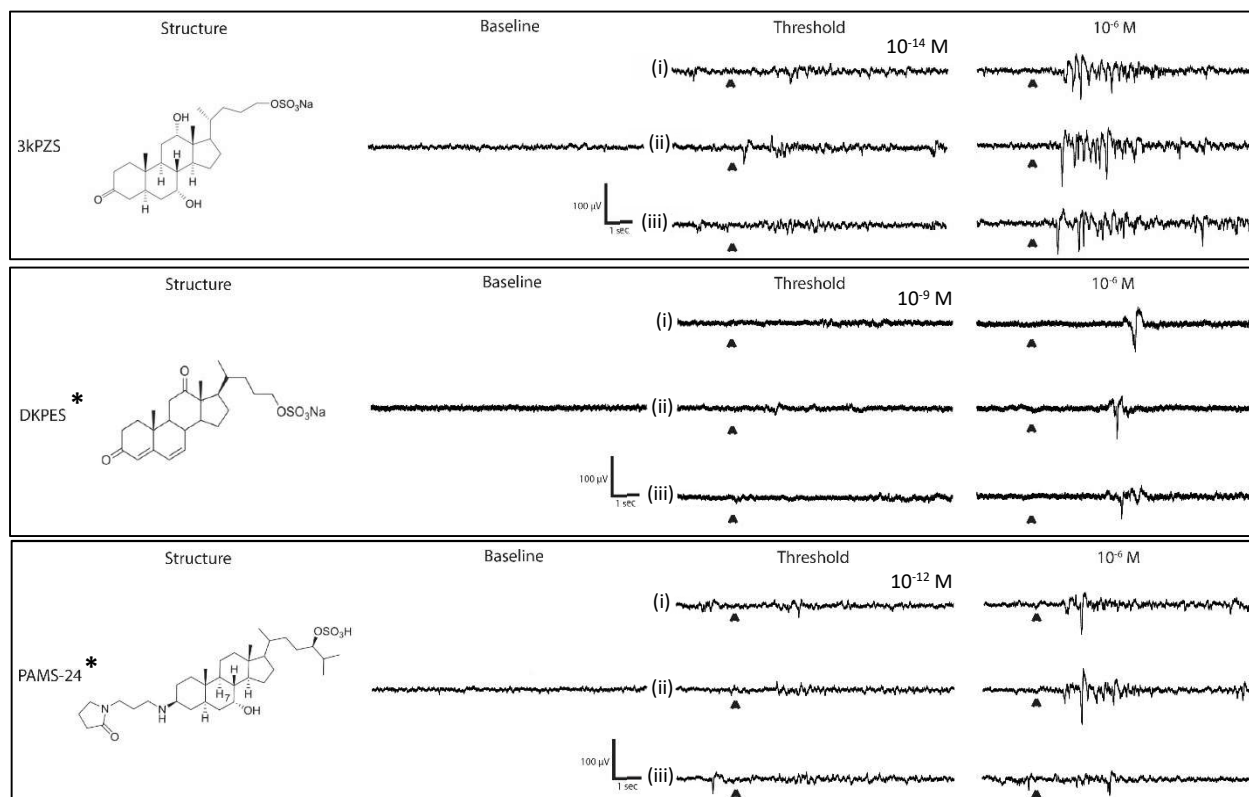
Figure 2.19 Spawning-stage dorsal olfactory bulb detection thresholds determined for three separate adult male sea lamprey pheromone components. The traces depicted are of local field potential recordings from the dorsal surface of the olfactory bulb in response to each pheromone component at 10^{-6} M (right) and threshold concentrations (center), with an example of the background baseline (left). For each pheromone component, one test preparation was used to elicit the response data shown. Each pheromone was tested three times and the offset of these 2 second deliveries are represented by the arrowheads under each trace. Asterisks denote recently elucidated putative pheromone components.

deviation was calculated and only responses with peak amplitudes greater than 3 times the baseline standard deviation were considered odour-evoked responses. Of the seven total pheromone component thresholds determined, four are recently elucidated, putative pheromone components including two male sex pheromone components DKPES and PAMS-24 (Figure 2.19) as well as two larval pheromone components 971 and 973 (Figure 2.20).
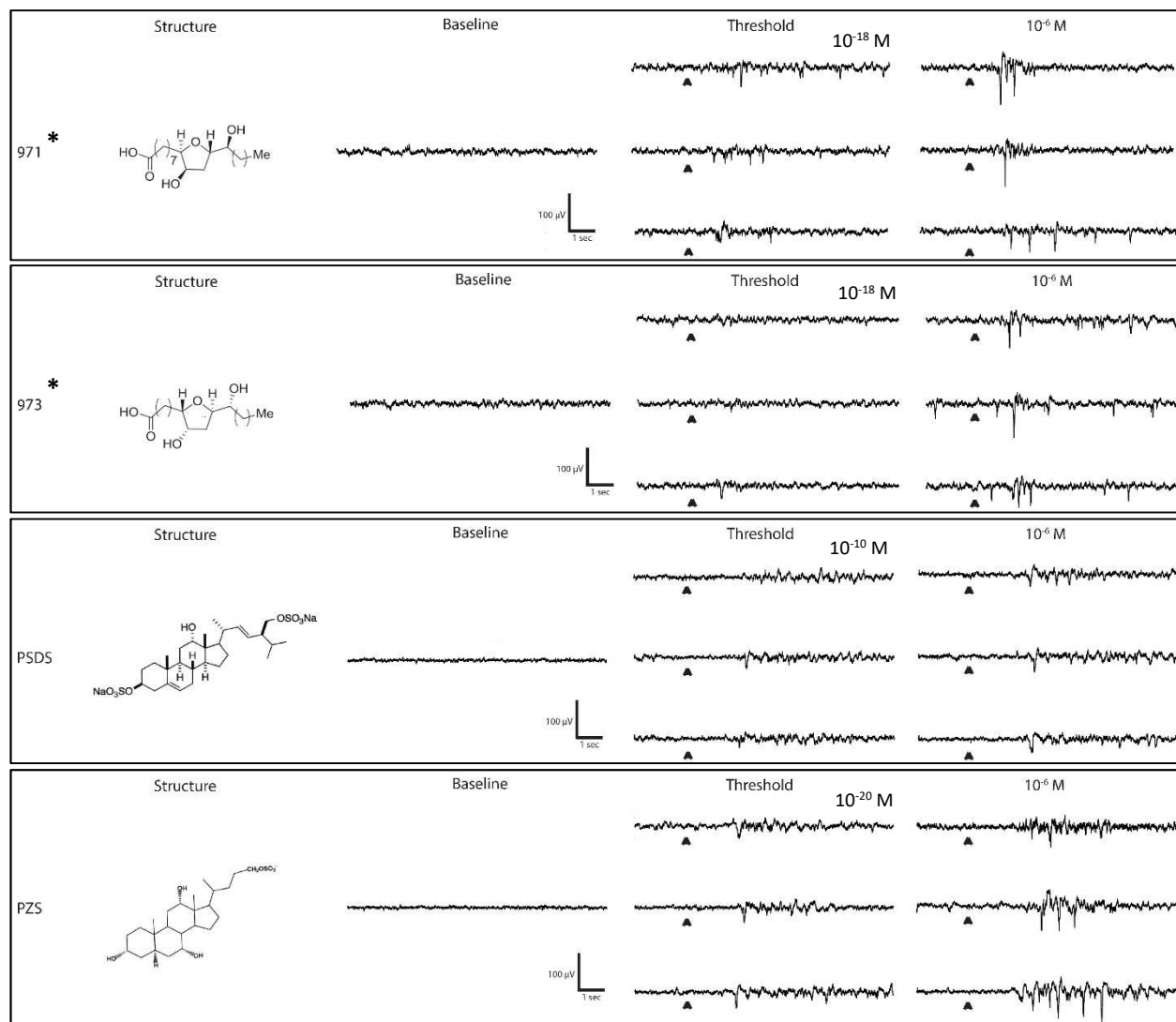
Figure 2.20 Spawning-stage dorsal olfactory bulb detection thresholds determined for four separate larval sea lamprey pheromone components. The traces depicted are of local field potential recordings from the dorsal surface of the olfactory bulb in response to each pheromone component at 10^{-6} M (right) and threshold concentrations (center), with an example of the background baseline (left). For each pheromone component, one test preparation was used to elicit the response data shown. Each pheromone was tested three times and the offset of these 2 second deliveries are represented by the arrowheads under each trace. Asterisks denote recently elucidated putative pheromone components.

2.3.6 Dose-response investigations of various pheromone components

A standard concentration series ranging from 10^{-12} M up to 10^{-6} M was delivered to spawning-stage sea lamprey to observe the potential correlation between the concentration of an odorant delivered and the subsequent response amplitude elicited. A total of 8 pheromone components (3 male sex pheromone and 5 larval pheromone components) were tested on olfactory bulb preparations from 8 spawning-stage sea lampreys. Each lamprey received serially diluted concentrations of one pheromone component (Figure 2.21a). Six of the eight pheromone components tested had the greatest average response amplitudes elicited by the highest concentration within the series.

Likewise, a concentration series ranging from 10^{-13} M up to 10^{-6} M was delivered to transformer stage sea lamprey to determine the nature of dose-dependent olfactory bulb responses. A total of nine pheromone components (4 male sex pheromone and 5 larval pheromone components) were tested on olfactory bulb preparations from 9 transformer lamprey sea. Each transformer lamprey received serially diluted concentrations of one pheromone component (Figure 2.21b). Two of the nine pheromone components tested had the greatest response amplitudes elicited by the highest concentration delivered.
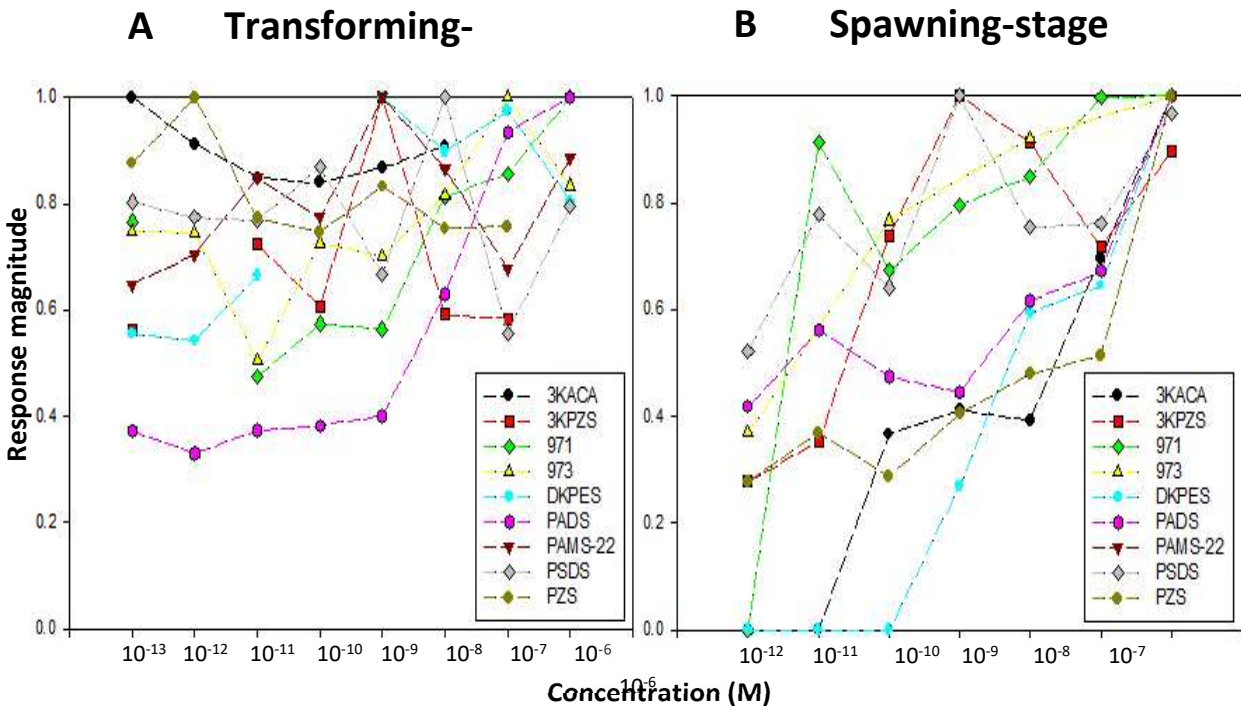
Figure 2.21 Average electrophysiological (local field potential) dose-response peak amplitudes recorded from the dorsal olfactory bulb surface of transformer-stage (A) and spawning-stage (B) sea lamprey. Each coloured series of plots represents a concentration series of a pheromone odorant delivered to the peripheral olfactory organ. The magnitude of the response amplitude is expressed as a ratio of the maximum response from that concentration series. A maximum response would thus have a y value of 1.0. Each odorant was tested on n=1 transformer-stage or spawner-stage sea lamprey for a total of n=9 transformer-stage preparations and n=8 spawner-stage preparations used.

2.3.7 Comparison of olfactory bulb electrophysiological responses to single vs multi-component odour stimuli

Male sex pheromone component 3kPZS (10^{-8} M), putative male sex pheromone component DKPES (10^{-8} M) and a mixture of both components DKPES:3kPZS (10^{-8} M:10^{-8} M) were delivered to the peripheral olfactory organ of five (n=5) transformer stage sea lamprey. The peak response amplitudes recorded from each lamprey were averaged for each odorant and

compared (Figure 2.22). After testing skewness (3kPZS z-score=1.459, DKPES z-score=1.611, DKPES:3kPZS z-score=1.586), kurtosis (3kPZS z-score=1.025, DKPES z-score=0.942, DKPES:3kPZS z-score=1.434), and Shapiro-Wilk value (3kPZS=0.430, DKPES=0.214, DKPES:3kPZS=0.265) it was determined that the data passed these tests of normality. Thus, a parametric ANOVA was used to determine that the LFP amplitude means were not significantly different (p=0.334).
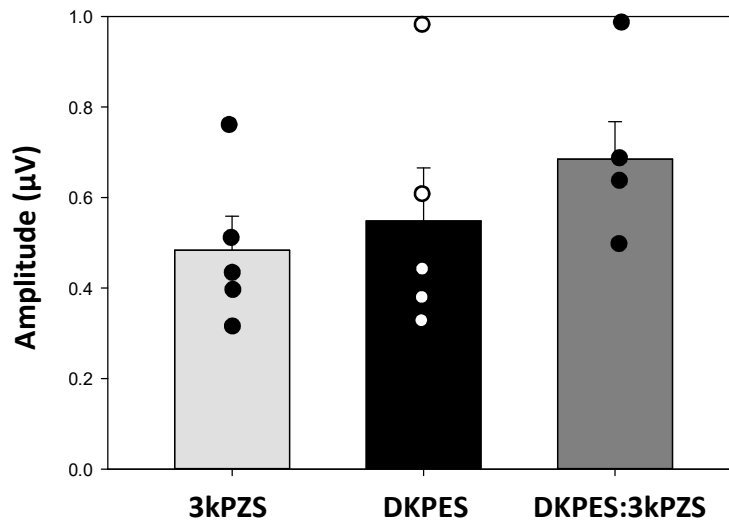
Figure 2.22 Transformer-stage olfactory bulb responses to individual pheromone components compared to mixture. The average peak amplitudes of local field potential recordings from the surface of the olfactory bulb in response to 10^{-8} M 3kPZS, 10^{-8} M DKPES, and a ratio mixture of 10^{-8} M DKPES:3kPZS (2:29.8) odorant applications to the peripheral olfactory organs of n=5 transformer stage sea lampreys. Constituent LFP values (dot overlays) comprising each average (represented by each bar) are displayed, superimposed over the corresponding bar. Data collected/analyzed with Michelle Farwell.

2.4 Discussion

Given the behavioural observations by Li *et al.* (2013) that a mixture of sex pheromone components 3kPZS and DKPES attracted a greater number of ovulating females than either individual component alone (with DKPES completely failing to elicit a behavioural response), this study sought to characterise how sea lamprey OSNs process odorant mixtures compared to single odorants and how this may affect neural activity at the surface of the olfactory bulb. The present study proposed that OSNs may be highly specific in responding to perspective ligands, thereby providing increased resolution and the ability for OSNs of the peripheral olfactory organ to respond to specific pheromone components. When presented with multiple odorants, individual OSNs were found to respond to a single odorant, often responding again to a mixture containing that odorant. Overall, 7 separate pheromone components, 2 amino acids and taurocholic acid were detected by separate OSNs of the olfactory epithelium without a single OSN responding to multiple odorants. Olfactory bulb detection thresholds in adult sea lampreys were determined for 7 pheromone components and found to range from 10^{-9} M (DKPES; n=1) to 10^{-20} M (PZS; n=1). All 4 newly discovered putative pheromone components tested (DKPES, PAMS-24, 971, and 973) elicited OSN responses as well as LFPs from the dorsal olfactory bulb region, demonstrating that these components are detected by the olfactory epithelium and that this sensory information is relayed to the brain (ie the olfactory bulb).

Across several separate olfactory epithelium preparations, OSNs were found to respond to one out of a series of odorants applied during each experiment. In each case, responding OSNs fluoresced to only one odorant, exhibiting high specificity for that odorant and often responding again if exposed to a mixture including the odorant previously responded to. Broadly tuned OSNs, responding to multiple odorants, have been observed in the necklace glomeruli of mice,

and while these broadly tuned OSNs have also been observed on the antennae of insects, so too have specialist OSNs, expressing only pheromone specific odour receptors showing high specificity for sex pheromone components (Christensen and Hildebrand, 1987; Hildebrand and Shepherd, 1997; Sato and Touhara, 2009; Greer *et al.* 2016). Nara *et al.* (2011) tested 13 separate odorant mixtures, as well as single odorants, on 3000 mouse OSNs and found both broadly tuned OSNs, responding to multiple odorant mixtures, as well as many cases of individual OSNs responding to only a single odorant. Interestingly, the single odorants to which individual OSNs were found to specifically respond to were all animal-related olfactory cues, including mouse pheromones, fecal odorants, and musk odorant components (Nara *et al.* 2011). These animal-related odorants could conceivably be involved in innate responses upon detection by OSNs of the olfactory epithelium, much in the same manner that sea lamprey pheromone components are believed to trigger innate behavioural responses. The importance of the detection of multiple pheromone components and their specific ratio within the released mixture has been demonstrated in a number of species. Nochuid moths, *Pelosi pisi* and *Pelosi flammea* employ the same two principle components in their respective pheromone blends, but these two closely related species use different concentrations of these components to aid in conspecific recognition (Kaissling and Kramer 1990). Similarly, while both the goldfish (*Carassius auratus*) and the closely related common carp (*Cyprinus carpio*) release prostaglandin $F_{2\alpha}$, 15keto-prostaglandin $F_{2\alpha}$, and 13,14-dihydro-15keto-prostaglandin $F_{2\alpha}$, male carp were more strongly attracted to the odour of conspecific ovulated females compared to the odour produced by ovulated goldfish (Lim and Sorensen 2011). It was determined that while both species release the same 3 prostaglandins, ovulated goldfish release these at a slightly greater rate and in a different ratio (Lim and Sorensen 2011). The ability to identify separate male sex pheromone and larval

migratory cue components could thus be advantageous for sea lamprey as this allows for varied behavioural responses based on the combination and ratio of mixture components (Li 2005; Johnson *et al.* 2008).

In this study, a mixture of 3kPZS and DKPES induced a significantly greater average LFP response amplitude from the dorsal olfactory bulb than 3kPZS when applied on its own. These two pheromone components elicited responses from separate OSNs, suggesting that these cells express unique odour receptors. OSNs expressing dissimilar odour receptors have been shown to project to different glomeruli in the mammalian olfactory bulb, with each glomerulus receiving axonal input from only OSNs expressing a single odour receptor gene (Ressler *et al.* 1994). Conceivably, the pheromone components in this study may be exhibiting specific glomerular activation similar to that seen in zebrafish, where Friedrich and Korsching (1997) showed that individual amino acids induced highly specific glomerular activity. As such, a mixture of 3kPZS and DKPES may be activating a greater number of glomeruli within the olfactory bulb than 3kPZS activates on its own, thereby generating greater neural activity reflected by a greater LFP response amplitude as seen in this study. LFP recordings represent the summed synaptic activity generated by inhibitory and excitatory postsynaptic potentials involving OSN axons, projection neuron dendrites, and interneurons, with greater LFP amplitudes being indicative of greater synaptic activity. While LFPs convey this general, odour-evoked information to higher brain regions, they do not provide information about the specific odour identity (Friedrich *et al.* 2004). Thus, these recordings cannot guarantee that the sensory information being sent to the recorded neurons is being passed on to higher brain structures to elicit a motor response. Behavioural responses to olfactory stimuli can also be taken into

consideration as an indication of the perception of an environmental odour (Johnson *et al.* 2006, 2009).

In the present study, calcium transients were elicited from OSNs in response to applications of 4 larval pheromone components (971, 973, PSDS, and PZS) and 3 male sex pheromone components (3kPZS, DKPES, and PAMS-24). These results bring cellular resolution to the findings from studies which used electro-olfactogram recordings of neural activity from the olfactory epithelium to illustrate sea lamprey responsiveness to 3kPZS (Li *et al* 2002), DKPES (Li *et al.* 2013), PAMS-24, 971, and 973 (Brant 2015), PSDS (Sorensen *et a*l 2005), and PZS (Siefkes and Li 2004) in the peripheral olfactory organ. This study also reports LFP responses recorded from the dorsal olfactory bulb region in response to 6 larval pheromone components (971, 973, PADS, PSDS, PZS, and ACA) and 4 male sex pheromone components (3kPZS, DKPES, PAMS-24, and 3kACA). The LFP responses elicited by 3kPZS, 3kACA, PZS, PADS, and PSDS echo the findings of Green *et al.* (2013, 2017) which also observed responses to a mixture containing these pheromone components from the dorsal olfactory bulb. Considering the previously reported electro-olfactogram responses to DKPES (Li *et al.* 2013), PAMS-24 (Brant 2015), and ACA (Bjerselius *et al.* 2000) recorded from the olfactory epithelium, it was not surprising to see neural activity elicited from the dorsal olfactory bulb by these components. This study reports an absence of pheromone-evoked LFP responses from the lateral olfactory bulb, as was also reported by Green *et al.* (2013, 2017). Additionally, there is structural similarity (ie. a shared tetracyclic (cholane) backbone with side-chain branching off the 5-carbon ring) between DKPES, PAMS-24, and ACA to the components of the pheromone mixture reported by Green *et al.* (2013, 2017) as being stimulatory. The current study expands these findings however by testing each component of the pheromone mixture employed by

Green *et al.* (2013, 2017) to characterise olfactory responsiveness to each component individually. Interestingly, putative pheromone components 971 and 973 do not share this tetracyclic backbone and instead represent novel dyhydroxylated tetrahydrofuran diol fatty acids (Brant 2015). Despite their departure from the classic cholane steroid template, these components were found to elicit neural activity from the olfactory epithelium based on electro-olfactogram recordings (Brant 2015) and calcium imaging data presented in this study showing individual OSNs responding to these components. This study also determined dorsal olfactory bulb response thresholds for 4 larval pheromone components (971, 973, PSDS, and PZS) and 3 male sex pheromone components (3kPZS, DKPES, and PAMS-24). Table 1 compares the olfactory detection thresholds determined for each component and compares these threshold values to the electro-olfactogram thresholds previously reported in the literature (Li *et al.* 2002, 2013; Siefkes and Li 2004; Sorensen *et al.* 2005; Brant 2015). Though the n value is too low for robust statistical analyses of these threshold values, if the various pheromone component LFP and electro-olfactogram thresholds are compared as a whole, it is observed that generally all LFP threshold values collected from adult lampreys, aside from PSDS (Sorensen *et al.* 2005), were found to be lower than the electro-olfactogram derived values for each pheromone component. One explanation for this observation may be OSN axonal convergence into olfactory bulb

	Molar (M) detection threshold						
	3KPZS	**PZS**	**PSDS**	**DKPES**	**PAMS-24**	**971**	**973**
Olfactory epithelium EOG	10^{-10} N=4	10^{-12} N=7	10^{-13} N=6	10^{-7} N=4	10^{-12}	10^{-11}	10^{-11}
Olfactory bulb LFP	10^{-14} N=1	10^{-20} N=1	10^{-10} N=1	10^{-9} N=1	10^{-14} N=1	10^{-18} N=1	10^{-18} N=1

Table 1. A comparison of dorsal olfactory bulb and olfactory epithelium response thresholds for individual sea lamprey pheromone components. LFP response thresholds from the dorsal olfactory bulb are compared to the response thresholds of electro-olfactogram recordings from the olfactory epithelium of adult lamprey in response to applications of individual pheromone components 3kPZS (Li *et al* 2002), DKPES (Li *et al.* 2013), PAMS-24, 971, and 973 (Brant 2015) PSDS (Sorensen *et a*l 2005), and PZS (Siefkes and Li 2004).

glomeruli. It has been shown in the mammalian olfactory system that axons from OSNs expressing the same odour receptor will converge within the same glomerulus to synapse with projection neuron dendrites (Ressler *et al.* 1994). Thus, this convergence may be summating sensory input from many, widespread OSNs scattered throughout the epithelium into far fewer glomeruli in the olfactory bulb from which LFP responses were recorded in this study. This then could have facilitated the detection of LFP responses from the olfactory bulb at concentrations below the detection threshold at the olfactory epithelium, where electro-olfactogram recordings may be recording the summed neural activity of only a portion of the OSNs activating the glomeruli from which LFP recordings were taken. Interestingly, the 3 lowest threshold values were produced by larval pheromone components (PZS, 971, and 973), this appears to shadow the general trend of relatively lower detection thresholds (electro-olfactogram) for migratory components compared to male sex pheromone components (Li *et al.* 1995, 2002, 2013; Sorensen *et al.* 2005). Additionally, natural in-stream pheromone concentrations have been measured as being in the range of 10^{-12} M to 10^{-13} M (Yun *et al.* 2002; Johnson *et al.* 2008), while behavioural

trials have shown ovulating female sea lamprey respond to in-stream concentrations as low as 10^{-14} M (3kPZS) (Johnson *et al.* 2008).

Interesting differences between the dose-response patterns produced by spawning-stage and transformer-stage lamprey exposed to pheromone component concentration series were observed. While 6 of 8 pheromone components delivered to spawning-stage lamprey had their maximum response magnitude elicited by the highest concentration delivered, this was the case for only 2 of 9 pheromone components delivered to transformer-stage lamprey. LFP peak response amplitudes represented the summed glomerular activity from OSN axons recruited to the recording region, projection neuron dendrites, as well as interneurons. These amplitudes were reported for each pheromone concentration tested as percentages of the maximum response for that concentration series. A decrease in LFP response amplitude coinciding with a decrease in concentration was observed for 5 of 8 pheromone component concentration gradients tested on spawning-stage lamprey while only 1 of 9 pheromone components (PADS) tested on transformer-stage lamprey exhibited a similar dose-response pattern. The difference between life-stage dose-response patterns could be influenced by the maximal raw LFP values recorded for each life stage. The maximal LFP values from spawning-stage lamprey tended to be greater for each concentration series than the maximal LFP values from transforming-stage lamprey. A greater maximum peak value per concentration series provides a larger range for a potential concentration-dependent response pattern to fall within. The greater LFP values produced by spawning-stage lamprey may be the result of a greater number of OSNs conveying sensory information to any one glomerulus, since the peripheral olfactory organ of spawning-stage lamprey is many-fold larger and contains far more OSNs than that of a transformer-stage lamprey (vanDenBossche *et al.* 1995). It could also be argued that the generally concentration-

invariant LFP amplitudes recorded from the majority of pheromone components tested on transformer-stage lamprey as well as a portion of those tested on spawning-stage lamprey may be expected. Wachowiak *et al.* (2001) observed in the box turtle, *Terrapene carolina*, that the glomerular activation patterns produced by an odorant at a low concentration did not alter significantly as the concentration was increased. As well, an orientation strategy relying on recognition of concentration gradients may not be effective for sea lamprey when tracking pheromones in their aquatic environment. Sea lamprey are monorhinic and thus use a single nostril to move scented water into and out of the olfactory epithelium which each respiratory cycle (Kleerekoper 1972). This restricts lamprey to sequential sampling of odour plumes, and this sampling rate may be too slow to reliably measure the dynamic properties in turbulent odour plumes (Webster and Weissburg 2001). Therefore, differences in bulbar activity level may not be expected to correlate with odorant concentration. Behavioural assays by Johnson *et al.* (2008) demonstrated upstream movement by ovulating female sea lampreys induced by in-stream plums of 10^{-14} M to 10^{-10} M 3kPZS with no significant difference in the time it took the lamprey to swim upstream into the trap between the various concentrations.

Sea lamprey OSNs are believed to posses G-protein coupled odorant receptors (Frontini *et al.* 2003, Ren *et al.* 2009), so forskolin, an indirect promoter of cyclic-AMP catalysis (resulting in depolarization and subsequent generation of a neural impulse), should elicit a response from any OSN employing this G-protein coupled receptor (Frings and Lindemann 1991; Leinders-Zufall *et al.* 1997; Wong *et al.* 2000). While we observed responses from multiple OSNs to forskolin, we did not observe an instance of an OSN responding to both an odorant as well as forskolin, as would be expected. A concentration of 10^{-6} M forskolin was used in this study, higher concentrations have been used in similar studies (10^{-5} M in Bozza *et al.*

2002) and this is an adjustment that could be easily made to determine if this may be affecting

OSN responses. Supporting this thought, while 30+ OSNs were observed responding to 3kPZS

during one experiment, the greatest number of OSNs seen responding to forskolin in our

experiments was 3. Another consideration, given the mechanism of action of forskolin, is that the

cellular membrane of the OSN may be leaky given the triton application during the calcium

loading process. This leakiness may be illustrated by the general decrease in baseline

fluorescence observed during calcium imaging experiments in this study. It could be that the

membrane may still be slightly solubilized, affecting the entry of forskolin or promoting its exit

out of the OSN, and thereby affecting OSN responses to its application. Regular odorants act

extracellularly on odour receptors and may be less affected.

An important qualifying note on much of the electrophysiological data collected from the

olfactory bulb in this study is the low n-value for the various threshold and dose-response

recordings. Several factors influenced the n-value including the time we had to work with the

animals. Spawning-stage lamprey undergo natural senescence regardless of whether mating has

occurred, thus from the time of collection (early May) until senescence (early to mid August in

our tanks) we had a relatively short window within which to work. Similarly, the transformer-

stage lamprey in our possession lasted on average from the time of collection (mid to late

October) until the animal quality degraded beyond usability (late March to early April).

Additionally, with limits on human resources, repeatability was sacrificed in order to gain as

much novel information as possible from as many different pheromone components (including

each of the 4 newly elucidated putative components) as possible for both threshold and dose-

response experiment sets. Given the knowledge gained through this study concerning the

approximate thresholds of the various pheromone components, these concentrations could be

targeted in future experiments as a means of more efficiently increasing the n value for these experiments. Based on the general trends observed in this study regarding dose-response patterns amongst spawning and transforming-stage sea lamprey, future experiments could focus more narrowly on a smaller set of pheromone odorants to test for potential life-stage effects.

The characterization of how the peripheral olfactory organ is responding to individual pheromone components and component mixtures, at the level of an individual OSN is an important addition to our knowledge of sea lamprey olfaction and may have farther reaching implications within vertebrate olfaction as well. As a basal vertebrate, the sea lamprey offers a glimpse into the evolution of the vertebrate olfactory system in terms of organization and function, thereby informing investigations of higher order vertebrates. From a population management standpoint, a greater understanding of how lamprey are processing pheromone mixtures in the peripheries of the olfactory system, and how this processing influences bulbar activity can significantly aid pheromone cocktail design. The characterization of 4 newly elucidated, putative pheromone components in terms of the ability of each of these components to stimulate olfactory responses from the olfactory bulb as well as individual cells within the olfactory epithelium also serves to better inform the potential further investigation of these compounds in behavioural studies. Ovulating females prefer whole spermiated male washings over any single fractionated component of the washings (Johnson *et al.* 2008), so identifying each component, and the relative attractiveness of each component, individually and in different combinations can prove useful. With discussions of pheromone communication in vertebrates often narrowly focused on mammals, the sea lamprey affords a well described, robust, and relatively simple model of vertebrate olfaction. This study represents the first description of OSN response characteristics in the sea lamprey and has outlined several pheromone components that

have elicited olfactory responses from individual OSNs that showed high specificity for the ligand to which they responded. The specificity in odour-evoked OSN responses seen here in the lamprey may offer insight into similar instances observed in the mouse and salamander (Zufall *et al.* 1998; Nara *et al.* 2011). In the future, it may be interesting to explore the effect of concentration on OSN stimulation. Mainly, are varying proportions of OSNs activated when the olfactory epithelium is exposed to 10^{-6} M 3kPZS compared to 10^{-14} M 3kPZS? When exposed to extremely concentrated pheromone odorants, do OSNs lose their specificity? This information may help better interpret the dose-response data reported in this study. It may also be interesting to compare the relative OSN activation thresholds of various pheromone odorants to the established electro-olfactogram thresholds. This study employed a relatively high concentration of 10^{-7} M for all pheromone concentrations unless otherwise explicitly stated.

The results of this study demonstrate that the OSNs of the sea lamprey olfactory epithelium appear to be very specifically tuned to separate odorant classes and to single odorants within that class, supporting the hypothesis that sea lamprey OSNs respond to just one pheromone component. The detection of neural activity (by LFP recordings from the dorsal olfactory bulb) elicited by pheromone concentrations below the thresholds reported for electro-olfactogram recordings of the olfactory epithelium in response to the same pheromone components, may help explain the low (ie. 10^{-14} M 3kPZS) concentrations known to elicit behavioural responses from sea lamprey that also fall below the reported electro-olfactogram recordings.

2.5 Literature cited

Applegate VC (1950) Natural history of the sea lamprey (Petromvzon marinus) in Michigan. U.S. Fish Wild l. Serv. Spec. Sci. Rep. Fish 35, 237.

Belanger RM, Pachkowski MD, Stacey NE (2010) Methyltestosterone-induced changes in electro-olfactogram responses and courtship behaviors of cyprinids. Chemical senses 35(1), 65-74.

Bergstedt RA and Seelye JG (1995) Evidence for lack of homing by sea lamprey. Transactions of the American Fisheries Society 124: 235–239.

Bjerselius R, Li W, Teeter JH, Seelye JG, Johnsen PB, Maniak PJ, Grant GC, Polkinghorne CN, Sorensen PW (2000) Direct behavioural evidence that unique bile acids released by larval sea lamprey function as a migratory pheromone. Can J Fish Aquat Sci 57: 557---569.

Bolduc, TG, & Sower, SA (1992). Changes in brain gonadotropin-releasing hormone, plasma estradiol 17-β, and progesterone during the final reproductive cycle of the female sea lamprey, Petromyzon marinus. Journal of Experimental Zoology, 264(1), 55-63.

Bozza T, Feinstein P, Zheng C, and Mombaerts P. (2002) Odorant receptor expression defines functional units in the mouse olfactory system. Journal of Neuroscience, 22(8), 3033-3043.

Brant, CO (2015). Characterization of sea lamprey pheromone components. Michigan State University.

Brocard F, Ryczko D, Fénelon K, Hatem R, Gonzales D, Auclair F, Dubuc R (2010) The transformation of a unilateral locomotor command into a symmetrical bilateral activation in the brainstem. J Neurosci 30(2):523-533.

Bryan MB, Zalinski D, Filcek B, Libants S, Li W, and Scribner KT (2005) Patterns of invasion and colonization of the sea lamprey (Petromyzon marinus) in North America as revealed by microsatellite genotypes. Molecular Ecology 14: 3757–3773.

Bryan MB, Scott AP and Li W (2007) The sea lamprey (Petromyzon marinus) has a receptor for androstenedione. Biol Reprod 77: 688-696.

Buck L and Axel R (1991) A novel multigene family may encode odorant receptors: a molecular basis for odor recognition. Cell, 65(1), 175-187.

Buck LB (1996) Information coding in the vertebrate olfactory system. Annu Rev Neurosci 19:517-544.

Christensen TA, Harrow ID, Cuzzocrea C, Randolph PW, Hildebrand JG (1995) Distinct Projections of 2 Populations of Olfactory Receptor Axons in the Antennal Lobe of the Sphinx Moth Manduca-Sexta. Chemical Senses 20:313-323.

Christensen TA, Hildebrand JG (1987) Male-Specific, Sex Pheromone-Selective Projection Neurons in the Antennal Lobes of the Moth Manducasexta. J Comp Physiol A-Sens Neural Behav Physiol 160:553-569.

Derjean D, Moussaddy A, Atallah E, St-Pierre M, Auclair F, Chang S, Ren X, Zielinski B, Dubuc R (2010) A novel neural substrate for the transformation of olfactory inputs into motor output. PLoS Biol 8(12):e1000567.

Døving KB, Sandvig K, and Kasumyan A (2009) Ligand-specific induction of endocytosis in taste receptor cells. Journal of Experimental Biology, 212(1), 42-49.

Drickamer LC (1999) Sexual attractants. In E. Knobil and J. D. Neill (eds.), Encyclopedia of Reproduction, Academic Press, New York 4: 444–448.

Eisenberg JF and Devra GK (1972) Olfactory communication in mammals. Annual Review of Ecology and Systematics 1-32.

Firestein S, Picco C, and Menini A (1993) The relation between stimulus and response in olfactory receptor cells of the tiger salamander. The Journal of Physiology, 468(1), 1-10.

Firestein S (2001) How the olfactory system makes sense of scents. Nature 413:211-218.

Forey PL and Janvier P (1993) Agnathans and origins of vertebrates. Nature 361:129-134.

Friedrich RW, Korsching SI (1997) Combinatorial and chemotopic odorant coding in the zebrafish olfactory bulb visualized by optical imaging. Neuron 18:737-752. 34

Friedrich RW, Korsching SI (1998) Chemotopic, combinatorial, and noncombinatorial odorant representations in the olfactory bulb revealed using a voltage-sensitive axon tracer. Journal of Neuroscience 18:9977-9988.

Frings S, and Lindemann B (1991) Current recording from sensory cilia of olfactory receptor cells in situ. I. The neuronal response to cyclic nucleotides. The Journal of general physiology, 97(1), 1-16.

Frontini A, Zaidi AU, Hua H, Wolak TP, Greer CA, Kafitz KW, Li WM, Zielinski BS (2003) Glomerular territories in the olfactory bulb from the larval stage of the sea lamprey Petromyzon marinus. J Comp Neurol 465:27-37.

Gray JM, Hill JJ, Bargmann CI (2005) A circuit for navigation in Caenorhabditis elegans. P Natl Acad Sci USA 102:3184-3191.

Green WW, Basilious A, Dubuc R, Zielinski BS (2013) The neuroanatomical organization of projection neurons associated with different olfactory bulb pathways in the sea lamprey, Petromyzon marinus. PLoS One 8:e69525.

Green WW, Boyes K, McFadden C, Daghfous G, Auclair F, Zhang H, Li W, Dubuc R, Zielinski BS (2017) Odorant organization in the olfactory bulb of the sea lamprey. Journal of Experimental Biology. 0, 1-10 dio:10.1242/jeb.150466.

Greer PL, Bear DM, Lassance JM, Bloom ML, Tsukahara T, Pashkovski SL, Masuda FK, Nowlan AC, Kirchner R, Hoekstra HE, Datta SR (2016). A family of non-GPCR chemosensors defines an alternative logic for mammalian olfaction. Cell, 165(7): 1734-1748.

Hagelin L Johnels AG (1955) On the structure and function of the accessory olfactory organ in lampreys. Acta Zool 36:113-125.

Hara TJ. (1986) Role of olfaction in fish behaviour. The behaviour of teleost fishes. Springer US. 152-176.

Hara TJ (1994) The diversity of chemical stimulation in fish olfaction and gustation, Rev. Fish Biol. Fish. 4:1-35.

Hara TJ, Zielinski B (2007) Olfaction. SensorySystems Neuroscience (Oxford:ElsevierAcademic Press) 1–43.

Hardisty MW (1965) Sex differentiation and gonadogenesis in lampreys (Parts I and II). Proc Zool Soc Lond 146:346-387.

Hasler AD and Scholz AT (1983) Olfactory Imprinting and Homing in Salmon. Berlin, New York: Springer-Verlag.

Hildebrand JG, Shepherd GM (1997) Mechanisms of olfactory discrimination: Converging evidence for common principles across phyla. Annu Rev Neurosci 20:595-631.

Iwema CL, Fang HS, Kurtz DB, Youngentob SL, Schwob JE (2004) Odorant receptor expression patterns are restored in lesion-recovered rat olfactory epithelium. Journal of Neuroscience 24:356-369.

Johnson BA, Woo CC, Leon M (1998) Spatial coding of odorant features in the glomerular layer of the rat olfactory bulb. J Comp Neurol 393:457-471.

Johnson NS, Siefkes MJ, Li W (2005) Capture of ovulating female sea lampreys in traps baited with spermiating male sea lampreys. N Am Fish Manage 25:67---72.

Johnson BA, Leon M (2007) Chemotopic odorant coding in a mammalian olfactory system. J Comp Neurol 503:1-34.

Johnson NS, Yun SS, Thompson HT, Brant CO, Li W (2009) A synthetized pheromone induces upstream movement in female sea lamprey and summons them into traps. Proc Natl Acad Sci USA 106:1021---1026.

Kaissling KE (1971) Insect olfaction. Olfaction. Springer Berlin Heidelberg 351-431.

Kaissling KE, and Kramer E (1990) Sensory basis of pheromone-mediated orientation in moths. Verhandlungen der Deutschen Zoologischen Gesellschaft, 83, 109-131.

Kleerekoper H (1972) The sense organs. In: Hardisty, M.W. and I.C. Potter (eds) The Biology of Lampreys. Academic Press, New York 2:373–404.

Laberge F and Hara TJ (2001) Neurobiology of fish olfaction: a review. Brain Res Rev 36:46-59.

Laframboise AJ, Ren X, Chang S, Dubuc R, Zielinski B (2007) Olfactory sensory neurons in the sea lamprey display polymorphisms. Neuroscience Letters 414:277-281.

Leinders-Zufall T, Rand MN, Shepherd GM, Greer CA, Zufall F (1997) Calcium entry through cyclic nucleotide-gated channels in individual cilia of olfactory receptor cells: spatiotemporal dynamics. J Neurosci 17:4136–4148.

Li K, Brant CO, Huertas M, Hur SK, Li W (2013) Petromyzonin, a hexahydrophenanthrene sulfate isolated from the larval sea lamprey (Petromyzon marinus L.). Org Lett 15(23):5924-5927.

Li K, Brant CO, Siefkes MJ, Kruckman HG, Li W (2013) Characterization of a novel bile alcohol sulfate released by sexually mature male sea lamprey (Petromyzon marinus). PLoS One. 8(7):e68157.

Li K, Siefkes MJ, Brant CO, Li W (2012) Isolation and identification of petromyzestrosterol, a polyhydroxysteroid from sexually mature male sea lamprey (Petromyzon marinus L.). Steroids 77(7):806-10.

Li W (1994) The olfactory biology of adult sea lamprey. University of Minnesota.

Li W, Scott AP, Siefkes, MJ, Yan H, Liu Q, Yun SS (2002) Bile acid secreted by male sea lamprey that acts as a sex pheromone. Science 296:138-141.

Li W, Sorensen PW (1992) The olfactory sensitivity of sea lamprey to amino acids is specifically restricted to arginine. Chem. Senses 17, 658.

Li W, Sorensen PW, Gallaher DG (1995) The olfactory system of the migratory sea lamprey (Petromyzon marinus) is specifically and acutely sensitive to unique bile acids released by conspecific larvae. J Gen Physiol 105:569---587.

Libants S, Carr K, Wu H, Teeter JH, Chung-Davidson Y, Zhang Z, Wilkerson C, Li W (2009) The sea lamprey Petromyzon marinus genome reveals the early origin of several chemosensory receptor families in the vertebrate lineage. BMC Evolutionary Biology 9.1: 180.

Lim H, and Sorensen PW (2011) Polar metabolites synergize the activity of prostaglandin F2α in a species-specific hormonal sex pheromone released by ovulated common carp. Journal of chemical ecology, 37(7), 695-704.

Luehring MA, Wagner CM, Li W (2010) The efficacy of two synthesized sea lamprey sex pheromone components as a trap lure when placed in direct competition with natural male odors. Biological Invasions 13(7):1589-1597.

Ma MH (2007) Encoding olfactory signals via multiple chemosensory systems. Crit Rev Biochem Mol Biol 42:463-480.

Mallatt J (1983) Laboratory growth of larval lamprey [Lampetra (Entosphenus) tridentata Richardson] at different food concentrations and animal densities. J. Fish Biol. 22: 293–301.

Mewes KR, Latz M, Golla H, Fischer A (2002) Vitellogenin from female and estradiol-stimulated male river lampreys (Lampetra fluviatilis L.). J Exp Zool 292:52-72.

Miyamichi K, Serizawa S, Kimura HM, Sakano H (2005) Continuous and overlapping expression domains of odorant receptor genes in the olfactory epithelium determine the dorsal/ventral positioning of glomeruli in the olfactory bulb. Journal of Neuroscience 25:3586-3592.

Moore HH, Schleen LP (1980) Changes in spawning runs of sea lamprey (Petromyzon marinus) in selected streams of Lake Superior after chemical control. Canadian Journal of Fisheries and Aquatic Sciences 37(11): 1851-1860.

Nara K, Saraiva LR, Ye X, and Buck LB (2011) A large-scale analysis of odor coding in the olfactory epithelium. Journal of Neuroscience, 31(25), 9179-9191.

Ngai, J., Chess, A., Dowling, M. M., Necles, N., Macagno, E. R. and Axel, R. (1993). Coding of olfactory information: Topography of odorant receptor expression in the catfish olfactory epithelium. Cell 72, 667-680.

Nikonov AA, Caprio J (2001) Electrophysiological evidence for a chemotopy of biologically relevant odors in the olfactory bulb of the channel catfish. J Neurophysiol 86:1869-1876.

Ren X, Chang S, Laframboise A, Green W, Dubuc R, Zielinski B (2009) Projections from the Accessory Olfactory Organ into the Medial Region of the Olfactory Bulb in the Sea Lamprey (Petromyzon marinus): A Novel Vertebrate Sensory Structure? J Comp Neurol 516:105–116.

Ressler KJ, Sullivan SL, Buck LB (1993) A Zonal Organization of Odorant Receptor Gene-Expression in the Olfactory Epithelium. Cell 73:597-609.

Ressler KJ, Sullivan SL, Buck LB (1994) Information Coding in the Olfactory System - Evidence for a Stereotyped and Highly Organized Epitope Map in the Olfactory-Bulb. Cell 79:1245-1255.

Restrepo D, Teeter JH, Schild D (1996) Second messenger signaling in olfactory transduction. J Neurobiol 30:37-48.

Rubin BD and Katz LC (1999) Optical imaging of odorant representations in the mammalian olfactory bulb. Neuron 23, 499–511.

Sansone A, Hassenklöver T, Offner T, Fu X, Holy TE, and Manzini I (2015) Dual processing of sulfated steroids in the olfactory system of an anuran amphibian. Frontiers in cellular neuroscience, 9.

Sato K, Touhara K (2009) Insect olfaction: receptors, signal transduction, and behavior. Results and problems in cell differentiation 47:121-138.

Schild D, Restrepo D (1998) Transduction mechanisms in vertebrate olfactory receptor cells. Physiol Rev 78:429-466.

Schneider D (1969) Insect Olfaction - Deciphering System for Chemical Messages. Science 163:1031-&.

Shepherd GM, Greer CA (1998) Olfactory Bulb. In: The synaptic organization of the brain. 4th Ed. (Shepherd GM, ed), pp 159-204. New York: Oxford University Press.

Siefkes MJ, Scott AP, Zielinski B, Yun SS, Li W (2003) Male sea lampreys, Petromyzon marinus L, excrete a sex pheromone from gill epithelia. Biol Reprod 69:125-132.

Siefkes MJ, & Li W (2004) Electrophysiological evidence for detection and discrimination of pheromonal bile acids by the olfactory epithelium of female sea lampreys (Petromyzon marinus). Journal of Comparative Physiology A, 190(3), 193-199.

Smetana R, Juvin L, Dubuc R, Alford S (2010) A parallel cholinergic brainstem pathway for enhancing locomotor drive. Nat Neurosci 13(6):731-738.

Smetana RW, Alford S, Dubuc R (2007) Muscarinic receptor activation elicits sustained, recurring depolarizations in reticulospinal neurons. J Neurophysiol 97(5):3181-3192.

Smith BR and Tibbles JJ (1980) Sea lamprey (Petromyzon marinus) in Lake Huron, Michigan, and Superior: history of invasion and control, 1936-1090. Canadian Journal of Fisheries and Aquatic Sciences 37, 1780–1801.

Sorensen PW and Stacey NE (1999) Evolution and specialization of fish hormonal pheromones. In R.E.Johnson,D.Müller-Schwarze, and P. W.Sorenson (eds.), Advances in Chemical Signals in Vertebrates, pp. 15–48. Kluwer Academic/Plenum, New York.

Sorensen PW, Vrieze LA (2003) The chemical ecology and potential application of the sea lamprey migratory pheromone. Journal of Great Lakes Research 29, 66-84.

Sorensen PW, Fine JM, Dvornikovs V, Jeffrey CS, Shoa F, Wang J, Vrieze LA, Anderson KR, Hoye TR (2005) Mixture of new sulfated steroids functions as a migratory pheromone in the sea lamprey. Nat Chem Biol 1:324---328.

Speca DJ, Lin DM, Sorensen PW, Isacoff EY, Ngai J, Dittman AH (1999) Functional identification of a goldfish odorant receptor. Neuron 23:487-498.

Stacey NE, Sorensen PW (2006) Reproductive pheromones. In: Sloman K, Balshine S, Wilson R (eds) Behaviour and physiology of fish, volume 24 (fish physiology). Academic Press, New York, pp 359–412.

Stacey NE and Sorensen PW (2009) 18 Hormonal Pheromones in Fish. Hormones, 1, 639-681.

Stengl M, Hatt H, Breer H (1992) Peripheral Processes in Insect Olfaction. Annu Rev Physiol 54:665-681.

Teeter J (1980) Pheromone communication in sea lampreys (Petromyzon marinus): implications United States Fish and Wildlife Service Special Scientific Report. Fisheries Service 55. Upper three Great lakes. Can. J. Fish. Aquat. Sci. 37: 1635–1640.

Tolbert LP, Hildebrand JG (1981) Organization and Synaptic Ultrastructure of Glomeruli in the Antennal Lobes of the Moth Manduca-Sexta - a Study Using Thin-Sections and Freeze-Fracture. Proc R Soc B-Biol Sci 213:279-+.

Tsien RW, Tsien RY (1990) Calcium channels, stores, and oscillations. Annu Rev Cell Biol 6:715–760

vanDenBossche J, Youson JH, Pohlman D, Wong E, Zielinski BS (1997) Metamorphosis of the olfactory organ of the sea lamprey (Petromyzon marinus L): Morphological changes and morphometric analysis. J Morphol 231:41-52.

Vassar R, Chao SK, Sitcheran R, Nunez JM, Vosshall LB, Axel R (1994) Topographic Organization of Sensory Projections to the Olfactory-Bulb. Cell 79:981-991.

Viana Di Prisco GV, Pearlstein E, Le Ray D, Robitaille R, Dubuc R (2000) A cellular mechanism for the transformation of a sensory input into a motor command. J Neurosci 20(21):8169-8176.

Viana Di Prisco GV, Pearlstein E, Robitaille R, Dubuc R (1997) Role of sensory-evoked NMDA plateau potentials in the initiation of locomotion. Science 278:1122-1125.

Wachowiak M and Cohen LB (2001) Representation of odorants by receptor neuron input to the mouse olfactory bulb. Neuron 32.4: 723-735.

Wisenden, B. D. (2015). The cue–signal continuum: a hypothesized evolutionary trajectory for chemical communication in fishes. *Fish pheromones and related cues*, 149-158.

Wong S, Trinh K, Hacker B, Chan G, Lowe G, Gaggar A, Xia Z, Gold G, Storm D (2000) Disruption of the type III adenylyl cyclase gene leads to peripheral and behavioral anosmia in transgenic mice. Neuron 27:487–497.

Youson JH (2003) The biology of the metamorphosis in sea lampreys; endocrine, environmental, and physiological cues and events and their potential application to lamprey control. Journal of Great Lakes Research 29, 26–49.

Electronic References:

Great Lakes Fishery Commission. 2001. Strategic Vision of the Great Lakes Fishery Commission for the First Decade of the New Millennium. Ann Arbor, MI, USA.

CHAPTER 3 *THESIS SUMMARY*

3.1 Summary

3.1.1 Overall goal

To understand how odorant mixtures stimulate a behavioural response in the sea lamprey.

3.1.2 General hypothesis

Each olfactory sensory neuron responds to a single pheromone component, rendering pheromone component mixtures more effective in stimulating a behavioural response (as seen in Li *et al.* 2013) than single components.

3.1.3 Brief background information

With its lineage as a basal vertebrate, its relatively large and easily accessible olfactory organs, and its ecological importance as an invasive species to the Laurentian Great Lakes, the sea lamprey has become a model system for the study of fish and vertebrate olfaction (Stoddart 1990). As such, the olfactory-locomotor pathway in the sea lamprey was described by Derjean *et al.* in 2010, Green *et al.* (2013) characterised the organisation of the olfactory bulb including the odour response characteristics of the medial, dorsal, and lateral olfactory bulb regions, showing that pheromones stimulate the dorsal bulbar region, which receives olfactory sensory input from the entire main olfactory epithelium. Various components of a migratory pheromone released by larval stage sea lamprey (Li *et al.* 1995; Bjerselius *et al.* 2000; Sorensen *et al.* 2005) as well as a number of male sex pheromone components (Li *et al.* 2002, 2013; Siefkes *et al.* 2003) have been elucidated with regard to structure. Behavioural studies by Li *et al.* in 2013 investigated the function of male sex pheromones 3-keto petromyzonol sulphate (3kPZS) and 3,12-diketo-4,6-

petromyzonene-24-sulfate (DKPES) and demonstrated reproductive female preference for a

mixture of the two components (2:29.8 DKPES:3kPZS) over 3kPZS used on its own to bait

traps, while DKPES on its own was unable to elicit any behavioural response. Although these

pheromone components elicited electro-olfactogram responses at the level of the olfactory

epithelium, the degree of specificity with which olfactory sensory neurons on the surface of the

epithelium bind various odour ligands is still unknown.

3.1.4 Research aims

1. Determine whether individual olfactory sensory neurons respond to one or to multiple pheromone components.
2. Determine the relative level of neural activity at the level of the olfactory epithelium and olfactory bulb in response to exposure to:
   a) Sex pheromone component combinations compared to the single components of that combination.
   b) Novel putative pheromone components DKPES, PAMS-22, 971, and 973.

3.1.5 Significance

- Determining whether olfactory sensory neurons respond to one ligand or multiple would

  aid in pheromone cocktail design and may help explain observed synergistic effects seen

  in behavioural studies (Li et al. 2013).

- Characterising olfactory bulb responses to new putative pheromones can expand current

  pheromone-based sea lamprey control arsenal while also determining whether

  behavioural studies involving these odours will be worthwhile.

3.1.6 Conclusions

Given that 144 separate OSNs over 29 olfactory epithelium preparations showed high specificity for one particular odorant when presented with multiple, there is appears to be support for the hypothesis that sea lamprey OSNs are very narrowly tuned in terms of odorants to which they respond. OSNs were also often observed responding to a mixture of odorants containing an odorant to which the cell previously responded when the odorant was applied individually.

Four putative sea lamprey pheromone components, 2 male sex pheromone components (DKPES and PAMS-24) and 2 larval pheromone components (971 and 973) were found to elicit olfactory responses from both the peripheral as well as the central olfactory organ. Calcium imaging experiments showed individual OSNs fluorescing upon exposure to each of the four putative pheromone odorants, indicating response elicitation from the sensory cells of the olfactory epithelium (in agreement with earlier electro-olfactogram studies of DKPES (Li *et al.* 2013), PAMS-24, 971, and 973 (Brant 2015). As well, this study found that these four putative pheromone components stimulated LFP activity from the dorsal olfactory bulb region of the sea lamprey upon exposure of the olfactory epithelium to each of the pheromone odorants, indicating the successful relay of sensory information generated at the peripheries of the olfactory system towards the olfactory bulb.

Olfactory bulb LFP response threshold to a number of pheromone components was examined in both spawning-stage and transforming-stage sea lamprey. In general, it was found that the LFP thresholds were lower than the electro-olfactogram thresholds found in the literature for each component tested. The LFP thresholds seemed to agree more with the thresholds for behavioural responses than the electro-olfactogram thresholds, except for 3 larval pheromone

components (PZS, 971, and 973) which exhibit extremely low threshold values (10^{-20} M, 10^{-18} M, and 10^{-18} M respectively) to which there are no published behavioural thresholds to compare.

Finally, an investigation of the potential synergy between pheromone components 3kPZS and DKPES yielded interesting results. The pheromone odorants were applied individually and in a mixture. The DKPES/3kPZS mixture was found to elicit a significantly greater LFP peak amplitude than pheromone component 3kPZS when it was applied individually.

3.1.7 Next steps

This study revealed interesting trends with regard to the relative neural activity elicited from the dorsal olfactory bulb of the sea lamprey in response to various pheromone components tested. However, until the n value on the threshold experiments done with spawning-stage lamprey is increased, robust statistical analysis will not be possible. As such, this should be prioritized, especially given the experimental protocol has been well established, and that the materials needed are not in short supply.

It would also be interesting to then determine the olfactory bulb detection thresholds for transformer-stage lamprey to then allow for comparison between the life stages. The dose-response experiments, carried out on both spawning and transforming-stage lamprey, should also be repeating in order to increase n value. Again, interesting dose-response patterns were brought to light in these experiments, with the two stages seemingly exhibiting different dose-response patterns.

Exploring the response characteristics of OSNs to varying concentrations of a single odorant could prove interesting. The number of responding OSNs to each concentration could be

tracked to determine concentration effects on OSN sensitivity. Sensitivity to pheromone

components could then be compared to that of other odour classes including amino acids.

3.2 Standard operating procedures and protocols

3.2.1 Calcium imaging

1. Switch camera cord to proper computer tower (tape indicates port to insert cord)

2. Turn on Nikon power supply

3. Turn on X-Cite power supply
   i. Wait for it to stop flashing (NB: if it is shut off; requires a 1 h cool down period)

4. Switch lens filter to DIA (blank)

5. Turn on chiller; should be set to 6 ºC (NB: requires ~30 mins to reach temp)

6. Turn on ADI power supply (next to Nikon)

7. Grab water-immersion objective from drawer

8. On computer:
   i. Open Lab Chart (set 10s intervals / pulse duration 5s / 1V amplitude)

   ii. Turn on camera (switch at back, on left)

   iii. Open Metafluor:
      1. Click begin new experiment
      2. Under "status"; click "log data"
         a. Save under "Calcium Imaging" (folder already in existence)
         b. Title experiment as today's data plus your initials
         c. Within folder; make a folder for each odorant tested
      3. Repeat a-c for "Save images" and "Save ratios"

   iv. Click focus

v. Pull slider (on right side of eyepiece)

vi. Click "Start focusing" → make necessary adjustments to expose and gain

vii. Click "Stop focusing"

viii. "Cfg acq" → set exposure time to what it is in "Focus"

ix. "Acq one"

x. Click "Regions"
    1. Click okay
    2. Click on "O"
    3. Circle each corner of field of view + a few cells
    4. Click save

xi. Click "start" on Lab Chart

xii. In Metafluor; click "Zero clock", click "Aquire", and in Lab Chart; enter comment. * **All 3 steps to be done simultaneously** *

xiii. In Lab Chart; Stimulate once (5s) at 100 cycles if the preceding 20 cycles were not noisy. Then stimulate again 200 cycles later

Things to keep in mind:

- The room should be kept as dark as possible
- Care should be taken to not bump the microscope or the table on which it sits
- Gloves should be worse throughout the experiment to prevent your odours from contaminating the ringer's etc.

3.2.1.1 imageJ/Matlab analysis

ImageJ:

1. "File"; "Import"; "Image sequence"
   a. Check Lab Chart file for the experiment that you're analysing to verify when stimulations took place

2. Click "open" on appropriate image
   a. adjust image range from dialogue box
   b. check "sort names numerically"; "okay"

3. Click "image"; "stacks"; "delete slice"

a. Do this while viewing the image you want deleted (the 1st image in a stack tends to be shifted compared to the rest)

4. To establish baseline fluorescence from 20 preceding images before stim:
   a. Click "image"; "stacks"; "z-project"
      i. If you stim'd at 100 c then baseline range is 80-100 c (want 10-20 images for baseline)
      ii. Projection type = "average intensity"

5. Analysis ΔF
   a. "Process"; "Image calc"
      i. Leave image 1 the way it is
      ii. Operation → "subtract"
      iii. Image 2 → "Average.."
      iv. Make sure both boxes are checked; "okay"

6. Analysis ΔF/F
   a. "process"; "image calc"
      i. Image 1 → "Result.."
      ii. Operation → "Divide"
      iii. Image 2 → "Average.."
      iv. Both boxes checked

7. Getting numerical values from processed images:
   a. "Analyze"; "Tools"; "ROI Manager"
      i. Select "freehand" tool and draw around responding cell
      ii. Click "add it"; shift+S; click "yes"
         1. Repeat for all responding cells + 1 non-responding cell (baseline)
      iii. Select all cells; "More"; "Save"
         1. File name should come up as "ROIset" *assuming you selected more than 1 cell*
         * To see all highlighted cells → check "show all"
         *Be sure to have current set of calculated images in view for next steps
   b. "More"; "Multimeasure"; click 1st 2 boxes, not the 3rd
      i. #'s are spit out; should be 0.### (between -1 and 1)
      ii. Save as (excel file)' no need to save other images
   c. Open excel file'; delete 1st row ("Mean 1, Mean 2, etc.."); "save as" Text (File delimited)

Matlab:

1. "Open"; script (a labmate will need to give you the appropriate script)
2. "Run and advance"; open (excel) Text file
3. "Lineplot"; "Colorplot"; or "both" are your options for figure output

3.2.2 Electrophysiology

3.2.2.1 Lab Chart analysis
Steps 1 – 2.c.i. are done 1 time for each odorant delivery regardless of number of peaks analyzed

1. Click start of solenoid trace in channel 3

2. Go to commands
   a. Set selection
   b. Unlick "active point"
   c. Click "as seconds"
      i. Want 5 seconds prior to solenoid onset (adjust time value accordingly)

3. Under channel: unclick channel 3; click channel 1

4. Click "data pad"
   a. Leave yourself 5 columns
      i. Column 1 – mean (ch 1)
      ii. Column 2 – click on "B" change to standard dev (ch 1)
      iii. Column 3 – go to "selection + active point"; click "selection end" (no ch)

5. Go to "Setup"
   a. Display settings
   b. Click "always seconds"
   c. Unlick "display date"
   d. Click "hide grid"
      i. Column 4 – click D; go to "stats"; click on "min value" (ch 1)
      ii. Column 5 – click E; go to "stats"; click on "time at min" (ch 1)

6. Click "Add to data pad"
   a. In upper left corner; click "A"

7. Want "baseline mean" and "baseline standard dev" from excel sheet (excel sheet to be given to you by a labmate)
   a. Get these values from data pad

8. Want "selection end"
   a. Get it from data pad → put it in excel sheet under "time of solenoid"

9. Drag threshold down; #'s will pop up

10. When highlighting a peak; start selection and end of selection should be level with each other (ie the trace)
    a. Add to data pad
       i. Not interested in first 3 values
       ii. Copy "min peak val"; paste in excel sheet under "Peak (min val)"

11. Take "Time of min" from data pad → paste under "Time of peak" in excel sheet

12. Drag and drop the 2 blank columns (response mag)

13. **Need to source the R-code: "EOG extract function messy peaks"
    i. (get this code from a labmate
    ii. File; source R-code → in R program
    iii. File; change dir; c://; users; z lab; desktop; LFP extract

14. In Lab Chart: click edit; copy lab chart data

15. Open new excel file
    a. Paste; unclick comments; unlick ch settings
        i. "Save as" into LFP extract file
            1. CSV, comma delimited

16. Back in R:
    a. EOG.extract2("File_name.csv","Output file_name.csv")
        i. Hit enter
    *** hitting up arrow will paste the previous line of code ***
    b. If flashing red line in R then peak successfully ran through
        i. In EOG extract folder there should now be a file with the same name as before but now with "output" preceding name
            1. Open this file and copy data except for "time"
                a. Paste them in original excel sheet

3.2.2.2 Obtaining local field potential traces

1. Start with black tract (channel 1)

2. drag down channel 1 (with digital filter) to expand the plot area

3. Click channel 1; digital filter; source channel 2; cut off = 100, low pass

4. Setup → display settings:
    - graticule → hide
    - click "always seconds"
    - click "display date"

5. Click on channel 3 on trace where you want to start copying

6. "Command"; "set selection" → "as seconds", "no active point"

7. "Channels" → unclick channel 3, click channel 1 (this will highlight channel 1

8. "Window zoom view" (magnifying glass icon)

9. "Stacked mode" (button on left; 4 buttons)

10. "Zoom in axis" *** keep all axis the same across all traces for a figure ***

11. "Edit" → copy zoom view

In Illustrator:

1. "File"; "new"; "landscape"

2. "Paste"

3. "View" → "outline"

4. Get rid of everything but the trace
    o   Ungroup
    o   Green lights up; right click; release clipping mask (x2)
    o   Delete; keep trace and axis

5. Click line segment tool; make x-axis of scale 1 second long; make y-axis of scale 100 um high → put both segments together and group

6. Group trace

7. Group with scale

8. Move to sheet

9. If it doesn't fit; artboard tool (#) to expand sheet

10. Save as jpeg; File → export; click "use artboard"

3.3 Practical lab information

3.3.1 Solution recipes

Molecule	Amount to add	Amount of solute	Final concentration
L-arginine	0.01742g	10mL ringer's	10^{-2} M
L-histidine	0.01552g	10mL ringer's	10^{-2} M
TCA	0.053768g	10mL ringer's	10^{-2} M
L-serine	0.010509g	10mL ringer's	10^{-2} M
L-glutamine	0.014615g	10mL ringer's	10^{-2} M
L-proline	0.02303g	20mL ringer's	10^{-2} M
L-glutamine	0.01502g	20mL ringer's	10^{-2} M
NaOH	10g	50mL DI H_2O	5 M
NaCl	5.84g	50mL DI H_2O	2 M

3.3.2 Pheromone component formula weights

Pheromone odorant	Aliquot volume (µL)	Into x µL of ringer's	Final concentration
3kPZS	49	9951	10-5 M
DKPES	49.5	9950.5	10-5 M
PAMS-24	64.6	9935.4	10-5 M
971	33	9967	10-5 M
973	33	9967	10-5 M
PZS	47.85	9952.15	10-5 M
PSDS	62.6	9937.4	10-5 M
PADS	74	9926	10-5 M
3kACA	40.6	9959.4	10-5 M

3.3.3 Triton x-100 recipe:

For 10 mL of Triton solution in DI water:
    10 mM NaCl, 0.1% triton 100x

    Add:
- 0.005844 g NaCl
- 10 uL Triton 100x (100x is part of its name)
- 9.99 mL DI water

* Aliquot into 100 uL and store in -20oC.

We then add a triton aliquot to an aliquot of calcium green dextran (a few crystals) and apply into the epithelium.

3.3.4 Anesthetizing lamprey:

Larvae/Transformers – 0.03g of MS-222 per 100mL (0.3g/L)

Spawners – 0.6g of MS-222 per 1L

APPENDIX: Supplementary Tables and Figures

Name	Origin	Behavioural Output	EOG Threshold
3kPZS	Spermiated male	Sex pheromone component; attracts ovulating females	10^{-10} M
DKPES*	Spermiated male	None on its own (synergistic affect in conjunction with 3kPZS	10^{-7} M
971*	Larva	TBD	10^{-11} M
973*	Larva	TBD	10^{-11} M
PAMS-24*	Spermiated male	Sex pheromone component advertising nest boundaries	10^{-12} M
PADS	Larva	Migratory pheromone component	10^{-13} M
PSDS	Larva	Migratory pheromone component	10^{-13} M
3kACA	Spermiated male	Suspected male sex pheromone component	10^{-10} M
PZS	Larva	Migratory pheromone component	10^{-12} M
ACA	Larva	Migratory pheromone component	10^{-10} M

Table A-1. A summation of the sea lamprey behavioural and EOG response data to pheromone components. Reported by Li *et al.* 2002 (3kPZS); Li *et al.* 2013 (DKPES); Brant 2015 (971, 973, and PAMS-24); Sorensen *et al.* 2005 (PSDS and PADS); Siefkes *et al.* 2003 (3kACA); Li *et al.* 1995 (PZS); and Bjerselius *et al.* 2000 (ACA).

Name	Origin	Behavioural Output	EOG Threshold	Local Field Potential	Calcium Imaging
3kPZS	Spermiated male	Sex pheromone component; attracts ovulating females	10^{-10} M	●	●
DKPES*	Spermiated male	None on its own (synergistic affect in conjunction with 3kPZS	10^{-7} M	●	●
971*	Larva	TBD	10^{-11} M	●	●
973*	Larva	TBD	10^{-11} M	●	●
PAMS-24*	Spermiated male	Sex pheromone component advertising nest boundaries	10^{-12} M	●	●
PADS	Larva	Migratory pheromone component	10^{-13} M	●	
PSDS	Larva	Migratory pheromone component	10^{-13} M	●	●
3kACA	Spermiated male	Suspected male sex pheromone component	10^{-10} M	●	
PZS	Larva	Migratory pheromone component	10^{-12} M	●	●
ACA	Larva	Migratory pheromone component	10^{-10} M	●	

Table A-2. A summation of the response data garnered from each pheromone component tested in this study as well as the behavioural output and EOG threshold of each component from the literature. Behavioural and EOG data reported by Li *et al.* 2002 (3kPZS); Li *et al.* 2013 (DKPES); Li (unpublished) (971, 973, and PAMS-24); Sorensen *et al.* 2005 (PSDS and PADS); Siefkes *et al.* 2003 (3kACA); Li *et al.* 1995 (PZS); and Bjerselius *et al.* 2000 (ACA). Newly identified putative pheromone components are denoted by *. Responses obtained from application of the associated odorant with the associated recording method are denoted by ●.
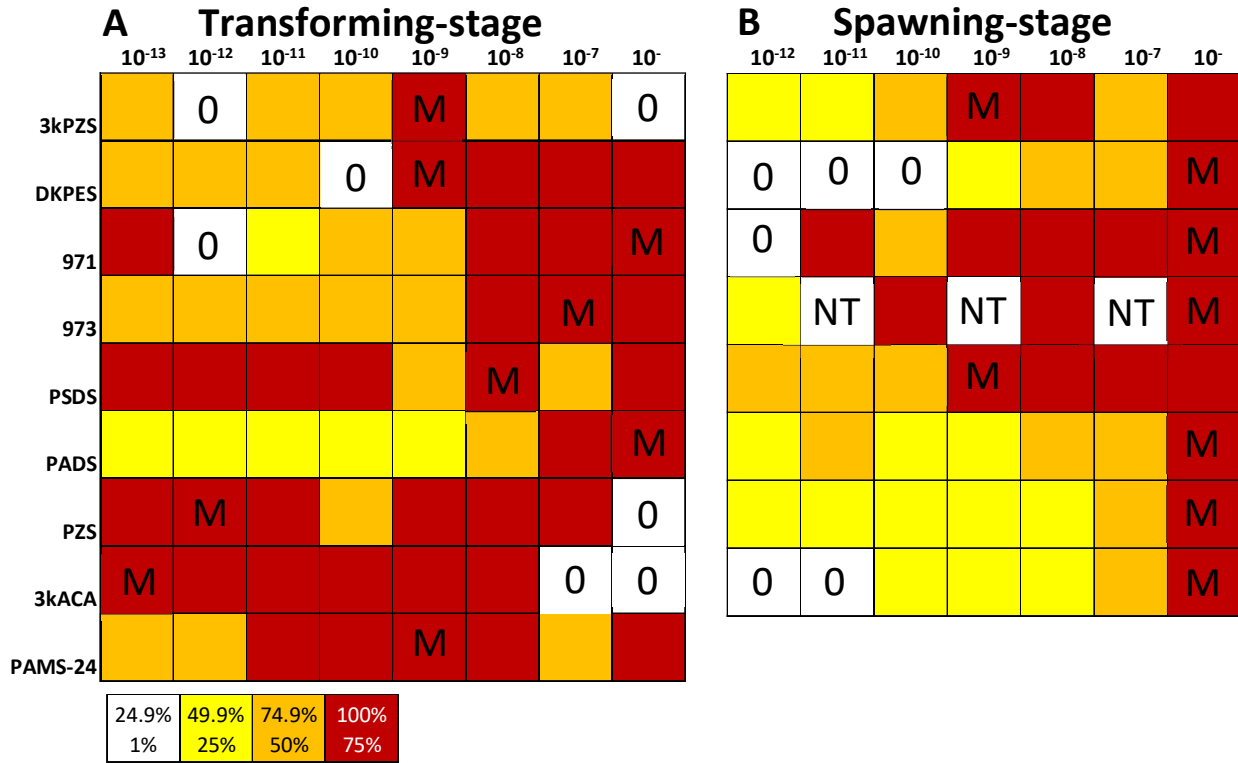
Figure A-1. Average electrophysiological (local field potential) response peak amplitudes recorded from the dorsal olfactory bulb surface of spawning-stage (A) and transformer-stage (B) sea lamprey. Each row represents a concentration series (10^{-12} M through 10^{-6} M for spawners and 10^{-13} M through 10^{-6} M for transformers) of a pheromone component delivered to the peripheral olfactory organ. The magnitude of the response amplitude (each cell) is expressed as a percentage (shaded box drawing) of the maximum response from that concentration series (M). Cells denoted with "0" indicate that a response was not detectable while cells denoted with "NT" represent concentrations not tested for the associated odorant.
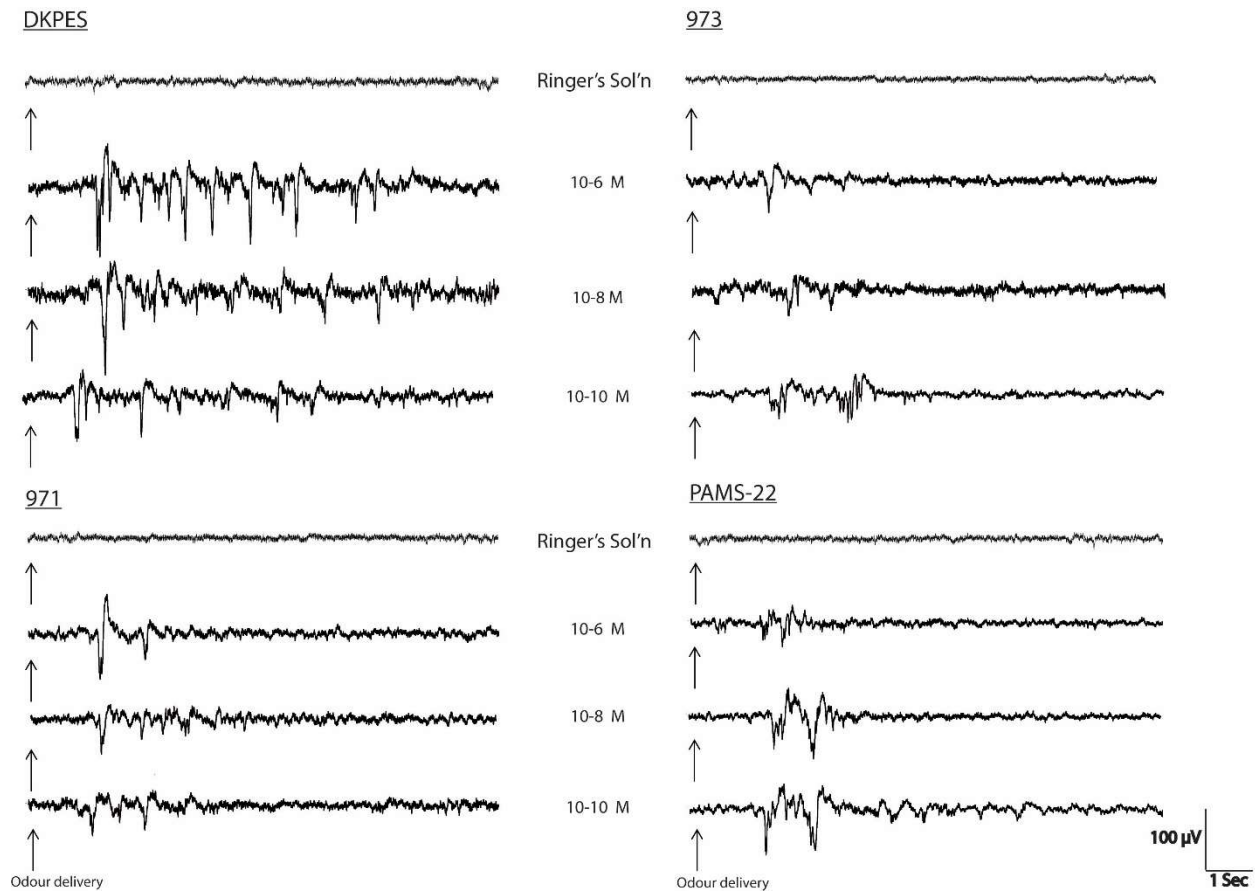
Figure A-2. Raw local field potential data in response to various concentrations of putative sea lamprey pheromone components DKPES, 973, 971, and PAMS-22. Arrows indicate the end of the odour delivery period for each local field potential recording.
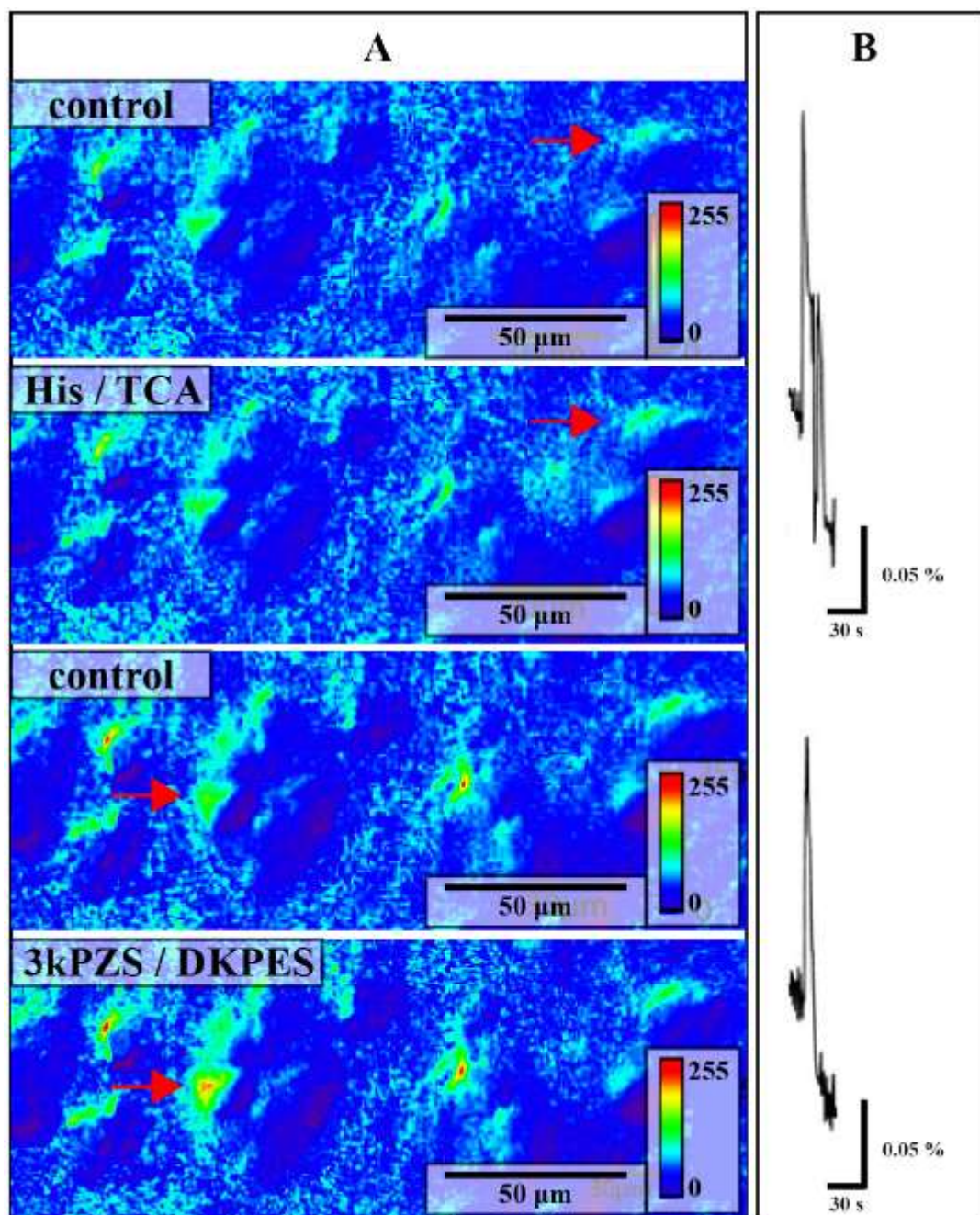
Figure A-3. Changes in fluorescence reflecting OSN responses to chemical stimuli. (A) A colour contour map was applied to the field of view to visually monitor changes in fluorescence of calcium green loaded OSNs. Blue represents less fluorescence and red represents more fluorescence. (B) Regions with Ca2+ transients are indicated by red arrows. Increases in fluorescence can be observed in both instances after a chemical stimulus was applied compared to immediately before the stimulus was applied. Note that different cells responded to the two mixtures. As well, a cluster of cells responded to 10-6M 3kPZS and DKPES. (B) Ca2+ transients of the indicated OSNs in (A).
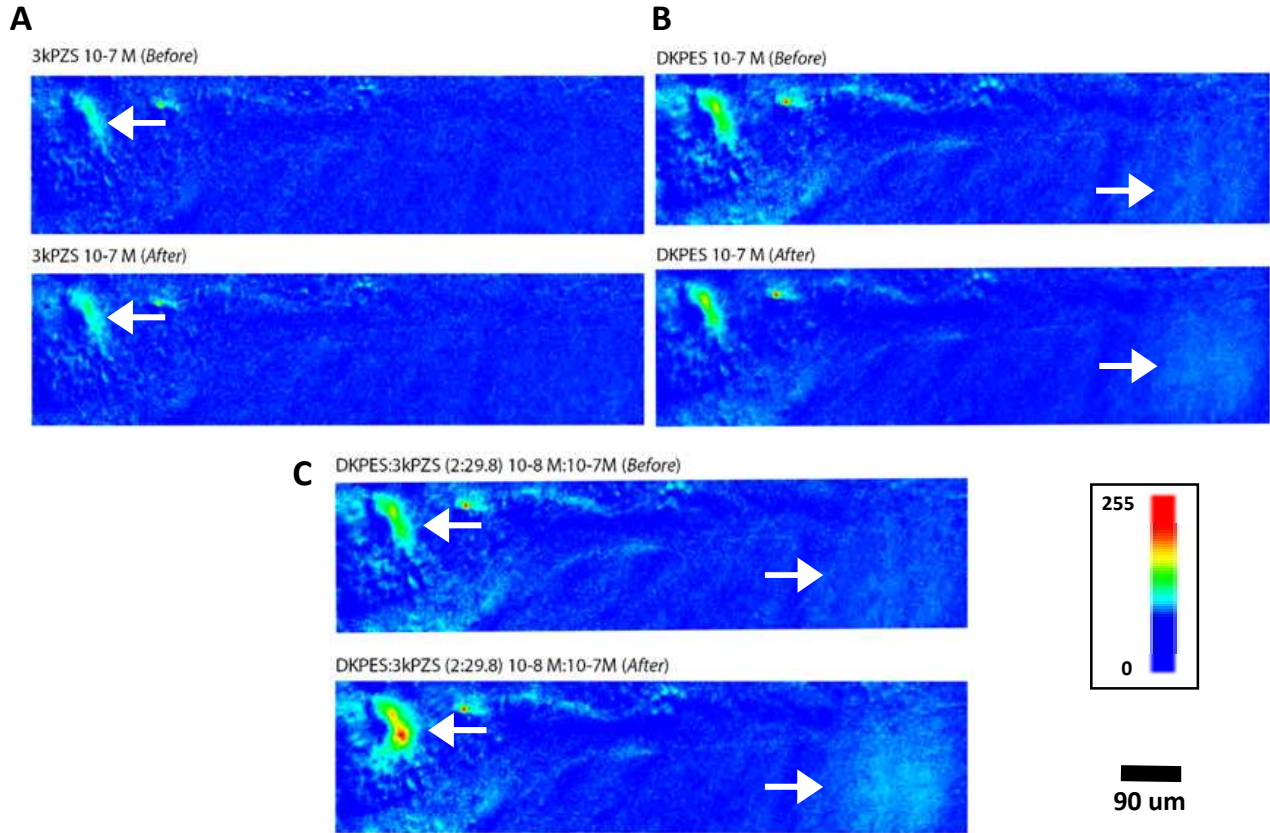
Figure A-4. Calcium imaging data collected from a transformer stage sea lamprey in response to male sex pheromone odorants 3kPZS and DKPES. A heat contour map was applied to each image ranging from blue (no fluorescence) to red (highest fluorescence). Panels A-C depict the same two OSNs in the same field of view with arrows indicating the fluorescing OSN in each case. Panel A shows the OSN on the left fluorescing in response to 3kPZS being applied to the epithelium at a concentration of 10^{-7} M while the right OSN does not respond. Panel B shows the OSN on the right responding to DKPES being applied at a concentration of 10^{-7} M while the left OSN does not respond. Finally, panel C shows both OSNs fluorescing in response to a mixture of both 3kPZS and DKPES components being applied simultaneously at 10^{-7} M.
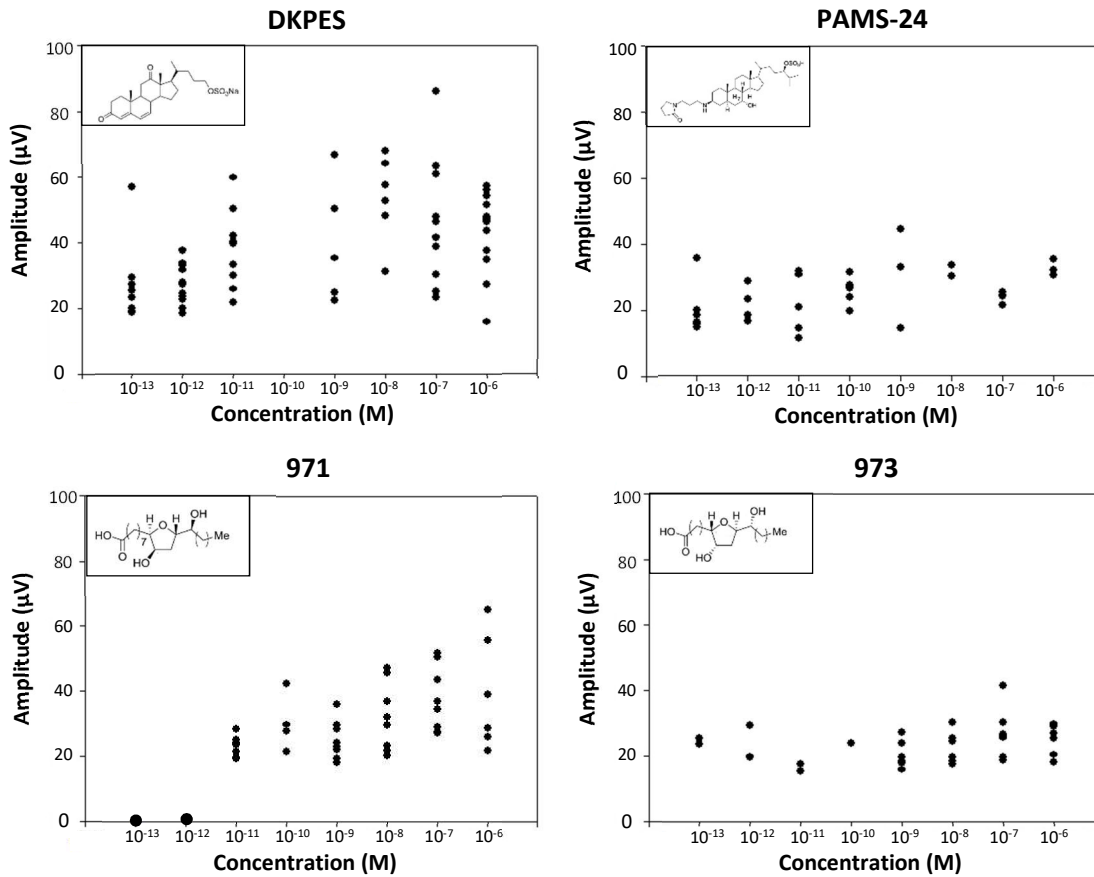
Figure A-5 Amplitude values of transformer stage sea lamprey LFP responses to four different putative pheromone components to a standardized concentration gradient ranging from 10^{-13} M to 10^{-6} M. Each point represents a single peak generated during a response to the associated odorant stimulus.
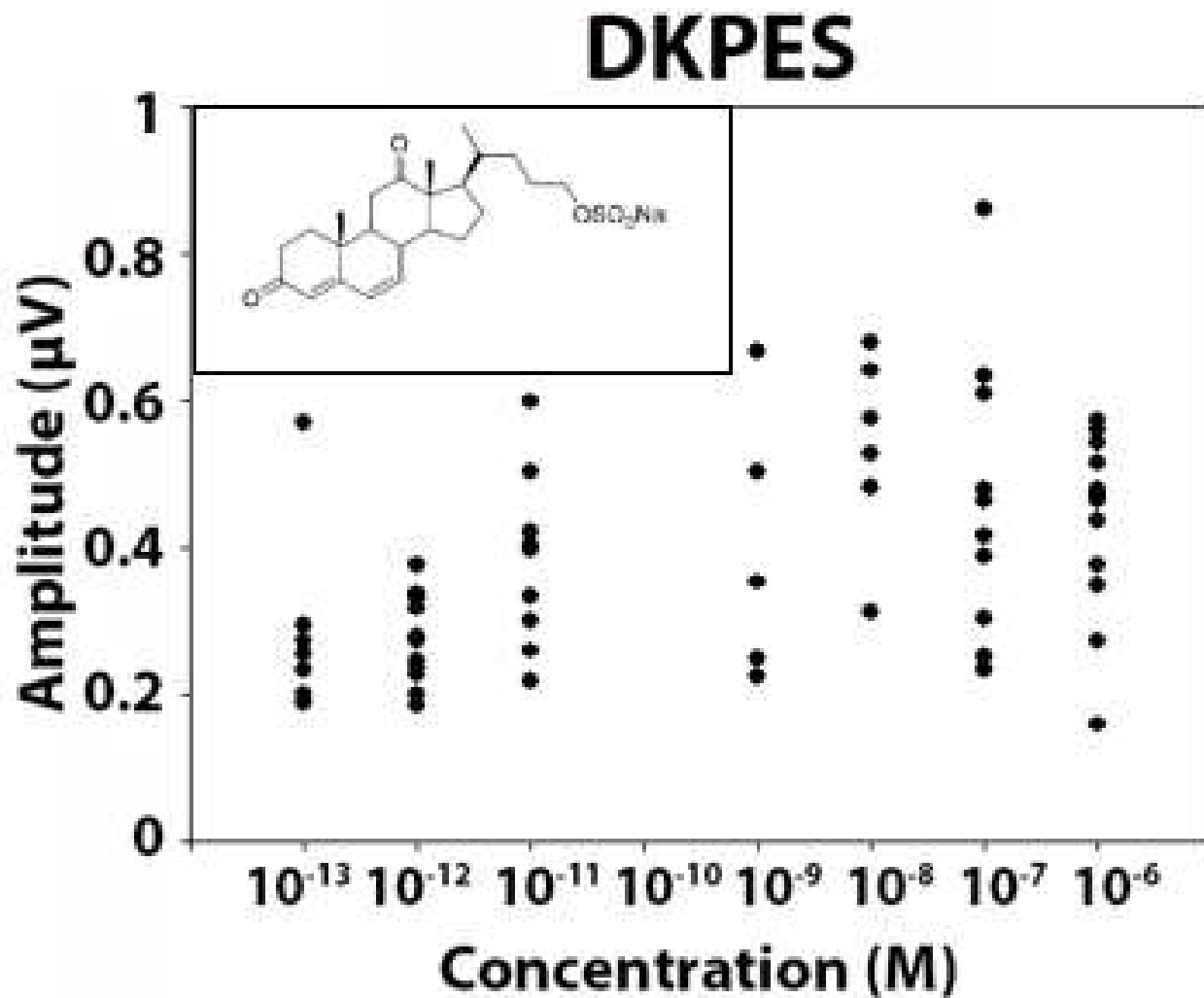
Figure A-6. Amplitude values of transformer stage sea lamprey LFP responses to putative male sex pheromone component DKPES over a standardized concentration gradient ranging from 10^{-13} M to 10^{-6} M. Each point represents a single peak generated during a response to the associated odorant stimulus (n=1).
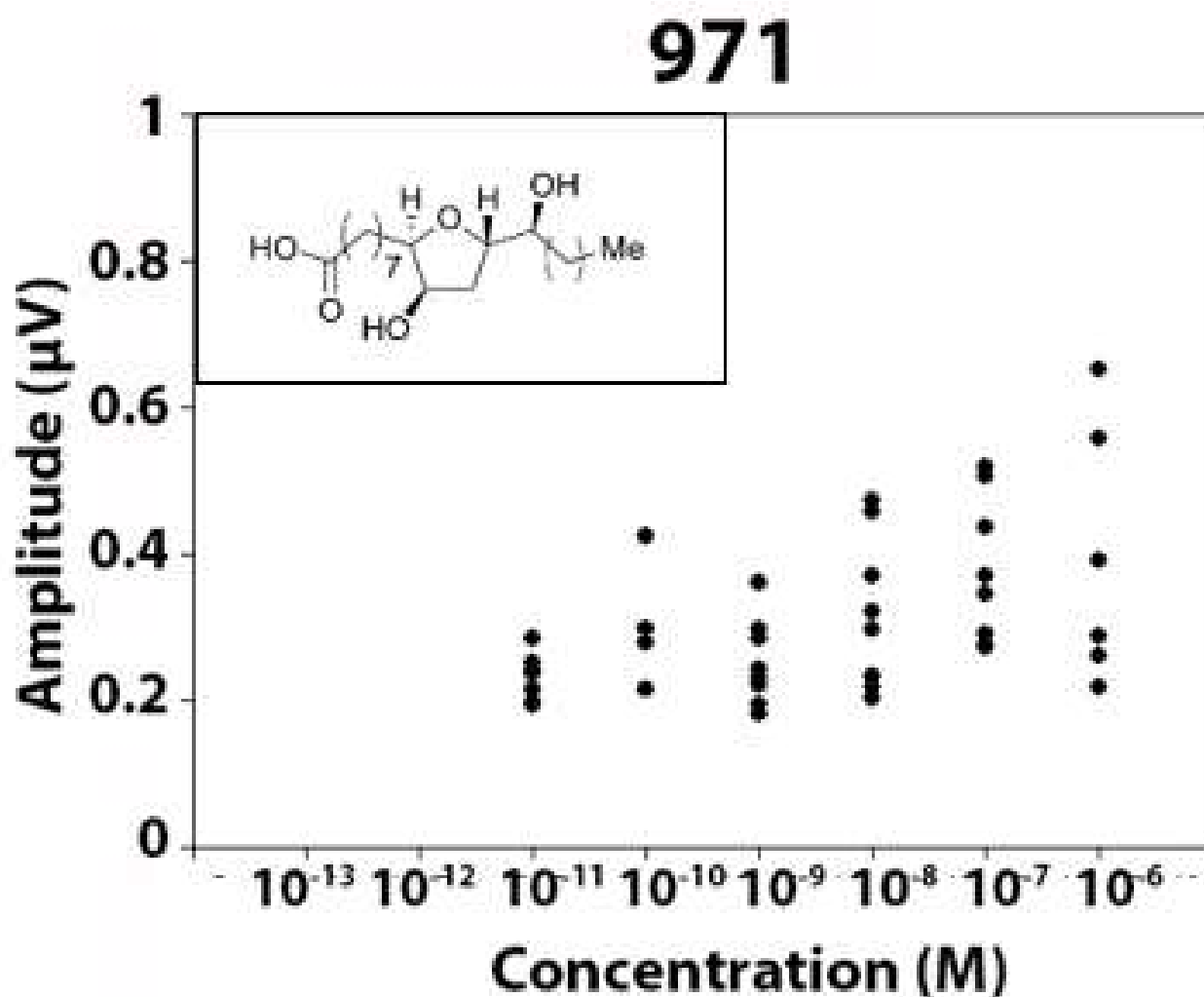
Figure A-7. Amplitude values of transformer stage sea lamprey LFP responses to putative larval pheromone component 971 over a standardized concentration gradient ranging from 10^{-13} M to 10^{-6} M. Each point represents a single peak generated during a response to the associated odorant stimulus (n=1).

973
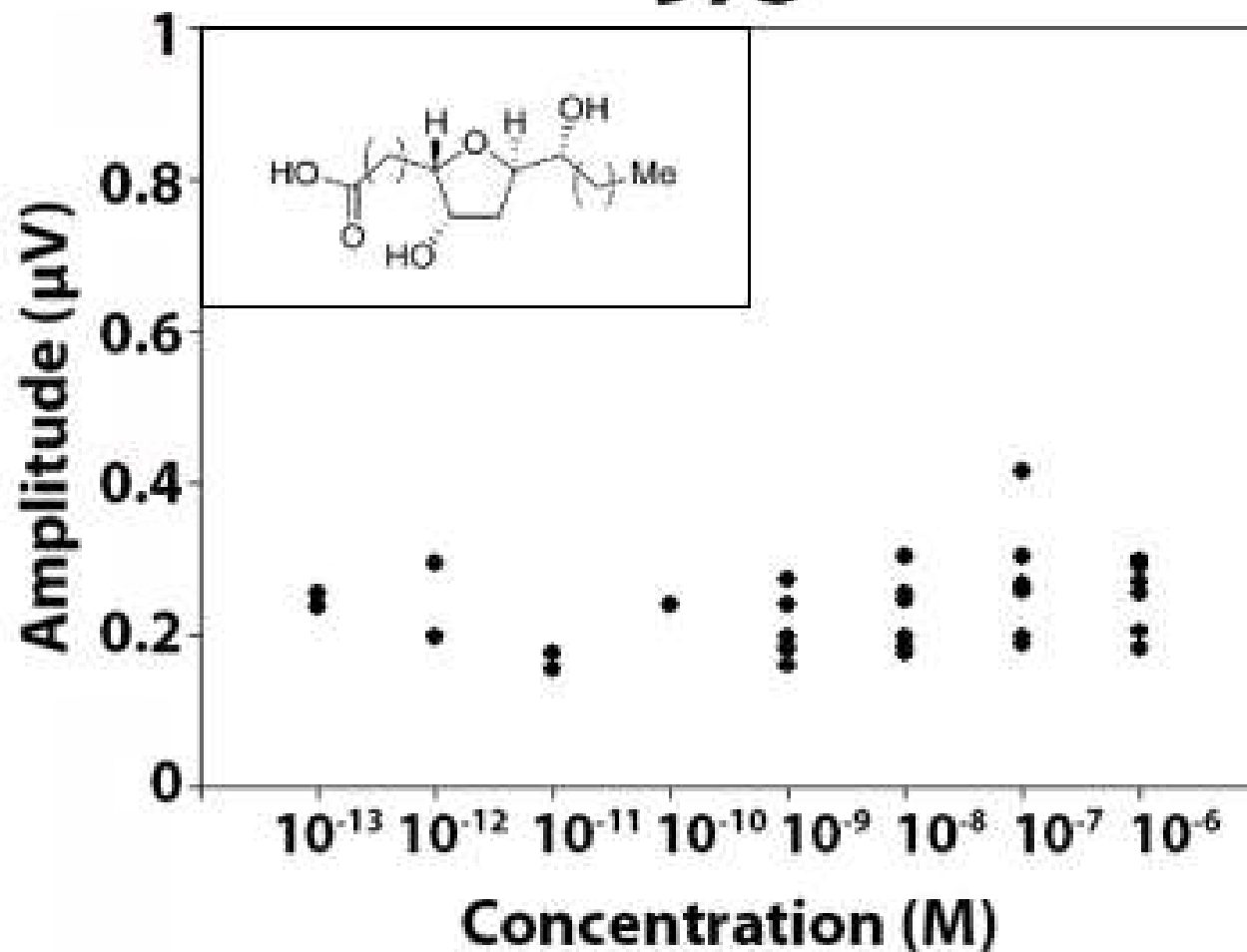
Figure A-8. Amplitude values of transformer stage sea lamprey LFP responses to putative larval pheromone component 973 over a standardized concentration gradient ranging from 10^{-13} M to 10^{-6} M. Each point represents a single peak generated during a response to the associated odorant stimulus (n=1).
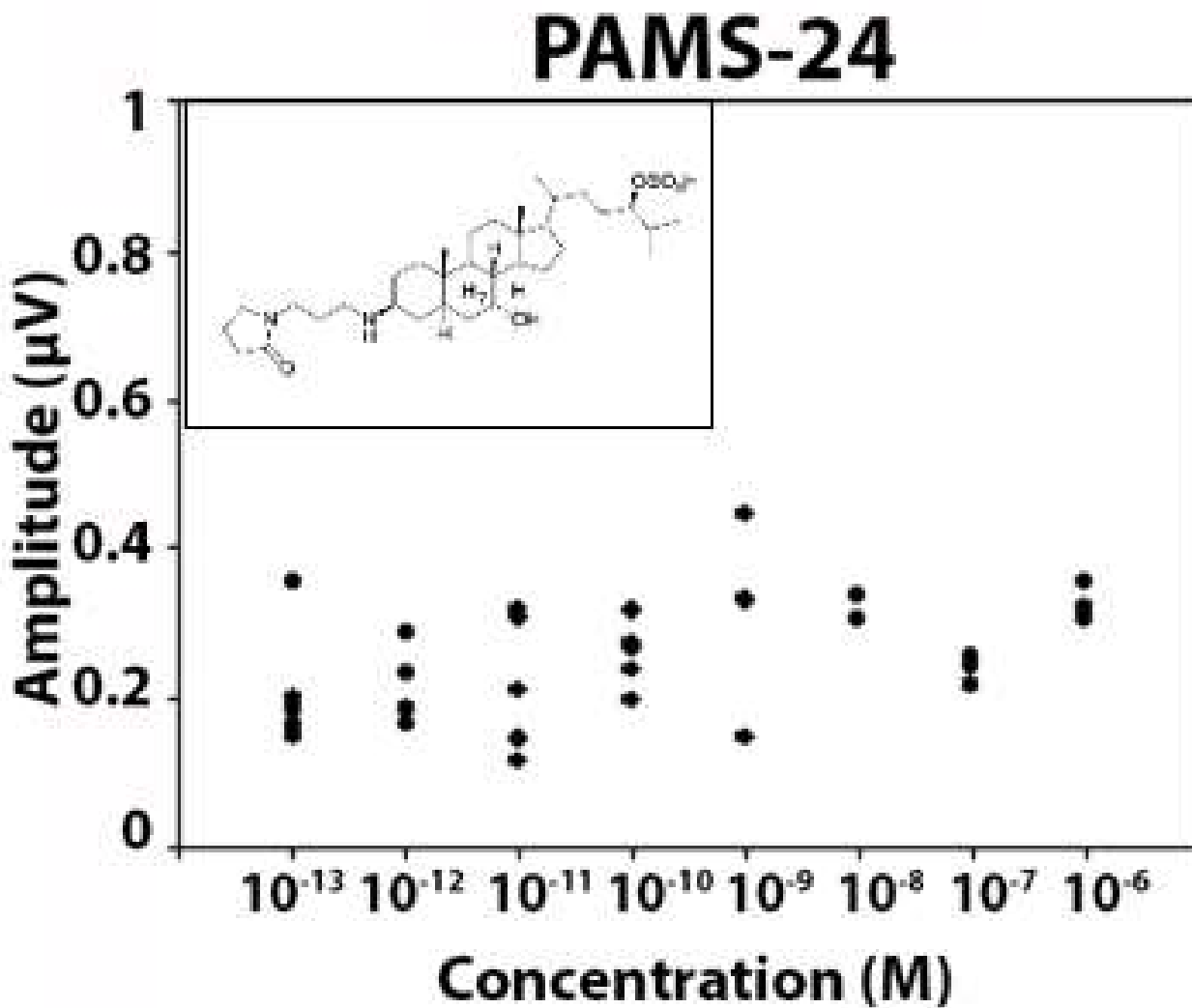
Figure A-9. Amplitude values of transformer stage sea lamprey LFP responses to putative male sex pheromone component PAMS-24over a standardized concentration gradient ranging from 10^{-13} M to 10^{-6} M. Each point represents a single peak generated during a response to the associated odorant stimulus (n=1).
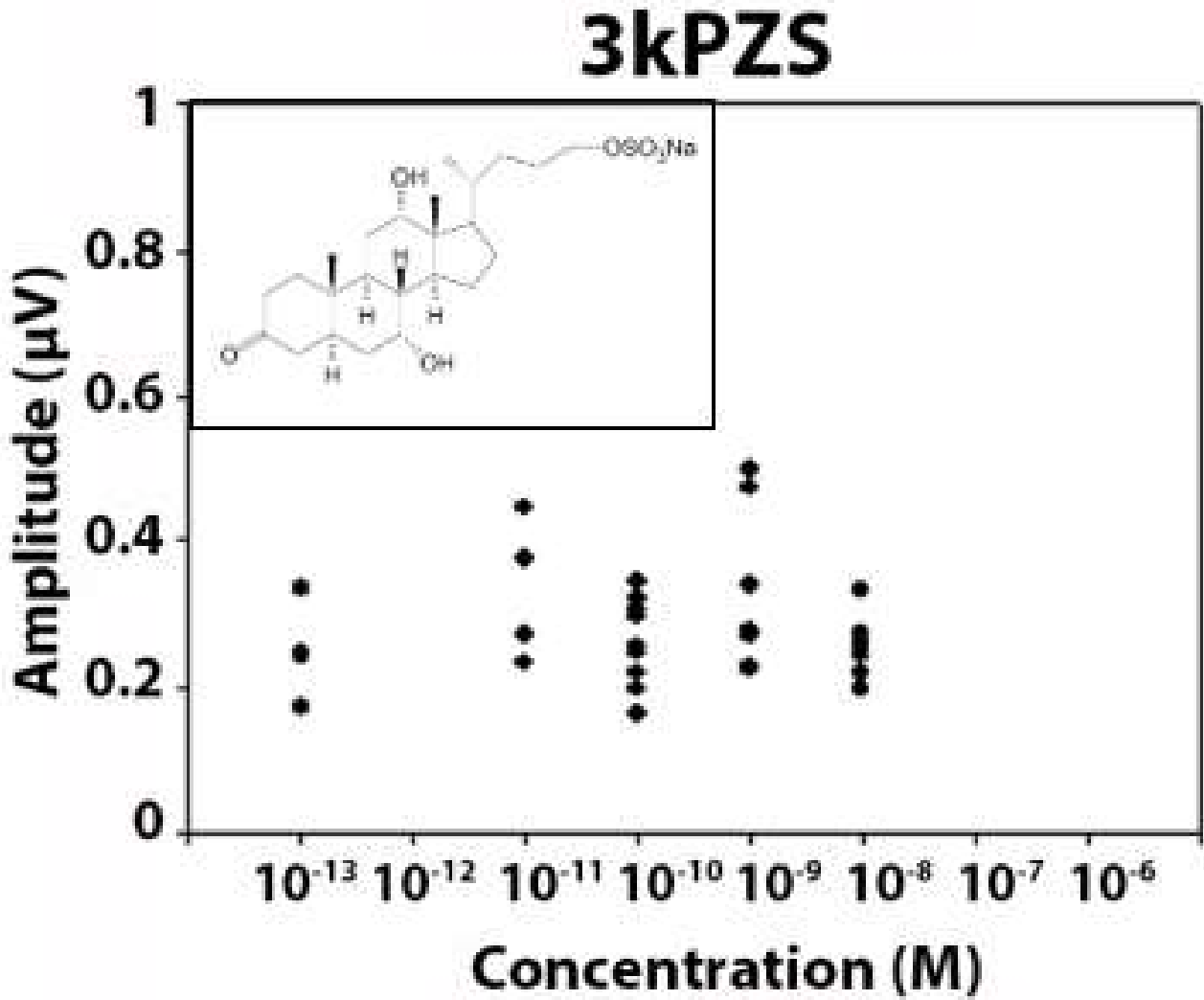
Figure A-10. Amplitude values of transformer stage sea lamprey LFP responses to male sex pheromone component 3kPZS over a standardized concentration gradient ranging from 10^{-13} M to 10^{-6} M. Each point represents a single peak generated during a response to the associated odorant stimulus (n=1).
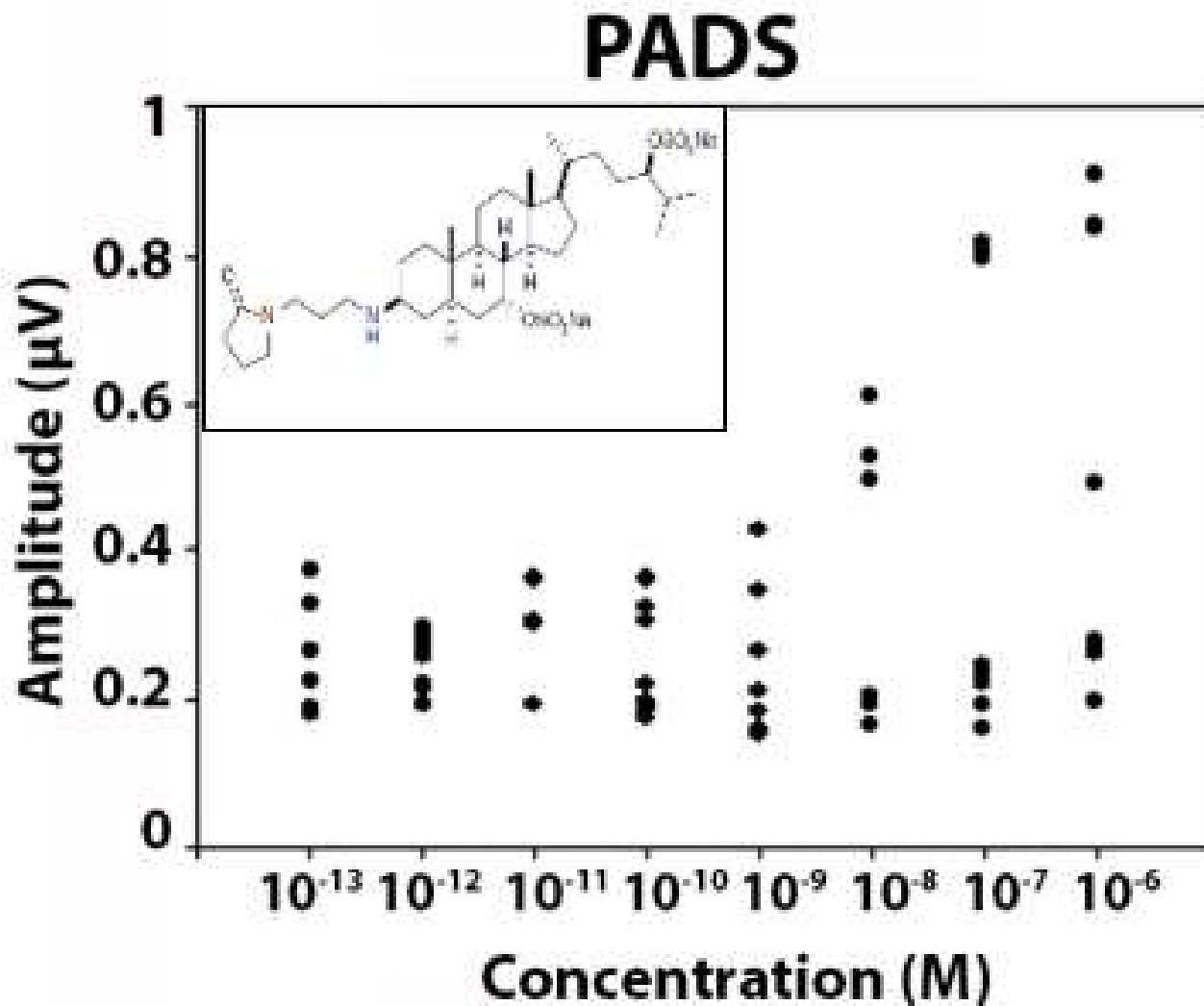
Figure A-11. Amplitude values of transformer stage sea lamprey LFP responses to larval migratory pheromone component PADS over a standardized concentration gradient ranging from 10^{-13} M to 10^{-6} M. Each point represents a single peak generated during a response to the associated odorant stimulus (n=1).
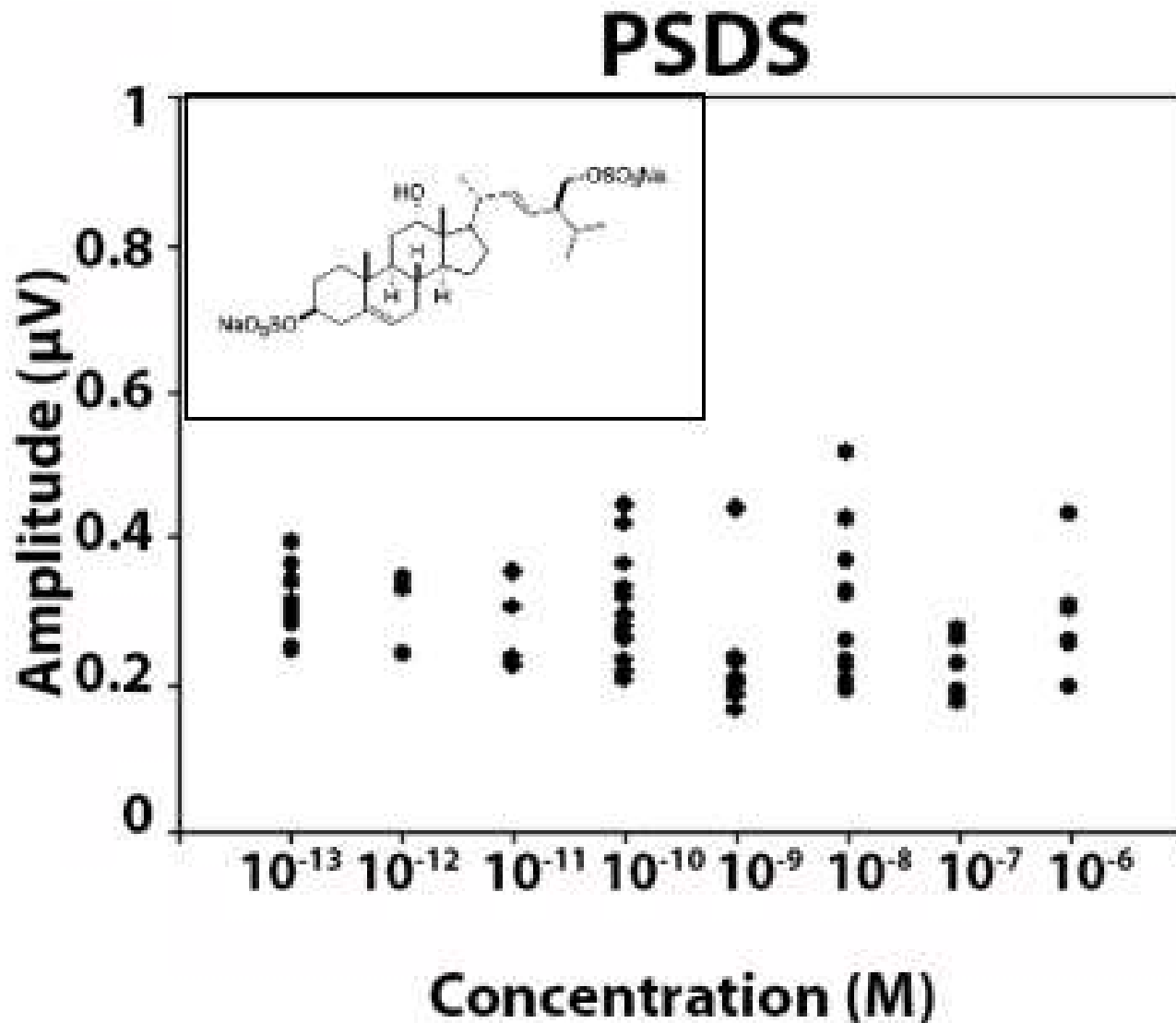
Figure A-12. Amplitude values of transformer stage sea lamprey LFP responses to larval migratory pheromone component PSDS over a standardized concentration gradient ranging from 10^{-13} M to 10^{-6} M. Each point represents a single peak generated during a response to the associated odorant stimulus (n=1).
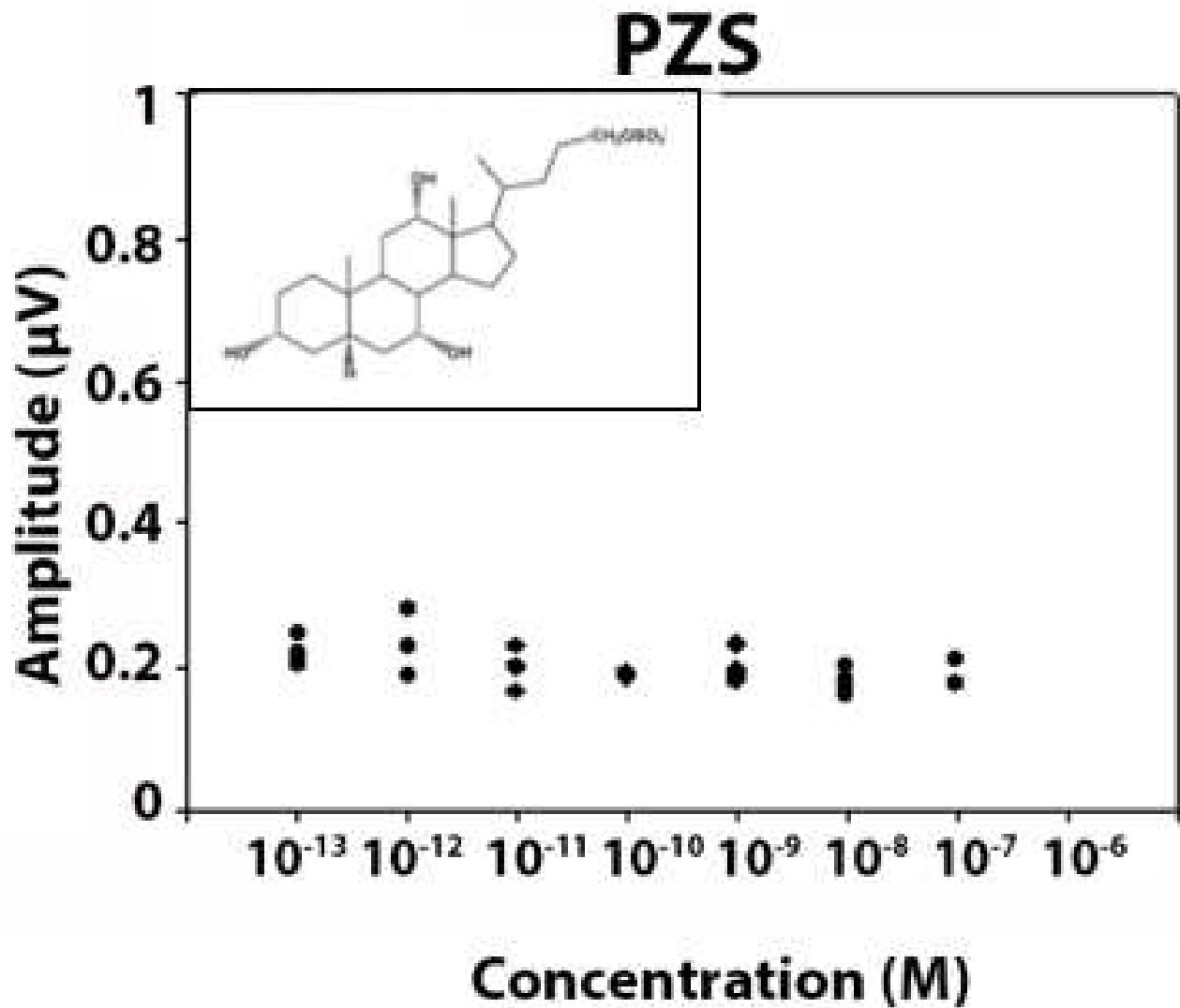
Figure A-13. Amplitude values of transformer stage sea lamprey LFP responses to larval migratory pheromone component PZS over a standardized concentration gradient ranging from 10^{-13} M to 10^{-6} M. Each point represents a single peak generated during a response to the associated odorant stimulus (n=1).
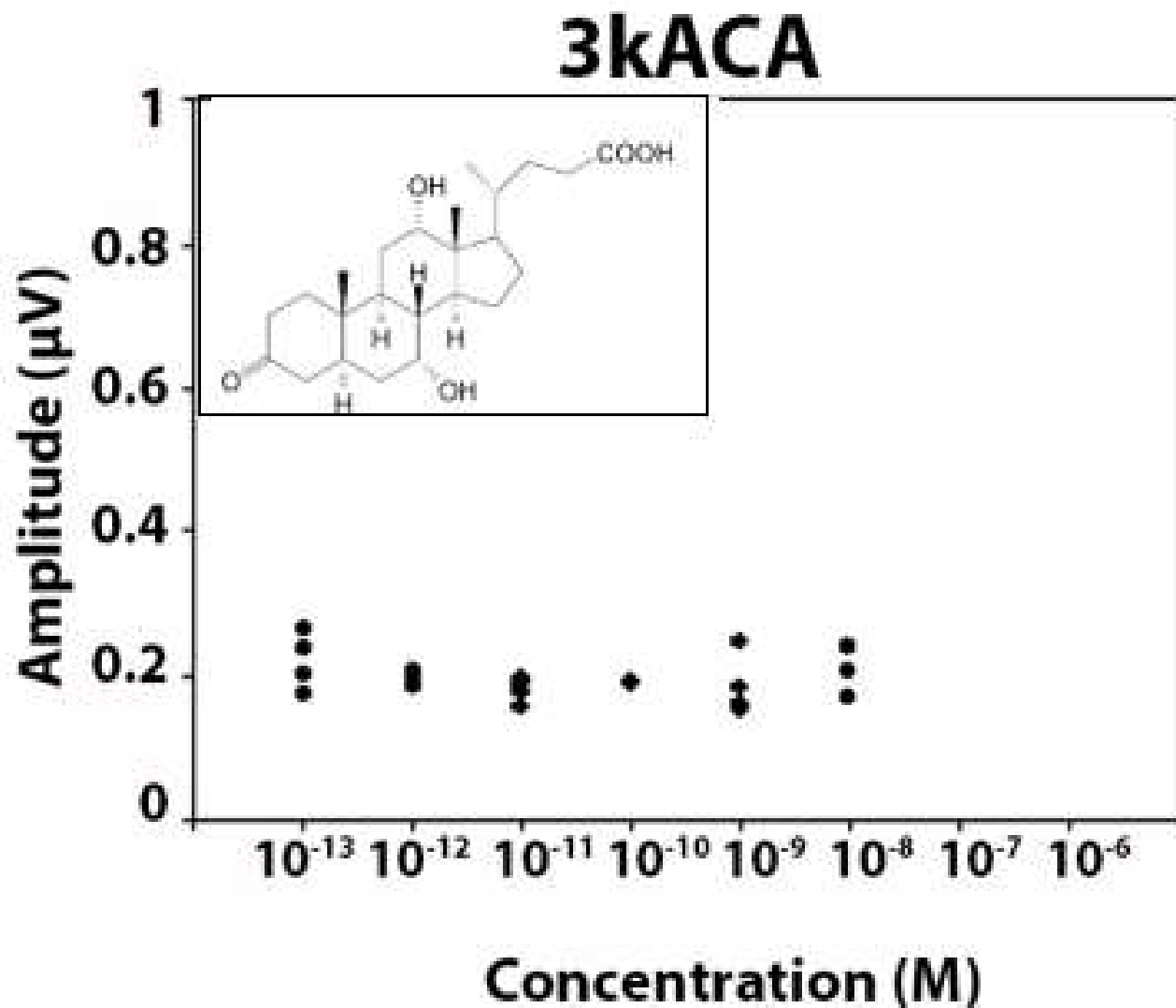
Figure A-14. Amplitude values of transformer stage sea lamprey LFP responses to male sex pheromone component 3kACA over a standardized concentration gradient ranging from 10^{-13} M to 10^{-6} M. Each point represents a single peak generated during a response to the associated odorant stimulus (n=1).
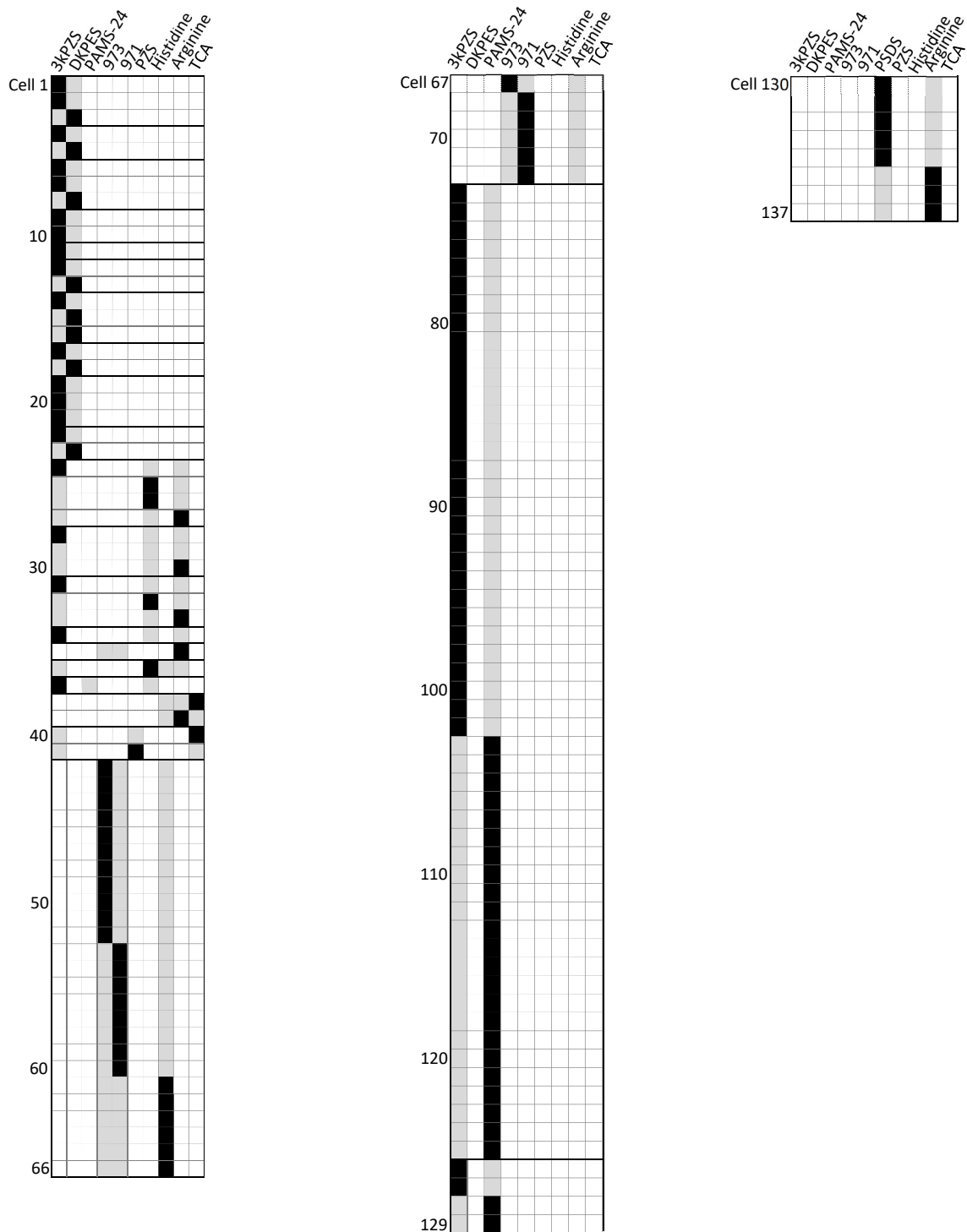
**Figure A-15. An overview of all 137 responding OSNs over 24 olfactory epithelium preparations.** OSNs (cells) are represented on the y-axis with tested pheromone components on the x-axis. Black cells indicate a response was observed by the associated cell, gray cells indicate

that the associated cell was exposed to that odorant but did not respond, and white cells indicate untested odorants.
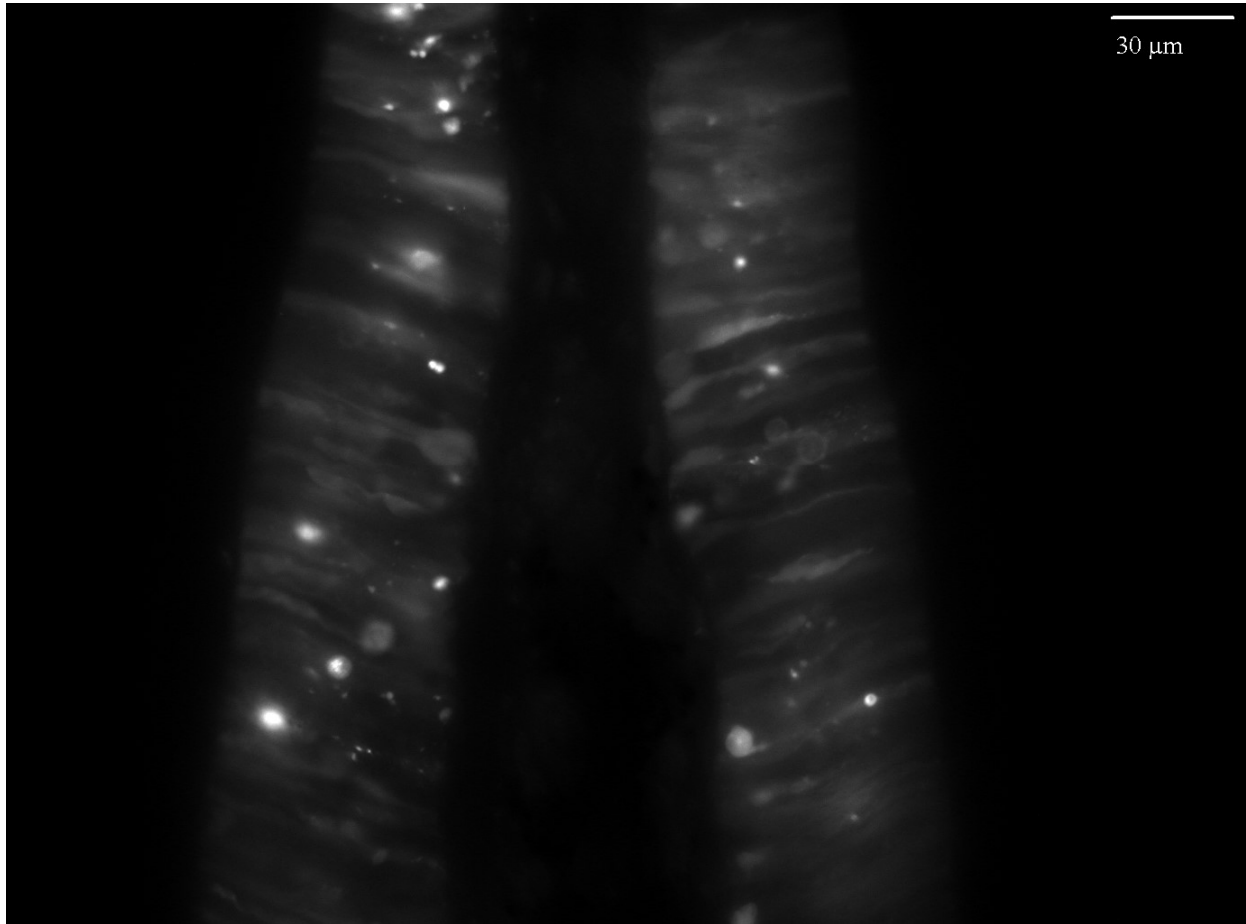
Figure A-16. Olfactory epithelial OSNs of a transformer-stage sea lamprey loaded with calcium green dextran.
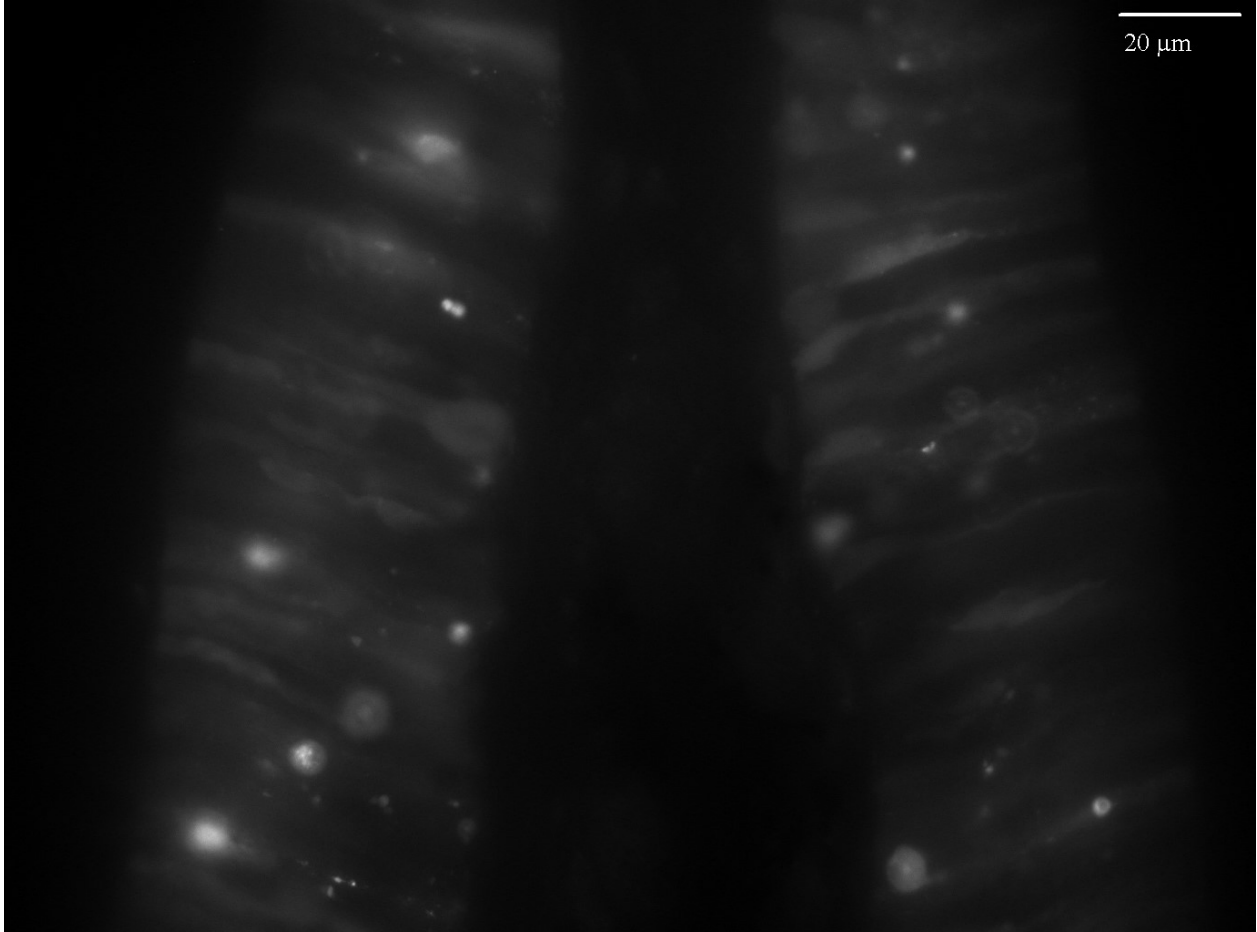
Figure A-17. Olfactory epithelial OSNs of a transformer-stage sea lamprey loaded with calcium green dextran.

Table A-3. A representative data set generated by analysis of fluorescence changes during calcium imaging of OSN. At each cycle, an image is taken and the resultant image stack is analyzed after the experiment. Analysis yields a fluorescence value for each cell analyzed at each cycle. In this way, changes in fluorescence can be tracked through time.

Cycle	Cell 1	Cell 2	Cell 3
1	0.02	0.023	0.028
2	0.019	0.024	0.029
3	0.018	0.021	0.027
4	0.013	0.017	0.02
5	-0.045	-0.045	-0.041
6	0.022	0.025	0.024
7	0.021	0.024	0.024
8	0.022	0.022	0.025
9	0.021	0.02	0.022
10	0.014	0.02	0.021
11	0.013	0.017	0.013
12	0.013	0.016	0.016
13	0.014	0.014	0.014
14	0.012	0.016	0.01
15	0.013	0.013	0.011
16	0.008	0.005	0.009
17	0.012	0.009	0.007
18	0.012	0.012	0.007
19	0.004	0.008	0.004
20	0.006	0.011	0.003
21	0.007	0.007	0.002
22	0.006	0.005	0.003
23	0.007	0.004	0.005
24	9.44E-04	0.002	6.73E-04
25	0.008	0.008	0.001
26	0.008	0.011	0.01
27	0.012	0.012	0.006
28	0.006	0.008	0.006
29	0.002	-0.002	-0.003
30	0.002	3.65E-04	-0.003
31	0.014	0.012	0.004
32	-0.009	-0.007	-0.01
33	-0.018	-0.017	-0.022
34	-0.015	-0.018	-0.022
35	-0.017	-0.016	-0.023
36	-0.021	-0.019	-0.026

37	-0.019	-0.019	-0.024
38	-0.017	-0.02	-0.025
39	-0.018	-0.019	-0.025
40	-0.018	-0.022	-0.026
41	-0.02	-0.021	-0.025
42	-0.02	-0.017	-0.027
43	-0.018	-0.023	-0.027
44	-0.021	-0.02	-0.027
45	-0.017	-0.022	-0.028
46	-0.022	-0.022	-0.026
47	-0.022	-0.024	-0.026
48	-0.022	-0.02	-0.027
49	-0.021	-0.026	-0.025
50	-0.021	-0.022	-0.026
51	-0.02	-0.024	-0.026
52	-0.02	-0.023	-0.026
53	-0.022	-0.022	-0.024
54	-0.02	-0.023	-0.023
55	-0.015	-0.022	-0.023
56	-0.007	-0.022	-0.024
57	-2.97E-04	-0.022	-0.021
58	0.038	0.011	0.011
59	0.035	0.008	0.008
60	0.003	-0.025	-0.024
61	0.005	-0.022	-0.028
62	0.008	-0.02	-0.025
63	0.012	-0.021	-0.019
64	0.008	-0.022	-0.008
65	0.04	0.01	0.044
66	0.039	0.007	0.05
67	0.009	-0.026	0.022
68	0.039	0.009	0.063
69	0.022	-0.007	0.047
70	-9.09E-04	-0.03	0.033
71	0.005	-0.027	0.029
72	0.006	-0.023	0.032
73	0.032	0.004	0.068
74	0.035	0.006	0.069
75	0.014	-0.014	0.051
76	0.004	-0.023	0.036
77	0.037	0.009	0.073
78	0.028	0.006	0.071
79	0.031	0.006	0.068

80	0.028	0.003	0.067
81	0.029	0.005	0.066
82	0.026	0.005	0.063
83	0.025	0.004	0.063
84	0.023	-0.001	0.053
85	0.025	0.001	0.052
86	0.022	-7.16E-04	0.052
87	0.02	-6.66E-04	0.049
88	0.017	-8.02E-04	0.049
89	-0.011	-0.03	0.015
90	0.02	-0.003	0.044
91	0.023	-0.002	0.044
92	0.018	-0.005	0.043
93	0.02	-0.003	0.04
94	0.016	-0.003	0.041
95	0.014	-0.007	0.035
96	0.016	-0.006	0.031
97	0.015	-0.005	0.037
98	0.013	-0.01	0.03
99	0.01	-0.008	0.027
100	0.013	-0.012	0.03
101	0.009	-0.01	0.03
102	0.012	-0.01	0.025
103	0.012	-0.011	0.023
104	0.011	-0.012	0.025
105	0.011	-0.01	0.022
106	0.009	-0.013	0.021
107	0.01	-0.012	0.019
108	0.004	-0.014	0.015
109	0.007	-0.013	0.021
110	0.008	-0.015	0.016
111	0.004	-0.019	0.02
112	0.005	-0.017	0.017
113	0.001	-0.015	0.016
114	0.002	-0.02	0.014
115	0.004	-0.016	0.016
116	6.59E-04	-0.019	0.01
117	-0.001	-0.019	0.01
118	-0.002	-0.024	0.008
119	-0.001	-0.02	0.009
120	9.90E-04	-0.027	0.009
121	-9.05E-04	-0.023	0.011
122	-0.001	-0.021	0.007

123	-0.002	-0.024	0.008
124	-0.003	-0.024	0.002
125	-0.005	-0.023	0.009
126	-0.007	-0.023	0.007
127	-0.008	-0.023	0.005
128	-0.005	-0.024	0.008
129	-0.009	-0.025	0.005
130	-0.008	-0.026	0.005
131	-0.011	-0.03	0.002
132	-0.013	-0.035	-0.005
133	-0.027	-0.044	-0.014
134	-0.032	-0.049	-0.022
135	-0.039	-0.055	-0.027
136	-0.037	-0.055	-0.025
137	-0.037	-0.056	-0.029
138	-0.041	-0.056	-0.027
139	-0.009	-0.026	0.007
140	-0.009	-0.026	0.005
141	-0.015	-0.036	0.003
142	-0.041	-0.058	-0.03
143	-0.013	-0.029	0.002
144	-0.04	-0.059	-0.029
145	-0.009	-0.029	0.005
146	-0.011	-0.029	0.004
147	-0.015	-0.028	0.007
148	-0.012	-0.029	0.007
149	-0.012	-0.027	0.005
150	-0.012	-0.033	0.008
151	-0.011	-0.032	0.003
152	-0.013	-0.03	0.007
153	-0.014	-0.033	0.006
154	-0.012	-0.031	0.004
155	-0.013	-0.032	0.005
156	-0.014	-0.034	0.006
157	-0.016	-0.035	0.001
158	-0.018	-0.036	0.001
159	-0.014	-0.037	1.50E-04
160	-0.018	-0.037	-4.52E-04
161	-0.021	-0.031	0.005
162	-0.014	-0.034	0.004
163	-0.019	-0.035	0.002
164	-0.02	-0.037	8.75E-04
165	-0.02	-0.036	0.002

166	-0.022	-0.036	0.004
167	-0.023	-0.038	8.81E-04
168	-0.022	-0.039	-0.001
169	-0.022	-0.039	9.73E-04
170	-0.02	-0.042	-0.002

Table A-4. A representative data set generated by the analysis of LFP recording data produced during dorsal olfactory bulb recordings. "Peak (min value)" values must exceed the "Threshold" values associated with that particular "delivery". The "threshold" is calculated as 3 times the "Baseline SD".

odour	delivery #	Baseline mean (V)	Baseline SD	Threshold (V)	Peak (min value)(V)
10-3 M arg/hist	1	-0.0189	0.2155	0.6276	-2.6587
				0	
3KPZS:DKPES (2:29.8)_10^-6:10^-7	1	-0.0383	0.0443	0.0946	-0.315
		-0.0383	0.0443	0.0946	-0.9016
				0	
	2	-0.0342	0.0477	0.1089	-0.9576
				0	
	3	-0.0343	0.0406	0.0875	-0.897
		-0.0343	0.0406	0.0875	-0.9099
				0	
L-Arg_10^-4	1	-0.0113	0.0393	0.1066	-0.5783
		-0.0113	0.0393	0.1066	-0.5734
				0	
	2	-0.0367	0.0461	0.1016	-0.5156
				0	
DKPES_10^-11	1	-0.0372	0.0623	0.1497	-0.703
		-0.0372	0.0623	0.1497	-0.7266
		-0.0372	0.0623	0.1497	-0.679
		-0.0372	0.0623	0.1497	-0.5886
		-0.0372	0.0623	0.1497	-0.7264
				0	
	2	-0.0357	0.0651	0.1596	-0.6017
		-0.0357	0.0651	0.1596	-0.621
		-0.0357	0.0651	0.1596	-0.6557
		-0.0357	0.0651	0.1596	-1.1162
		-0.0357	0.0651	0.1596	-0.6545
				0	

	3	-0.0356	0.0732	0.184	-0.8694
		-0.0356	0.0732	0.184	-0.8174
		-0.0356	0.0732	0.184	-0.4717
				0	
DKPES_10^-8	1	-0.0344	0.0479	0.1093	-0.6146
				0	
	2	0.2092	0.8182	2.6638	-0.6335
		0.2092	0.8182	2.6638	-0.6145
		0.2092	0.8182	2.6638	-0.8366
				0	
	3	-0.0347	0.0573	0.1372	-0.7004
		-0.0347	0.0573	0.1372	-0.6455
		-0.0347	0.0573	0.1372	-0.6576
		-0.0347	0.0573	0.1372	-0.8414
				0	
3KPZS_10^-11	1	-0.0376	0.0456	0.0992	-0.7809
		-0.0376	0.0456	0.0992	-0.5383
		-0.0376	0.0456	0.0992	-0.6327
				0	
	2	-0.0363	0.0554	0.1299	-0.9495
		-0.0363	0.0554	0.1299	-0.8101
		-0.0363	0.0554	0.1299	-0.8431
				0	
	3	-0.0372	0.0602	0.1434	-0.6838
		-0.0372	0.0602	0.1434	-0.7344
		-0.0372	0.0602	0.1434	-0.916
3KPZS_10^-8	1	-0.0375	0.0498	0.1119	-0.9764
		-0.0375	0.0498	0.1119	-0.5832
		-0.0375	0.0498	0.1119	-0.5361
		-0.0375	0.0498	0.1119	-0.8251
				0	
	2	-0.0366	0.0549	0.1281	-0.853
		-0.0366	0.0549	0.1281	-0.7161
		-0.0366	0.0549	0.1281	-0.7653
				0	
	3	-0.0366	0.0444	0.0966	-0.6161
		-0.0366	0.0444	0.0966	-0.8154
	1	-0.0189	0.2155	0.6276	-2.6587
				0	
	1	-0.0354	0.0269	0.0453	-0.3724
		-0.0354	0.0269	0.0453	-0.1855
				0	
	2	-0.0372	0.0275	0.0453	-0.3277
		-0.0372	0.0275	0.0453	-0.1787

				0	
	3	-0.0379	0.0294	0.0503	-0.2224
		-0.0379	0.0294	0.0503	-0.2623
				0	
	1	-0.0371	0.0313	0.0568	-0.1923
		-0.0371	0.0313	0.0568	-0.2135
		-0.0371	0.0313	0.0568	-0.2943
				0	
	2	-0.0361	0.0292	0.0515	-0.2848
		-0.0361	0.0292	0.0515	-0.2562
				0	
	3	-0.0357	0.0339	0.066	-0.217
		-0.0357	0.0339	0.066	-0.2724
				0	
	1	-0.0153	0.1124	0.3219	-0.3044
				0	
	2	-0.0362	0.0307	0.0559	-0.2985
				0	
	3	0.4007	1.0583	3.5756	-0.1909
		0.4007	1.0583	3.5756	-0.3617
				0	
	1	-0.0391	0.0334	0.0611	-0.303
				0	
	2	-0.0373	0.0232	0.0323	-0.2175
		-0.0373	0.0232	0.0323	-0.1881
		-0.0373	0.0232	0.0323	-0.1952
		-0.0373	0.0232	0.0323	-0.3238
				0	
	3	-0.035	0.0228	0.0334	-0.1827
		-0.035	0.0228	0.0334	-0.1729
		-0.035	0.0228	0.0334	-0.3606
				0	
	1	-0.0373	0.0235	0.0332	-0.1493
		-0.0373	0.0235	0.0332	-0.2647
				0	
	2	-0.038	0.0227	0.0301	-0.1831
		-0.038	0.0227	0.0301	-0.2078
		-0.038	0.0227	0.0301	-0.4255
				0	
	3	-0.0315	0.0273	0.0504	-0.1567
		-0.0315	0.0273	0.0504	-0.3457
				0	
	1	0.1383	0.6408	2.0607	-0.1634
		0.1383	0.6408	2.0607	-0.6078
				0	
	2	0.246	0.9018	2.9514	-0.2019

	0.246	0.9018	2.9514	-0.4945
			0	
3	-0.0378	0.0242	0.0348	-0.5273
	-0.0378	0.0242	0.0348	-0.1915
			0	
1	-0.035	0.0225	0.0325	-0.7942
	-0.035	0.0225	0.0325	-0.1601
	-0.035	0.0225	0.0325	-0.243
			0	
2	-0.0361	0.0178	0.0173	-0.2381
	-0.0361	0.0178	0.0173	-0.8049
	-0.0361	0.0178	0.0173	-0.1914
			0	
3	-0.0399	0.022	0.0261	-0.8165
	-0.0399	0.022	0.0261	-0.2196
	-0.0399	0.022	0.0261	-0.2212
			0	
1	-0.0375	0.0238	0.0339	-0.8372
			0	
2	-0.0363	0.0182	0.0183	-0.8398
	-0.0363	0.0182	0.0183	-0.2774
	-0.0363	0.0182	0.0183	-0.1961
			0	
3	-0.0433	0.0215	0.0212	-0.9081
	-0.0433	0.0215	0.0212	-0.4921
	-0.0433	0.0215	0.0212	-0.2611

VITA AUCTORIS

NAME: Gianfranco Grande

PLACE OF BIRTH: Windsor, Ontario

YEAR OF BIRTH: 1990

EDUCATION: B.Sc. Biological Sciences
University of Windsor

Windsor, ON

2008-2012

B.Ed. Intermediate/Senior
University of Windsor

Windsor, ON

2012-2013

M.Sc. Biology
University of Windsor

Windsor, ON

2015-2017